THE STRESSED BRAIN: NEURAL SIGNATURES OF ACUTE STRESS AND THEIR RELEVANCE FOR LONG-TERM STRESS VULNERABILITY

Wei Zhang

Support

The work described in this thesis was carried out at the Donders Institute for Brain, Cognition and Behaviour, and the Behavioural Science Institute, Radboud University Nijmegen, The Netherlands, with financial support from a VICI grant (#453-12-001) from the Netherlands Organization for Scientific Research (NWO) and a consolidator grant from the European Research Council (ERC_CoG-2017_772337) awarded to Prof. dr. Karin Roelofs.

ISBN: 978-94-628-4996-9

Cover Illustration: Wei Zhang

Lay-out: Proefschriftmaken

Print: Proefschriftmaken | https://www.proefschriftmaken.nl

The stressed brain: Neural signatures of acute stress and their relevance for long-term stress vulnerability

Proefschrift

ter verkrijging van de graad van doctor aan de
Radboud Universiteit Nijmegen
op gezag van de
rector magnificus

prof. dr. J.H.J.M. van Krieken,

volgens besluit van het college van decanen
in het openbaar te verdedigen op dinsdag

19 november 2019 om 15.00 uur precies

door

Wei Zhang
geboren op 26 november 1979
te Chongqing, China

Promotor: Prof. dr. K. Roelofs

Copromotor: Dr. F. Klumpers

Manuscriptcommissie:

Prof. dr. G.S.E. Fernández
Prof. dr. B.M. Elzinga (Universiteit Leiden)
Dr. I. Veer (Charité – Universitätsmedizin Berlin, Duitsland)

The stressed brain: Neural signatures of acute stress and their relevance for long-term stress vulnerability

Doctoral Thesis

to obtain the degree of doctor from
Radboud University Nijmegen
on the authority of the
Rector Magnificus

prof. dr. J.H.J.M. van Krieken,

according to the decision of the Council of Deans
to be defended in public on

Tuesday, November 19, 2019 at 15.00 hours

by

Wei Zhang
born on November 26, 1979
in Chongqing, China

Supervisor: Prof. dr. K. Roelofs

Co-supervisor: Dr. F. Klumpers

Doctoral Thesis Committee:

Prof. dr. G.S.E. Fernández
Prof. dr. B.M. Elzinga (Universiteit Leiden)
Dr. I. Veer (Charité – Universitätsmedizin Berlin, Duitsland)

献给亲爱的爹娘..✍

Table of Contents

CHAPTER I

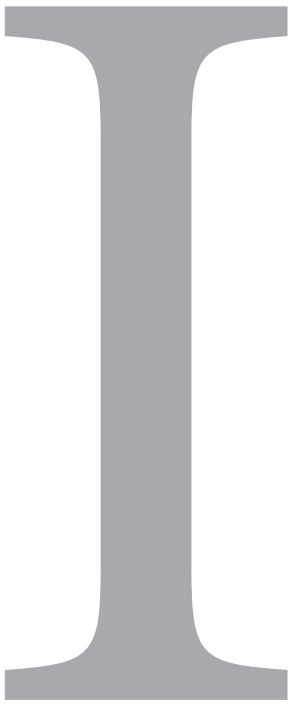

GENERAL INTRODUCTION

One of the hallmark questions in neuropsychiatry is why some people develop stress symptoms and others do not, even when being exposed to similar stressors or traumatic events. An answer to this question would not only offer valuable insight into concepts like stress resilience versus vulnerability, it could also help facilitate more precise assessments and (preventive) interventions for stress-related disorders. In the work described in this thesis, I test whether individual differences in acute stress responses may be predictive of long-term stress vulnerability.

Stress-related disorders are a burden not just for individuals, but also for society as a whole. In fact, a large number of individuals experience stress-related disorders. In Europe alone, up to 25% of the population suffers from depression or anxiety each year ("Each year, up to 25%", 2012), and the lifetime prevalence of post-traumatic stress disorder (PTSD), another common stress-related neuropsychiatric disorder, has been estimated to be up to 7% (Wittchen et al., 2011). With higher frequency of severe stressor exposure, occupational groups such as police officers and firefighters are at high risk for the development of mental health disturbances, including PTSD symptoms. Early findings from the largest force-wide survey in the UK recently found that 90% of police workers had been exposed to trauma, and nearly 20% of them reported experiencing PTSD symptoms ("Close to one in five police officers", 2019). The economic impact of stress-related disorders is enormous, with an estimated annual cost of more than €200 billion in Europe, including €8.4 billion for PTSD alone (Olesen et al., 2012).

It has recently been suggested that psychological and neuroendocrine adaptation to acute stressors may be relevant for understanding long-term stress vulnerability and resilience (Michopoulos et al., 2015; Kalisch et al., 2017). As an example, cortisol reactivity to acute stress prior to traumatization has been shown to predict the PTSD symptom levels after trauma exposure (Galatzer-Levy et al., 2014; Steudte-Schmiedgen et al., 2015). Given that these peripheral endocrine measures may only indirectly reflect the underlying neural mechanisms, it would be of interest to directly investigate whether acute stress responses at the neural level could predict trauma-related symptom development. Importantly, existing investigations into stress resilience and vulnerability at the neural level have predominantly involved cross-sectional studies of patients with stress-related disorders. Furthermore, limited prospective studies often focus on the identification of neural biomarkers in rest and leave neuroendocrine adaptations to acute stressors largely unnoticed with respect to predicting long-term stress effects. The field is therefore in great need of prospective longitudinal studies to reveal which neural stress mechanisms are predictive and which are acquired factors that put one at risk (Pitman et al., 2012; Admon et al., 2013; Kalisch et al., 2017).

To elucidate these stress processes, the current thesis aims to identify predictive biomarkers of stress-related symptom development. To this end, the first objective was to locate neural biomarkers that are of potential interest for acute stress

responses, including changes in functional connectivity of large-scale networks in response to acute psychosocial stressors. Subsequently, I investigated whether these potential biomarkers could predict stress-related symptom development in a longitudinal fashion. For these purposes, I tested 340 police recruits before and after a stressful period in their training phase characterized by numerous trauma exposures. A previous study in the Netherlands employed a similar prospective design and showed that this paradigm could elicit (sub-threshold) post-traumatic stress symptoms in 34% of police recruits (Carlier et al., 1997). Furthermore, I also explored the neural correlates of memory contextualization, a process that has been implicated in PTSD psychopathology. Before describing the specific research questions, I will first briefly explain the concept of stress, including relevant stress responses at neurobiological level and associated psychopathologies, such as PTSD.

Stress

What is stress? On the one hand, this term is generally used to refer to a stressor – namely, an internal or external stimulus, either physical or psychological, threatening the homeostasis of an organism (Selye, 1936). On the other hand, the term is also used to indicate a response to noxious or aversive stimuli. This definition of stress has been emphasized by studies investigating stress in terms of physiological and psychological responses (Seley, 1956). From a more clinical point of view, stress can be defined as a dynamic process that describes "a particular relationship between the person and the environment that is appraised by the person as taxing or exceeding his or her resources and endangering his or her well-being" (Lazarus and Folkman, 1984). Exposure to such a process in a repeated or chronic manner will lead to allostatic overload – "the wear and tear on the body" – which may further result in maladaptation and psychopathology (McEwen, 1998; McEwen et al., 2015). In this thesis, the term stress will be primarily used to indicate stress responses.

Stress Responses

Stress responses are assessed at different levels, including physiological, cognitive, emotional and behavioral levels. Concerning physiological stress responses, there are two main stress systems, namely the fast autonomic nervous system (ANS) and the slower hypothalamic-pituitary-adrenal (HPA) axis. Below, I will briefly introduce these two systems as well as associated neural mechanisms.

ANS and related stress response

Upon threat exposure, incoming sensory information rapidly (within seconds) triggers the activation of the ANS. Through the sympathetic nervous system (SNS) and the parasympathetic nervous system (PNS), the ANS causes fast reactions in

organs throughout the entire body by the fast release of (nor)adrenaline from the adrenal medulla into the bloodstream. Functions of the ANS in response to stress can typically be measured by changes in, among others, heart rate, blood pressure and skin conductance (see review by Zygmunt & Stanczyk, 2010). In human research, alpha-amylase is increasingly assessed as a general proxy of ANS arousal (Nater et al., 2006; Granger et al., 2007). Studies using this measure have linked changes in alpha-amylase response to pathological dysregulation of the ANS in patients with stress-related disorders (Schumacher et al., 2013).

HPA axis and related stress response

In contrast to the ANS, the HPA axis is a relatively slower system, the activation of which ensures a long-lasting response to stress. As indicated by the name, this system involves three key components: the hypothalamus, the pituitary gland and the adrenal cortex (*Figure 1* on the next page). Exposure to stress activates the paraventricular nucleus (PVN) of the hypothalamus to secrete corticotropin-releasing hormone (CRH) and vasopressin. These hormones then act on the anterior pituitary to facilitate the secretion of adrenocorticotropic hormone (ACTH). Ultimately, ACTH simulates the adrenal cortex to initiate the synthesis and release of glucocorticoid hormones (mainly cortisol in humans). Importantly, glucocorticoids, in turn, act back on the hypothalamus and pituitary in a negative feedback cycle, making the HPA an intricate but efficient system. The HPA end product, cortisol, is often referred to as the "stress hormone" and usually only peaks 20–30 minutes after the initiation of stress, with the elevation remaining up to more than one hour (Droste et al., 2008; Hermans, Henckens, Joëls, & Fernández, 2014; Joels, Sarabdjitsingh, & Karst, 2012). Importantly, elevated cortisol levels prepare the body for a fight-or-flight response by mobilizing resources to increase energy that can facilitate the addressing and resolving of the challenge (McKinley and Oldfield, 1998). Cortisol has also been implicated in restoring homeostasis in the aftermath of stress exposure (De Kloet et al., 1999, 2005).

Stress responses at neural level

It has long been acknowledged that, due to its plasticity, the brain can be shaped and remodeled by experiences (Bennett et al., 1964). A large number of studies, both in animals and humans, have shown that stressful experiences can cause functional and structural changes in many brain regions, including the prefrontal cortex (PFC), the amygdala and the hippocampus (see review by McEwen & Gianaros, 2010). In addition to identifying the isolated activity within specific brain regions under certain conditions, researchers have also studied the inter-regional temporal relationships between different brain regions as a measure of functional connectivity (FC) – that is, "the temporal correlations between spatially remote neurophysiological events" (Friston, Frith, Liddle, & Frackowiak, 1993; Lee,

Harrison, & Mechelli, 2003). Advancing from initial FC studies that have focused on task states, recent years have witnessed an increased focus on FC in a resting state, with resting-state functional magnetic resonance imaging (rs-fMRI) being used as a measurement tool (Biswal et al., 2010).

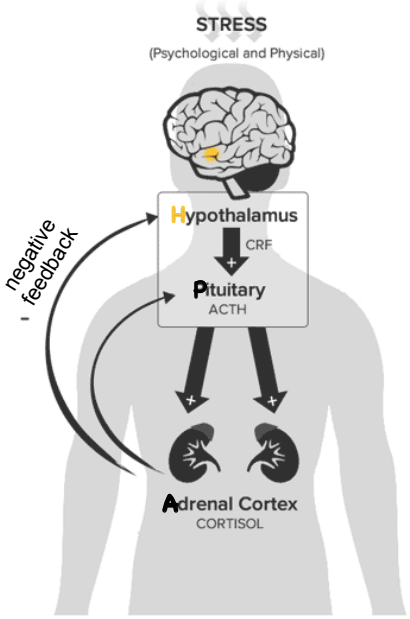

Hypothalamus-Pituitary-Adrenal axis is one of the major biological stress response systems.

Exposure to a stressor activates hypothalamic release of CRF that leads to the release of ACTH and ultimately simulates adrenal release of cortisol.

When cortisol centration in the blood reaches certain level, negative feedback is excerted to inhibit CRF and ACTH release. Homeostasis returns.

(Image adapted from Integrative Blog at https://www.integrativepro.com/Resources/Integrative-Blog/2016/The-HPA-Axis)

Figure 1. *HPA-axis*

Resting-state connectivity and large-scale networks

Acquisition of rs-fMRI focuses on measuring low-frequency spontaneous activity in the brain. Such brain activity is typically present even in the absence of an externally prompted task and is thus referred to as intrinsic. As connectivity can be considered to be coherent fluctuations in brain activity across distributed regions, brain circuits exhibiting such fluctuations in the absence of any overt task or experimental manipulations are often referred as intrinsic connectivity networks (ICNs; Fox & Raichle, 2007; Vincent et al., 2007). The most well-known ICNs are the default mode network (DMN), the salience network (SN) and the central executive network (CEN). Investigations on the FC of these networks to study alterations in brain functions have become increasingly popular over recent years, particularly in the clinical setting (*Figure 2*).

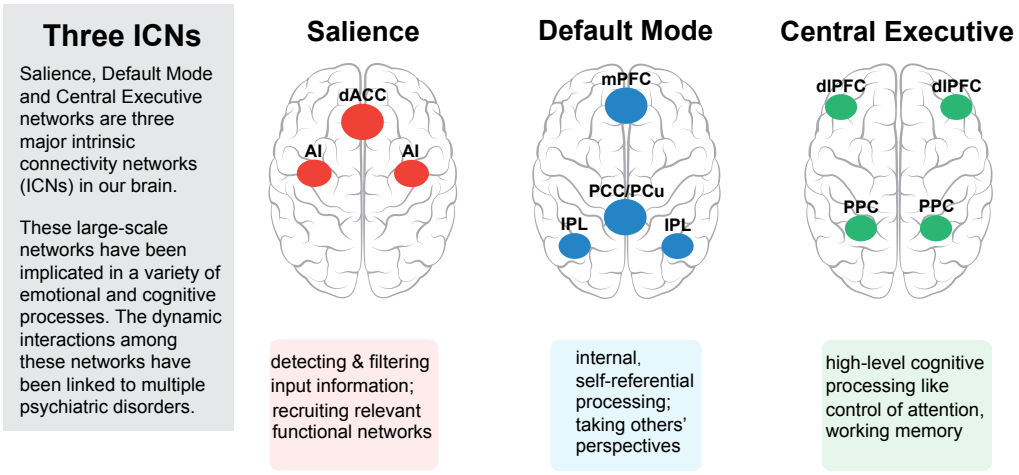

Figure 2. *A simplified sketch of three major intrinsic connectivity networks in our brain.*

In general, the DMN is known to activate preferentially when individuals focus on internal tasks, such as mind wandering, envisioning the future, retrieving autobiographic memory and taking others' perspectives (Greicius et al., 2003; Buckner et al., 2008). Anatomically, this network comprises several hub regions, including the medial PFC (mPFC), posterior cingulate cortex (PCC)/precuneus (PCu), inferior parietal lobule (IPL) and a few subsystems. The DMN has been shown to be negatively correlated with brain systems that are engaged in processing external signals, such as attention networks (Broyd et al., 2009). The SN is primarily anchored at the anterior insula (AI) and dorsal anterior cingulate cortex (dACC), with subcortical regions like amygdala, putamen and thalamus showing intrinsic connectivity with these crucial nodes (Seeley et al., 2007). The SN is involved in detecting and filtering relevant interoceptive, autonomic and emotional information, as well as in recruiting relevant functional networks (Seeley et al., 2007; Menon and Uddin, 2010). The CEN is a parietal-frontal system which includes the dorsolateral prefrontal cortex (dlPFC) and the posterior parietal cortex (PPC). This network is crucial for actively maintaining and manipulating information in working memory, for rule-based problem solving and for decision making in the context of goal-directed behavior (Petrides, 2005; Damoiseaux et al., 2006; Müller and Knight, 2006; Koechlin and Summerfield, 2007).

Stress effects on ICN connectivity

Few studies have directly investigated stress effects on FC at large-scale network level. Nevertheless, existing (seed-based) findings suggest aberrant FC of the amygdala in stress-related processing (Janak & Tye, 2015; Ressler, 2010; Zhang et al., 2018), as well as altered activity and connectivity of key ICN regions (such as dACC in the SN and PCC in the DMN) underlying dampened executive functions after

stressor exposure (Hermans et al., 2011; Liu et al., 2017). It has been hypothesized that the SN could initiate the dynamic switch between the DMN and CEN, assuring the mediation between attention to endogenous and exogenous events (Sridharan et al., 2008; Daniels et al., 2010; Menon and Uddin, 2010). Yet, most stress studies predominantly adopt a seed-based approach to investigate FC of selective areas of these ICNs, and infer the results with respect to the network-level functionality (see review by van Oort et al., 2017). Direct investigations into network-level FC for these ICNs as a function of stress have just begun to emerge (Hermans et al., 2011; Young et al., 2016). However, the findings thus far have been observed under task conditions. Consequently, it remains unclear whether the observed network reorganization also occurs in the absence of ongoing task demands.

Stress-related Psychopathology

Responses to stress can be associated with positive effects. However, excessive stress can lead to allostatic overload and result in maladaptation and psychopathology (McEwen, 1998; McEwen et al., 2015). There is a large group of psychiatric disorders that are related to stress, including mood and anxiety disorders, psychotic disorders, addiction and PTSD. In particular, due to the existence of a variety of clinical phenotypes that are consistent with PTSD diagnostic criteria, PTSD is now classified as one of the "trauma and stress-related disorders." Given the focus of my study, I will mainly focus on the psychopathology of PTSD.

PTSD is a mental condition that is triggered by a traumatic event – either experiencing or witnessing it. According to the DSM-5, PTSD is characterized by four clusters of symptoms: re-experiencing, avoidance, negative alteration in cognition and mood, and arousal symptoms (American Psychiatric Association, 2013). Re-experiencing symptoms include recurrent, unwanted distressing memories of the traumatic event, flashbacks, nightmares and emotional/physical responses to trauma reminders. Symptoms of avoidance include avoidance of distressing memories, thoughts, feelings or external reminders of the event. Negative alterations in cognition and mood refer to lack of interest in activities, difficulties in experiencing positive emotions and maintaining close relationships, negative thoughts about oneself and others, inability to remember important aspects of the traumatic event and feeling emotionally numb. The last cluster, consisting of arousal symptoms, includes irritability, increased startle response, reckless or self-destructive behavior, hypervigilance and sleeping problems (American Psychiatric Association, 2013).

Neurobiological markers of PTSD

Cortisol responses

Neurobiological processes have been receiving increasing attention as possible

factors linked to the onset and exacerbation of PTSD symptoms. This perspective is also in line with the US National Institute of Mental Health's Research Domain Criteria initiative, which aims to develop a classification system for mental disorders that is dimensional and links to neurobiological systems (Cuthbert and Insel, 2013). One of the most widely investigated systems is the HPA axis. The role of this system in PTSD psychopathology has been primarily studied through cortisol measurements. Whereas some studies observed blunted basal cortisol level in PTSD in comparison to healthy controls, other studies reported no differences (for review see Meewisse, Reitsma, De Vries, Gersons, & Olff, 2007). When taking into account potential methodological confounds, lower cortisol levels were observed among females with PTSD and survivors of sexual or physical abuse with PTSD (Meewisse et al., 2007). In contrast, other studies reported the opposite pattern, with elevated cortisol levels in women with PTSD after reading personalized trauma scripts (Elzinga et al., 2003), or after assessing long-term cortisol levels accumulated in hair (Schalinski et al., 2015). In the few available longitudinal studies on basal HPA-axis activity, inconclusive results also emerge. Lower levels of urinary cortisol were found to predict PTSD 4–6 weeks later among adults who had experienced motor vehicle accidents (Delahanty et al., 2000, 2003), but higher levels of urinary cortisol predicted PTSD among children and adolescents aged 8–18 with a variety of traumatic injuries (Delahanty et al., 2005). A similar pattern was observed in a study among rape victims: lower cortisol in the days following a rape was predictive of future PTSD in survivors with a history of assault, but higher levels of cortisol were associated with survivors without such a history (Resnick et al., 1995).

In short, studies regarding basal cortisol levels are inconclusive, and measuring cortisol reactivity to challenges has been suggested as a more promising approach (Michopoulos et al., 2015). A recent empirical study on police students found that blunted cortisol reactivity to acute stress exposure was associated with increased prospective risk for PTSD (Galatzer-Levy et al., 2014). Steudte-Schmiedgen et al. (2015) observed similar effects, where blunted cortisol stress reactivity predicted PTSD symptom development following trauma exposure in male soldiers.

Regional to network-level responses

In addition to investigating the HPA axis, neuroscientists who are interested in understanding the neurobiological mechanism underlying PTSD have started to examine the neurocircuitry involved in stress processing. As has been described above, stressful experiences can shape and remodel our brain structure, and some of the brain regions – such as the PFC, amygdala and hippocampus – are particularly sensitive to this stress effect. Early studies on stress effects in the brain primarily focused on the activity and connectivity of these key regions in relation to psychopathology. For example, overall hyper-activity of the amygdala and hypo-activity of the medial PFC have been consistently observed in PTSD patients

in contrast to healthy controls in cross-sectional studies, while hippocampal dysregulation has been suggested underlying the deficits of PTSD population in memory performance and information processing (Etkin and Wager, 2007; Shin and Liberzon, 2010; Pitman et al., 2012; Koch et al., 2016). Subsequent studies, mostly using a seed-based connectivity analysis, observed functional abnormalities in patients with PTSD in brain circuits associated with the amygdala, medial prefrontal cortex (mPFC), cingulate gyrus and insula (see review by Fenster, Lebois, Ressler, & Suh, 2018; also by Liberzon & Sripada, 2007). Later on, studies expanded the focus from these fronto-limbic circuits to the interaction of three major ICNs, namely the DMN, SN and CEN. A triple-network model has been proposed to better understand the psychopathology of a few major psychiatric and neurological disorders, including PTSD (Menon, 2011). This model suggests that the "SN, and most notably the anterior insula (AI), is an integral hub in mediating dynamic interactions between other large-scale brain networks involved in externally oriented attention and internally oriented self-related mental processes." Importantly, the model generally matches the observations on aberrant organization and functioning of the key regions from the DMN, SN and CEN in individuals with PTSD in contrast to trauma-exposed or trauma-unexposed individuals (see review for Admon et al., 2013; Koch et al., 2016; Michopoulos et al., 2015; Pitman et al., 2012). However, most of these studies focus on a limited number of key regions – that is, use a seed-based approach – and only infer the results at the network level. Very few studies have directly tested alterations of these networks in relation to stress effects (Hermans et al., 2011; Young et al., 2016), and no investigations thus far have tested whether these networks interactions under stress can predict subsequent symptom development after trauma exposure.

Characterizing the interactions of these three networks (DMN, SN and CEN) may provide us with greater understanding of the fundamental brain mechanisms underlying psychopathology in, for example, PTSD; hence, in this research, I investigated how these networks respond to experimentally induced acute stress (**Chapter 2**) and whether such acute stress-induced network connectivity patterns are predicative of post-traumatic stress levels (**Chapter 4**). Although a network-level approach can provide better insight into cohesive behavior of networks as a whole, by nature such an approach can overlook functional characteristics at the local level. Approaches accounting for regional attributes, such as graph theory-based analyses, may help address this issue (Bressler and Menon, 2010; Cohen and D'Esposito, 2016). In this research, I used a novel method that combines the guidance from a priori knowledge about ICNs that are sensitive to stress effects with the strength of a more data-driven approach to investigate which functional units (i.e., units defined by their FC) are most critically affected by acute stress (**Chapter 3**).

Additionally, in acknowledgment of heterogeneity in PTSD symptoms and the common comorbidity with other psychiatric and general medical conditions, it is likely more prudent for future studies to identify valid biomarkers for specific clusters of symptoms (Galatzer-Levy et al., 2013; Murphy et al., 2019). For example, the loss of "pattern separation" (or loss of memory precision over time) has been suggested as a key process that gives rise to memory intrusion or flashbacks (Moore and Zoellner, 2007; Snyder et al., 2011; Besnard and Sahay, 2016). At the neural level, some studies associate the abnormal PFC functioning with this process, whereas others suggest a crucial role of the hippocampus in information integration (Eichenbaum, 2000; Davachi, 2006; Summerfield et al., 2006; Ranganath, 2010). In this research, I designed a task to manipulate the degree of memory contextualization (i.e., a process that an item binds to its context) and explored the neural correlates of this process (**Chapter 5**).

Outline of the thesis

To gain a better understanding of neural mechanisms related to acute stress responses, and to test whether such responses can predict long-term consequences upon exposure to real-life stressors, in this thesis I set out to address the following questions and hypotheses (ordered by chapter):

1. *How do large-scale intrinsic networks respond to acute stressors with regard to FC?* Will brain structures exhibit similar reorganization as has been shown under task conditions when there are no external task demands? Based on existing evidence, I predicted increased connectivity of SN but decreased connectivity of DMN following acute stress induction. I further expected to observe an association between such stress-induced network connectivity changes and cortisol stress responsiveness.
2. *What are the sub-structures of these large-scale brain networks that acute stress influences the most in terms of their connectivity patterns?* Can we tell the stressed from the non-stressed state in the brain based on these patterns? Using a novel approach, I tested whether sub-structures of SN and DMN were critically affected by acute stress induction.
3. *Can acute stress responses at endocrinal and neural-network level predict the development of PTSD symptom levels?* Can individual differences in these acute stress responses serve as a vulnerability marker for long-term consequences after trauma exposure? I predicted that increases in SN connectivity and decreases in DMN connectivity in response to acute stress induction would predict higher levels of post-trauma stress resilience.
4. *What are the neural correlates of memory contextualization?* Are brain regions involved in such a process also known to be implicated in PTSD psychopathology? In particular, I was interested in testing the role of the prefrontal cortex and hippocampus in the contextualization process.

General approach

To address **Questions 1 and 2**, I investigated changes in resting-state connectivity of large-scale networks using rs-fMRI data acquired before and after an experiment of psychosocial stress induction. This experiment was part of a large longitudinal study that enables further investigation into **Question 3** – namely, can I predict long-term symptom development using baseline stress reactivity? More specifically, Questions 1–3 are addressed using a prospective longitudinal study among 340 police recruits who were tested before and after a 16-month stressful period in their training. A similar experimental paradigm has previously been shown to elicit symptoms in 34% of police recruits (Carlier et al., 1997). In addition, I developed a contextualization task to address **Question 4** by identifying neural correlates of context-dependent memory, using fMRI data. Below, I will briefly describe the general methods used in the Police-in-Action (PIA) project that covers the studies found in **Chapters 2–4**.

General methods for PIA-study

Experimental Design: The procedure used in these studies, in addition to other tasks that were implemented in the PIA project (i.e., questionnaires, a fear-conditioning task, a reversal learning task, an emotional go/nogo shooting task, structural T1 acquisition, and an approach/avoidance task), has been pre-registered (Koch et al., 2017). Relevant for Chapter 2–4, an acute stress-induction experiment was conducted at both baseline and follow-up (see experimental design in *Figure 3*).

Participants

A total of 427 participants were initially recruited, including 340 police students from the Dutch Police Academy. All police recruits were receiving education at school during Wave 1 assessment, and around 90% of them went through Wave 2 assessment after an average of 16-months' exposure to real-life traumas during emergency aid training.

Acute Stress Induction

Acute stress responses were induced by sequential administration of a socially evaluated cold pressor task (SECPT) and a mental arithmetic (MA) task – a procedure that has been shown to successfully induce psychophysiological and subjective stress responses (Schwabe et al., 2008; Luo et al., 2018). The full procedure took about 8 minutes, including instructions, with each task lasting for 3 minutes. Salivary cortisol and subjective reports on negative affect were collected during the time course of the experiment. The rs-fMRI data for two sessions of approximately 6 minutes each were acquired before and after the experiment (*Figure 3*).

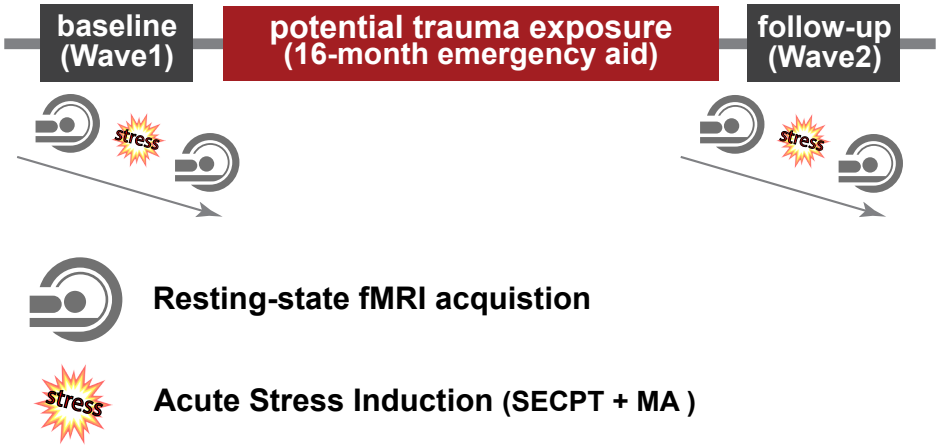

Figure 3. *Simplified experimental design of studies relevant for Chapter2-4 from PIA project. Two assessments (i.e., baseline Wave 1 and follow-up Wave 2) were conducted before and after an averaged 16-month exposure to real life trauma, respectively. In each assessment, two sessions of resting-state fMRI were acquired, before and after a formal stress induction that was consisted of a Socially Evaluated Cold Pressure Task (SECPT) and a Mental Arithmetic (MA) task.*

References

Admon R, Milad MR, Hendler T (2013) A causal model of post-traumatic stress disorder: Disentangling predisposed from acquired neural abnormalities. Trends Cogn Sci 17:337–347.

American Psychiatric Association (2013) Diagnostic and Statistical Manual of Mental Disorders (DSM). CoDAS 25:191–192.

Besnard A, Sahay A (2016) Adult Hippocampal Neurogenesis, Fear Generalization, and Stress. Neuropsychopharmacology 41:24–44.

Biswal BB et al. (2010) Toward discovery science of human brain function. Proc Natl Acad Sci U S A 107:4734–4739.

Bressler SL, Menon V (2010) Large-scale brain networks in cognition: emerging methods and principles. Trends Cogn Sci 14:277–290.

Broyd SJ, Demanuele C, Debener S, Helps SK, James CJ, Sonuga-Barke EJS (2009) Default-mode brain dysfunction in mental disorders: a systematic review. Neurosci Biobehav Rev 33:279–296.

Buckner RL, Andrews-Hanna JR, Schacter DL (2008) The brain's default network: Anatomy, function, and relevance to disease. Ann N Y Acad Sci 1124:1–38.

Carlier IVE, Lamberts RD, Gersons BPR (1997) Risk factors for posttraumatic stress symptomatology in police officers: A prospective analysis. J Nerv Ment Dis 185:498–506.

Cohen JR, D'Esposito M (2016) The Segregation and Integration of Distinct Brain Networks and Their Relationship to Cognition. J Neurosci 36:12083–12094.

Cuthbert BN, Insel TR (2013) Toward the future of psychiatric diagnosis: The seven pillars of RDoC. BMC Med 11.

Damoiseaux JS, Rombouts SARB, Barkhof F, Scheltens P, Stam CJ, Smith SM, Beckmann CF (2006) Consistent resting-state networks across healthy subjects. Proc Natl Acad Sci 103:13848–13853.

Daniels JK, Mcfarlane AC, Bluhm RL, Moores KA, Richard Clark C, Shaw ME, Williamson PC, Densmore M, Lanius RA (2010) Switching between executive and default mode networks in posttraumatic stress disorder: Alterations in functional connectivity. J Psychiatry Neurosci 35:258–266.

Davachi L (2006) Item, context and relational episodic encoding in humans. Curr Opin Neurobiol 16:693–700.

De Kloet ER, Joëls M, Holsboer F (2005) Stress and the brain: From adaptation to disease. Nat Rev Neurosci 6:463–475.

De Kloet ER, Oitzl MS, Joëls M (1999) Stress and cognition: Are corticosteroids good or bad guys? Trends Neurosci 22:422–426.

Delahanty DL, Nugent NR, Christopher NC, Walsh M (2005) Initial urinary epinephrine and cortisol levels predict acute PTSD symptoms in child trauma victims. Psychoneuroendocrinology 30:121–128.

Delahanty DL, Raimonde AJ, Spoonster E (2000) Initial posttraumatic urinary cortisol levels predict subsequent PTSD symptoms in motor vehicle accident victims. Biol Psychiatry 48:940–947.

Delahanty DL, Raimonde AJ, Spoonster E, Cullado M (2003) Injury severity, prior trauma history, urinary cortisol levels, and acute PTSD in motor vehicle accident victims. J Anxiety Disord 17:149–164.

Depression in Europe: facts and figures. (2012). Retrieved from http://www.euro.who.int/en/health-topics/noncommunicable-diseases/mental-health/news/news/2012/10/depression-in-europe/depression-in-europe-facts-and-figures

Droste SK, De Groote L, Atkinson HC, Lightman SL, Reul JMHM, Linthorst ACE (2008) Corticosterone levels in the brain show a distinct ultradian rhythm but a delayed response to forced swim stress. Endocrinology 149:3244–3253.

Eichenbaum H (2000) A cortical-hippocampal system for declarative memory. Nat Rev Neurosci 1:41–50.

Elzinga BM, Schmahl CG, Vermetten E, Van Dyck R, Bremner JD (2003) Higher cortisol levels following exposure to traumatic reminders in abuse-related PTSD. Neuropsychopharmacology 28:1656–1665.

Etkin A, Wager TD (2007) Functional neuroimaging of anxiety: a meta-analysis of emotional processing in PTSD, social anxiety disorder, and specific phobia. Am J Psychiatry 164:1476–1488.

Fenster RJ, Lebois LAM, Ressler KJ, Suh J (2018) Brain circuit dysfunction in post-traumatic stress disorder: from mouse to man. Nat Rev Neurosci 19:535–551.

Fox MD, Raichle ME (2007) Spontaneous fluctuations in brain activity observed with functional magnetic resonance imaging. Nat Rev Neurosci 8:700–711.

Friston KJ, Frith CD, Liddle PF, Frackowiak RSJ (1993) Functional connectivity: The principal-component analysis of large (PET) data sets. J Cereb Blood Flow Metab 13:5–14.

Galatzer-Levy IR, Ankri Y, Freedman S, Israeli-Shalev Y, Roitman P, Gilad M, Shalev AY (2013) Early PTSD Symptom Trajectories: Persistence, Recovery, and Response to Treatment: Results from the Jerusalem Trauma Outreach and Prevention Study (J-TOPS). PLoS One 8.

Galatzer-Levy IR, Steenkamp MM, Brown AD, Qian M, Inslicht S, Henn-Haase C, Otte C, Yehuda R, Neylan TC, Marmar CR (2014) Cortisol response to an experimental stress paradigm prospectively predicts long-term distress and resilience trajectories in response to active police service. J Psychiatr Res 56:36–42.

Granger DA, Kivlighan KT, El-Sheikh M, Gordis EB, Stroud LR (2007) Salivary α-Amylase in Biobehavioral Research. Ann N Y Acad Sci 1098:122–144.

Greicius MD, Krasnow B, Reiss AL, Menon V (2003) Functional connectivity in the resting brain: A network analysis of the default mode hypothesis. Proc Natl Acad Sci 100:253–258.

Hermans EJ, Henckens MJAG, Joëls M, Fernández G (2014) Dynamic adaptation of large-scale brain networks in response to acute stressors. Trends Neurosci 37:304–314.

Hermans EJ, van Marle HJF, Ossewaarde L, Henckens MJ a. G, Qin S, van Kesteren MTR, Schoots VC, Cousijn H, Rijpkema M, Oostenveld R, Fernandez G (2011) Stress-Related Noradrenergic Activity Prompts Large-Scale Neural Network Reconfiguration. Science 334(6059):1151–1153.

Janak PH, Tye KM (2015) From circuits to behaviour in the amygdala. Nature 517:284–292.

Joels M, Sarabdjitsingh RA, Karst H (2012) Unraveling the Time Domains of Corticosteroid Hormone Influences on Brain Activity: Rapid, Slow, and Chronic Modes. Pharmacol Rev 64:901–938.

Kalisch R et al. (2017) The resilience framework as a strategy to combat stress-related disorders. Nat Hum Behav 1:784–790.

Koch SBJ, Klumpers F, Zhang W, Hashemi MM, Kaldewaij R, van Ast VA, Smit AS, Roelofs K (2017) The role of automatic defensive responses in the development of

posttraumatic stress symptoms in police recruits: protocol of a prospective study. Eur J Psychotraumatol 8:1412226.
Koch SBJ, van Zuiden M, Nawijn L, Frijling JL, Veltman DJ, Olff M (2016) Aberrant resting-state brain activity in posttraumatic stress disorder: A meta-analysis and systematic review. Depress Anxiety 33:592–605.
Koechlin E, Summerfield C (2007) An information theoretical approach to prefrontal executive function. Trends Cogn Sci 11:229–235.
Lazarus RS, Folkman S (1984) The Stress Concept in the Life Sciences. In: Stress, Appraisal, and Coping, pp 1–21.
Lee L, Harrison LM, Mechelli A (2003) A report of the functional connectivity workshop, Dusseldorf 2002. In: NeuroImage, pp 457–465.
Liberzon I, Sripada CS (2007) The functional neuroanatomy of PTSD: a critical review. In: Progress in Brain Research, pp 151–169.
Liu Y, Li L, Li B, Feng N, Li L, Zhang X, Lu H, Yin H (2017) Decreased Triple Network Connectivity in Patients with Recent Onset Post-Traumatic Stress Disorder after a Single Prolonged Trauma Exposure. Sci Rep 7.
Luo Y, Fernández G, Hermans E, Vogel S, Zhang Y, Li H, Klumpers F (2018) How acute stress may enhance subsequent memory for threat stimuli outside the focus of attention: DLPFC-amygdala decoupling. Neuroimage.
McEWEN BS (1998) Stress, Adaptation, and Disease: Allostasis and Allostatic Load. Ann N Y Acad Sci 840:33–44.
McEwen BS, Bowles NP, Gray JD, Hill MN, Hunter RG, Karatsoreos IN, Nasca C (2015) Mechanisms of stress in the brain. Nat Neurosci 18:1353–1363.
McEwen BS, Gianaros PJ (2010) Stress- and Allostasis-Induced Brain Plasticity. Annu Rev Med 62:431–445.
McKinley MJ, Oldfield BJ (1998) The brain as an endocrine target for peptide hormones. Trends Endocrinol Metab 9:349–354.
Meewisse M-L, Reitsma JB, De Vries G-J, Gersons BPR, Olff M (2007) Cortisol and post-traumatic stress disorder in adults. Br J Psychiatry 191:387–392.
Menon V (2011) Large-scale brain networks and psychopathology: A unifying triple network model. Trends Cogn Sci 15:483–506.
Menon V, Uddin LQ (2010) Saliency, switching, attention and control: a network model of insula function. Brain Struct Funct 214:655–667.
Michopoulos V, Norrholm SD, Jovanovic T (2015) Diagnostic Biomarkers for Posttraumatic Stress Disorder: Promising Horizons from Translational Neuroscience Research. Biol Psychiatry 78:344–353.
Moore SA, Zoellner LA (2007) Overgeneral Autobiographical Memory and Traumatic Events: An Evaluative Review. Psychol Bull 133:419–437.
Müller NG, Knight RT (2006) The functional neuroanatomy of working memory: Contributions of human brain lesion studies. Neuroscience 139:51–58.
Murphy D, Ross J, Busuttil W, Greenberg N, Armour C (2019) A latent profile analysis of PTSD symptoms among UK treatment seeking veterans. Eur J Psychotraumatol 10:1558706.
Nater UM, La Marca R, Florin L, Moses A, Langhans W, Koller MM, Ehlert U (2006) Stress-induced changes in human salivary alpha-amylase activity - Associations with adrenergic activity. Psychoneuroendocrinology 31:49–58.
Olesen J, Gustavsson A, Svensson M, Wittchen HU, Jönsson B (2012) The economic cost of brain disorders in Europe. Eur J Neurol 19:155–162.

Petrides M (2005) Lateral prefrontal cortex: Architectonic and functional organization. Philos Trans R Soc B Biol Sci 360:781–795.

Pitman RK, Rasmusson AM, Koenen KC, Shin LM, Orr SP, Gilbertson MW, Milad MR, Liberzon I (2012) Biological studies of post-traumatic stress disorder. Nat Rev Neurosci 13:769–787.

Police workforce: Almost one in five suffer with a form of PTSD. (2019). Retrieved from https://www.cam.ac.uk/policeptsd.

Ranganath C (2010) Binding Items and Contexts: The Cognitive Neuroscience of Episodic Memory. Curr Dir Psychol Sci 19:131–137.

Resnick HS, Yehuda R, Pitman RK, Foy DW (1995) Effect of previous trauma on acute plasma cortisol level following rape. Am J Psychiatry 152:1675–1677.

Ressler KJ (2010) Amygdala Activity, Fear, and Anxiety: Modulation by Stress. Biol Psychiatry 67:1117–1119.

Schalinski I, Elbert T, Steudte-Schmiedgen S, Kirschbaum C (2015) The cortisol paradox of trauma-related disorders: Lower phasic responses but higher tonic levels of cortisol are associated with sexual abuse in childhood. PLoS One 10, e0136921.

Schumacher S, Kirschbaum C, Fydrich T, Ströhle A (2013) Is salivary alpha-amylase an indicator of autonomic nervous system dysregulations in mental disorders?-A review of preliminary findings and the interactions with cortisol. Psychoneuroendocrinology 38:729–743.

Schwabe L, Haddad L, Schachinger H (2008) HPA axis activation by a socially evaluated cold-pressor test. Psychoneuroendocrinology 33:890–895.

Seeley WW, Menon V, Schatzberg AF, Keller J, Glover GH, Kenna H, Reiss AL, Greicius MD (2007) Dissociable Intrinsic Connectivity Networks for Salience Processing and Executive Control. J Neurosci 27:2349–2356.

SELYE H (1956) Stress and psychiatry. Am J Psychiatry 113:423–427.

Shin LM, Liberzon I (2010) The neurocircuitry of fear, stress, and anxiety disorders. Neuropsychopharmacology 35:169–191.

Snyder JS, Soumier A, Brewer M, Pickel J, Cameron H a (2011) Adult hippocampal neurogenesis buffers stress responses and depressive behaviour. Nature 476:458–461.

Sridharan D, Levitin DJ, Menon V (2008) A critical role for the right fronto-insular cortex in switching between central-executive and default-mode networks. Proc Natl Acad Sci U S A 105:12569–12574.

Steudte-Schmiedgen S, Stalder T, Schönfeld S, Wittchen HU, Trautmann S, Alexander N, Miller R, Kirschbaum C (2015) Hair cortisol concentrations and cortisol stress reactivity predict PTSD symptom increase after trauma exposure during military deployment. Psychoneuroendocrinology 59:123–133.

Summerfield C, Greene M, Wager T, Egner T, Hirsch J, Mangels J (2006) Neocortical connectivity during episodic memory formation. PLoS Biol 4:855–864.

van Oort J, Tendolkar I, Hermans EJ, Mulders PC, Beckmann CF, Schene AH, Fernández G, van Eijndhoven PF (2017) How the brain connects in response to acute stress: A review at the human brain systems level. Neurosci Biobehav Rev 83:281–297.

Vincent JL, Patel GH, Fox MD, Snyder AZ, Baker JT, Van Essen DC, Zempel JM, Snyder LH, Corbetta M, Raichle ME (2007) Intrinsic functional architecture in the anaesthetized monkey brain. Nature 447:83–86.

Wittchen HU, Jacobi F, Rehm J, Gustavsson A, Svensson M, Jönsson B, Olesen J, Allgulander C, Alonso J, Faravelli C, Fratiglioni L, Jennum P, Lieb R, Maercker A, van Os J, Preisig M,

Salvador-Carulla L, Simon R, Steinhausen HC (2011) The size and burden of mental disorders and other disorders of the brain in Europe 2010. Eur Neuropsychopharmacol 21:655–679.

Young CB, Raz G, Everaerd D, Beckmann CF, Tendolkar I, Hendler T, Fernandez G, Hermans EJ (2016) Dynamic shifts in large-scale brain network balance as a function of arousal. J Neurosci.

Zhang X, Ge TT, Yin G, Cui R, Zhao G, Yang W (2018) Stress-induced functional alterations in amygdala: Implications for neuropsychiatric diseases. Front Neurosci 12.

Zygmunt A, Stanczyk J (2010) Methods of evaluation of autonomic nervous system function. Arch Med Sci 6:11–18.

CHAPTER II

II

ACUTE STRESS ALTERS THE 'DEFAULT' BRAIN PROCESSING

This chapter has been published as Wei Zhang, Mahur M. Hashemi, Reinoud Kaldewaij, Saskia B.J. Koch, Christian Beckmann, Floris Klumpers and Karin Roelofs* (2019) Acute stress alters the 'default' brain processing. Neuroimage 189: 870-877.*

**Equal contributions*

Abstract

Active adaptation to acute stress is essential for coping with daily life challenges. The stress hormone cortisol, as well as large scale re-allocations of brain resources have been implicated in this adaptation. Stress-induced shifts between large-scale brain networks, including salience (SN), central executive (CEN) and default mode networks (DMN), have however been demonstrated mainly under task-conditions. It remains unclear whether such network shifts also occur in the absence of ongoing task-demands, and most critically, whether these network shifts are predictive of individual variation in the magnitude of cortisol stress-responses.

In a sample of 335 healthy participants, we investigated stress-induced functional connectivity changes (delta-FC) of the SN, CEN and DMN, using resting-state fMRI data acquired before and after a socially evaluated cold-pressor test and a mental arithmetic task. To investigate which network changes are associated with acute stress, we evaluated the association between cortisol increase and delta-FC of each network.

Stress-induced cortisol increase was associated with increased connectivity within the SN, but with decreased coupling of DMN at both local (within network) and global (synchronization with other brain regions) levels.

These findings indicate that acute stress prompts immediate connectivity changes in large-scale resting-state networks, including the SN and DMN in the absence of explicit ongoing task-demands. Most interestingly, this brain reorganization is coupled with individuals' cortisol stress-responsiveness. These results suggest that the observed stress-induced network reorganization might function as a neural mechanism determining individual stress reactivity and, therefore, it could serve as a promising marker for future studies on stress resilience and vulnerability.

Introduction

Beyond traditional group-level analyses, recent investigations have moved towards characterizing individual profiles of functional connectivity (FC), which predict cognitive and behavioral performance at the single-subject level (Finn et al., 2017; Marquand, Haak, & Beckmann, 2017). FC fingerprints, derived from resting-state fMRI (rs-fMRI) data in particular, have been widely used in studies examining the abnormalities of connectivity profiles in patients with stress-related psychiatric disorders (Koch et al., 2016; Nicholson et al., 2015; Oathes, Patenaude, Schatzberg, & Etkin, 2015). However, it remains unclear how stress induction leads to changes in resting-state FC (rs-FC) profiles and how those changes may be linked to central stress-response systems, the major of which is the hypothalamic pituitary adrenal (HPA) axis.

Stress-related disorders like post-traumatic stress disorder (PTSD) have been suggested to be characterized by abnormal organization and functioning of three major large-scale brain networks, namely the salience network (SN), central executive network (CEN) and default model network (DMN; Menon, 2011). The interpretability of these findings however, hinges on whether they can be linked to quantitative biological markers of acute stress states such as the HPA-axis activity and its end product cortisol, which have extensively been linked to stress adaptation (De Kloet, Joëls, & Holsboer, 2005; McEwen, 1998). To understand the functional implications of neural network shifts in relation to stress adaptation, a number of recent investigations directly manipulated acute stress states and found that exposure to stress-induction helps reveal the fundamental neural origins of individual stress responsiveness (Cousijn et al., 2010; Henckens, van Wingen, Joëls, & Fernández, 2012; van Oort et al., 2017). At the network level, a small number of promising studies have revealed a stress-induced re-allocation of neural resources entailing increases in SN connectivity at the cost of decreases in CEN connectivity (Hermans et al. 2011; Hermans et al. 2014). This dynamic re-prioritization can generally be beneficial as it allows for adaptive responses to changing environmental conditions.

Importantly, these large-scale network shifts after stress induction have mainly been identified under task conditions so far (Hermans et al., 2014; Hermans et al., 2011; McMenamin et al., 2015; Young et al., 2016). Due to the dominant roles of the SN and CEN to meet ongoing task-demands (Dosenbach et al., 2007; Seeley et al., 2007), this potentially biases the observed network shifts towards states involving SN and CEN functioning, and reduces variations in internally-driven neural fluctuations (i.e., resting-state DMN). It therefore remains unclear whether stress induction could result in similar network shifts when external task demands are absent, as in a resting-state. So far, there has been very little investigation of system-level resting-state network connectivity changes after stress induction.

While limited evidence from studies using a seed-based approach suggest a general increase in the SN connectivity and mixed patterns in different DMN regions after stress induction (see review by van Oort et al. 2017), observations from clinical populations with stress-related disorders indicate the involvement of increased SN and reduced DMN connectivity in psychopathology (Admon, Milad, & Hendler, 2013; Koch et al., 2016). Accordingly, we predicted that with our network approach, we would observe similar increases in the SN connectivity and decreases in the DMN connectivity after stress induction while no changes in CEN connectivity were expected.

Most critically, despite the well-known variation in individual stress-responses, it remains unclear whether those network shifts are associated with individual stress response sensitivity, in part because most of those studies were not adequately powered to detect individual differences (van Oort et al., 2017). Until now, limited evidence has suggested that stress-induced FC increases in the SN under task conditions might be linked to individual variances in cortisol, α-amylase and subjective stress responses (Hermans et al. 2011), as well as to instant heart-rate changes (Young et al., 2016). This leaves the question open whether these observations are linked to specific task conditions or represent a shift in default functioning of these neural networks. In the current study, we aimed to test the hypothesis that acute stress-induced rs-FC changes in large-scale networks would occur as a function of individual differences in the cortisol stress-responses. Specifically, we expected stronger cortisol increases to be associated with increased SN and decreased DMN connectivity.

We tested our hypothesis in a well-powered sample of healthy individuals (N=335), who underwent a formal stress induction, preceded and followed by rs-fMRI scans (i.e. without external stimuli input). In specific, we investigated stress-induced network connectivity changes within the SN, CEN and DMN (i.e. local connectivity changes), as well as their synchronization with other brain regions (i.e., global connectivity changes; Cole, Yarkoni, Repovs, Anticevic, & Braver, 2012; Cole, Anticevic, Repovs, & Barch, 2011; Gonzalez-Castillo et al., 2015). By assessing both local and global connectivity changes, the current study aimed to capture a wider picture of the connectivity patterns following stress induction, not only specifically within the restricted areas (i.e., within each network) but also in the areas extending beyond our network definition. Further, to understand functional implications of these network reorganizations, we tested if these connectivity changes would occur as a function of the individual cortisol-stress reactivity.

Materials and Methods

Participants

A total of 372 participants completed the current study. An additional group of 23 participants were tested to generate independent resting-state network templates (see details below). Exclusion criteria included any current psychiatric or neurological disorder, history of, or current endocrine or neurological treatment, current use of psychotropic medication, and current drug or alcohol abuse (full details in Koch et al., 2017). After exclusion (see more details below), data from a total of 335 participants, including 276 police students who had recently started their education at the police academy, were analysed. Sixty-one out of a total of N=80 female participants in this sample reported hormonal contraceptive uses.

As part of a larger project consisting of multiple tests including approach-avoidance, reversal learning and emotional Go-NoGo tasks, the current study was implemented as the last experiment in the late afternoon (please refer to Koch et al., 2017 for a complete overview of the project) and was conducted in accordance with the principles of the Declaration of Helsinki and approved by the Independent Review Board Nijmegen (IRBN), the Netherlands. All participants gave their written informed consent before the study and all data were collected at the Donders Institute for Brain, Cognition and Behavior in Nijmegen, The Netherlands.

Experimental design and procedure

The experiment took place after 4PM, when cortisol levels are relatively stable because of the diurnal rhythm, so reliable individual stress-responses could be obtained (Miller et al., 2016). Two runs of fMRI scanning were implemented, one before and one after stress induction. This experiment was placed in the last imaging session of the experimental day, i.e. participants were already acquainted with the scanning procedure and thus not scanner naïve (full details of experiment protocols in Koch et al., 2017).

Stress responses were induced by sequential administration of a socially evaluated cold pressor task (SECPT) and a mental arithmetic (MA) task, a procedure that has been shown to successfully induce psychophysiological and subjective stress responses (Luo et al., 2018; Schwabe, Haddad, & Schachinger, 2008). Following a similar procedure as in previous studies (Luo et al., 2018; Vogel et al., 2015), participants were instructed to immerse their right foot in icy-cold (0-3°C) water for three minutes. Immediately after SECPT, a 3-minute MA task was administered. Participants were instructed to count back out loud from 2053 in steps of 17 as quickly and accurately as possible. The full stress-induction procedure lasted approximately 8 minutes, including instructions (full details in Supplemental

Methods and Materials).

Data acquisition and analysis

fMRI data acquisition

Each fMRI run involved one 6-minute long resting-state fMRI scan (RS1 and RS2) and one 2-minute long field-mapping scan (not used for the current analyses), leading to a total of 8 min per fMRI run. Participants were instructed to lie still and to stare at a small white cross at the screen center during both scanning runs, which has been suggested to increase the reliability of within-network connectivity (Birn et al., 2013). All images were collected using a 3T Siemens Magnetom Prisma^{fit} MRI scanner (Erlangen, Germany) with a 32-channel head coil. T2*-weighted EPI BOLD-fMRI images were acquired for the resting-state scans, using a multi-band 8 protocol with an interleaved slice acquisition sequence *(slice number=64, TR=735ms, TE=39ms, flip angle=52°, voxel size=2.4×2.4×2.4mm^3, slice gap=0mm, FOV=210mm)* that was optimized from the standard recommended scanning protocol of the Human Connectome Project (http://protocols.humanconnectome.org/HCP/3T/imaging-protocols.html). High-resolution structural images (1×1×1mm^3) were also acquired, using a T1-weighted MP-RAGE sequence *(TR=2300ms, TE=3.03ms, flip angle=8°, FOV=256×256×192mm^3)*.

Stress measurement collection

In total, five salivary samples were taken using Salivettes® collection tubes (Sarstedt, Germany) at -10, 0, +10, +20, and +30 minutes with respect to the onset time of stress induction (*Figure 1*). In a group of 61 participants, the last sample (i.e., at +30 min) has not been obtained, resulting in a sample of N=311 participants with complete measurements.

Together with saliva sampling, self-reported ratings of positive and negative affect (PANAS; Watson et al., 1988) were collected. Subjective ratings on negative affect were based on the sum of the scores of the 10 negative affect items for each participant. Each rating took place on a 5-point likert scale, with the sum score consequently ranging between 10 and 50. The same subsample as mentioned above (N=311) was measured with complete measurements at all five time points (see *Figure 1*).

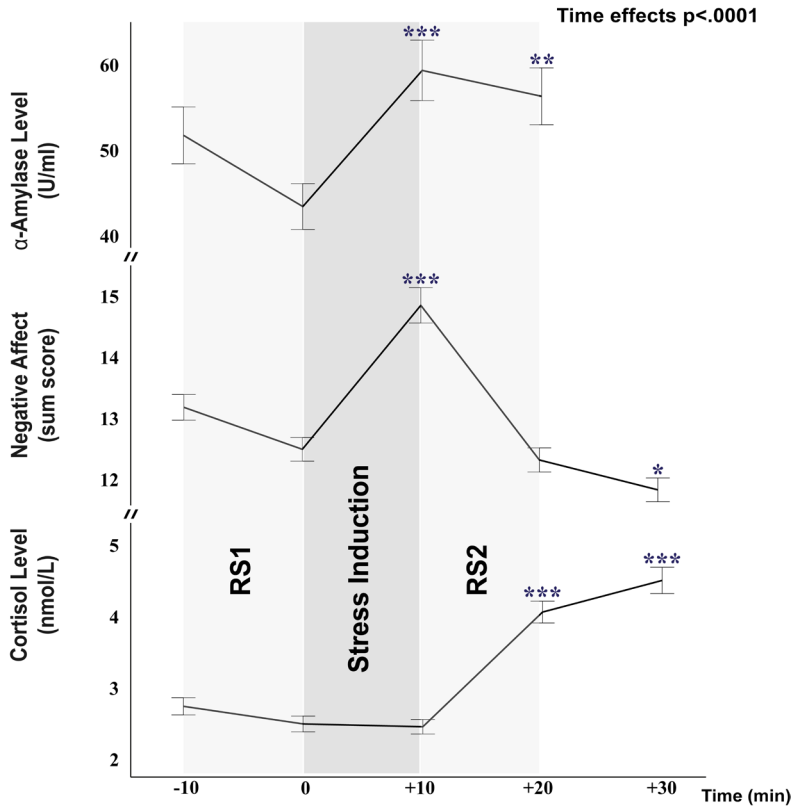

***Figure 1**. Stress measures.*
*Stress induction took place in between two runs of rs-fMRI scans (RS1 & RS2). Salivary samples and subjective affect reports were collected in a total of five times (i.e., -10m to +30m), with time interval between each sample being approximately 10 minutes. Increases in cortisol were observed 20 and 30 minutes after the onset of stress induction while increases in α-amylase and ratings of negative affect were observed immediately after stress induction (i.e., at time +10m), in comparison to baseline measurement at time 0. Of note, the last sample of α-amylase (i.e., at +30 min) was removed from the analysis due to large increases resulting from physical movement of the participants exiting the scanner room. Asterisks indicated statistically significant differences relative to time 0 immediately preceding stress induction (***p<.0001, **p<.001, *p<.05).*

Analyses on stress measures

Statistical analyses on stress measures were carried out separately on the sample of participants with complete data for all individual stress measurements (N=311), and on the full sample (N=372). Only the results from the sample with complete data are reported below. Results from the full sample were highly similar and can be found in Supplemental Results.

Main effects of sampling time (subsequent time points) on salivary cortisol, α-amylase levels and negative affect sum-scores were tested to index acute stress effects, using a linear mixed model with a random intercept for each individual. As

salivary cortisol has been shown to be a robust and reliable measure, frequently used as a biomarker of stress responses (Bozovic, Racic, & Ivkovic, 2013; Hellhammer, Wüst, & Kudielka, 2009), cortisol level increases (the difference between time 20 min and baseline 0 min) were used to investigate the association with imaging measures. To evaluate the typical gender effect on cortisol (Kudielka & Kirschbaum, 2005; Reschke-Hernández, Okerstrom, Bowles Edwards, & Tranel, 2017), as well as potential group effects (i.e., police students vs. remaining participants) in our sample, cortisol increases were compared between those groups. In short, while we observed typical gender (but not group) effects on cortisol responses (males > females), the main resulting associations between cortisol and neural responses were found to hold when taking into account gender. Full details of these supplementary analyses can be found in Supplemental Methods and Materials.

fMRI preprocessing and analysis
Preprocessing

Imaging data from 10% (N=37) of the total participants were excluded from analysis due to technical issues (N=4), motion (based on the mean value of the relative displacement; top 5% participants from each rs-fMRI scan leading to a total of 8.5%, with N=32 from the entire sample; Pruim et al., 2015) and incidental neurological findings (N=1), which resulted in a sample of 335 participants, including 276 police students.

To allow for $T2^*$ equilibration effects, the first five images of each resting-state scan were discarded. Analysis of fMRI data was performed with FSL5.0.9 (FMRIB, Oxford, UK). Preprocessing included motion correction by aligning all images to the first scan using rigid body transformations, spatial smoothing with a 5mm FWHM kernel, denoising using ICA-AROMA (Pruim et al., 2015), and high-pass filtering with a cut-off of 100 seconds. The preprocessed images were then fed into a general linear model to regress out nuisance effects. Specifically, twenty-four head motion parameters (i.e., the six realignment parameters, their temporal derivatives and the quadratic terms of both the original parameters and derivatives; Caballero-Gaudes et al., 2017; Friston et al., 1996; Zu Eulenburg et al., 2012) were included in the model to minimize the motion artefacts. Additionally, each individual T1 image was segmented for subject-specific white matter and CSF masks that were subsequently thresholded with a 95% probability and registered with functional image. Mean signal intensities of white matter and CSF were extracted and included in the GLM (Caballero-Gaudes & Reynolds, 2017; Satterthwaite et al., 2013).

The residual images from this linear model were normalized to the Montreal Neurological Institute template (MNI152), using linear and nonlinear transformations via boundary based registration (BBR; Greve et al., 2009), FLIRT (Greve & Fischl, 2009; Jenkinson, Bannister, Brady, & Smith, 2002; Jenkinson & Smith, 2001) and

FNIRT (Andersson, Jenkinson, & Smith, 2007). Consequently, each participant had two normalized residual images (i.e., cleaned rs-fMRI data) that index BOLD signal fluctuations, before and after acute stress induction, respectively.

Identifying delta-FC of RSNs

Group-level network templates based on data of 23 independently tested non-stressed participants were produced, using group independent component analysis (ICA) as implemented in MELODIC (Beckmann & Smith, 2005). ICA components showing the highest cross-correlation of mean time-series with pre-selected functional ROIs (i.e., anterior SN, left CEN, right CEN and ventral DMN) from the Stanford FIND atlas (Shirer, Ryali, Rykhlevskaia, Menon, & Greicius, 2012) were identified as RSNs of interest. This approach allowed us to select RSNs of interest that were not biased towards the data either before or after stress induction. Importantly, the final selected RSN templates involves all major nodes/areas that are typically considered as hub regions in those networks (*Figure S1*). For example, the selected SN included the bilateral anterior insula, dorsal ACC and amygdala; the CEN included dorsolateral prefrontal cortex and posterior parietal cortex while the DMN included ventromedial prefrontal cortex, parahippocampal gyrus, posterior cingulate cortex and precuneus. Connectivity changes after stress induction (i.e., delta-FC) were defined as the differences in each network of interest before and after stress induction. All individual increased (after>before) and decreased (before>after) delta-FC images were then tested at the group-level, using permutation tests via Randomise (Winkler, Ridgway, Webster, Smith, & Nichols, 2014), to examine significant delta-FC after stress induction for each network at both local (i.e., within network) and more global (i.e., synchronization with regions both within and outside our network definitions) levels.

The results from these initial exploratory tests were considered significant using a family-wise-error (FWE) corrected p-value of 0.00625, derived from a threshold-free cluster enhancement approach (Smith & Nichols, 2009) that accounts for the number of individual networks (i.e., SN, LCEN, RCEN, DMN), as well as the number of connectivity change directions (i.e., increases and decreases) involved in the comparisons.

Linking delta-FC of RSNs to stress responses

Although the lack of a non-stressful control group of adequate size precluded a direct group comparison for testing the specificity of the observed stress effects in the initial group analysis, the large sample size (N=335) of the current study allowed us to verify that the observed connectivity changes in large-scale networks indeed covaried with individual responsiveness of the HPA axis, and therefore linked to changes in the stress response. To this end, increased cortisol level was added as a

covariate in the permutation tests to link the connectivity changes to acute stress-responses. To examine significant stress-related changes within each network (i.e., local delta-FC), we used our group ICA templates (see above) as the masks for small volume correction (SVC) to directly test our a priori hypotheses. As we had no hypothesis to test the CEN unilaterally, individual delta-FC of the left and right CEN for each participant were combined for these, and all following hypothesis-testing analyses. Results from group permutation tests with cortisol increase as covariates were considered significant with a FWE corrected p-value of 0.0167 that takes into account the number of hypothesis tests for three networks (i.e., SN, CEN and DMN), using Bonferroni correction.

In addition to the standard univariate voxel-wise approach described above, we also investigated individual differences at the network level. To this end, mean coefficients of delta-FC were extracted from the clusters that showed significant connectivity changes after stress induction (*Figure S2*). These coefficients indicated the strength of delta-FC between each RSN and all brain regions that showed changes in connectivity after stress induction (i.e., widespread changes referred as global synchronization including both changes with brain regions within- and outside the network), and were correlated with cortisol increase across participants. To test whether any association between delta-FC coefficients and cortisol increases existed specifically within each network (i.e., local changes), mean coefficients of individual delta-FC maps were extracted with masks of our group ICA templates. We firstly tested statistical significance of mean coefficients, using one-sample t-test (see results in the Supplemental Methods and Materials). Subsequently, Spearman rank correlation analyses were used to test above associations, which minimize the potential influences from extreme values in the variables. Results were considered significant with an adjusted p-value of $p<.0167$ to account for the number of analyses that were carried out to test our a priori hypotheses on three RSNs. Bootstrapped confidence intervals (boot.CI) were calculated for these rank correlation analyses, using the adjusted bootstrap percentile (BCa) method with n=1000 iterations.

Results

Stress measures

Stress-induction was successful as was indicated by significant increases in all stress measures. Specifically, main effects of sampling time were observed for salivary cortisol ($F(4,1182.08)=145.76$, $p<.0001$), α-amylase ($F(3,830.97)=9.78$, $p<.0001$) and negative affect ratings ($F(4,1230.01)=99.24$, $p<.0001$; *Figure 1*).

In line with the delayed cortisol stress responses (Schwabe et al., 2008; Kirschbaum et al., 1994), cortisol levels significantly increased at +20 and +30 minutes after the onset of stress induction compared to pre-stress baseline (i.e., at time 0 min;

all p's <.0001), while no significant difference was observed between +20 and +30 minutes (t(1181.93)=-2.64, p=.06; *Figure 1*). As expected, α-amylase and subjective stress levels peaked immediately after stress induction (i.e., at time +10 min; $t_{\alpha\text{-amylase}}(829.36)=-4.68$, p<.0001; $t_{affect}(1229.13)=-14.18$, p<.0001). While α-amylase level remained high (i.e., at time +20 min; t(831.08)=-4.03, p<.001), subjective scores of negative affect quickly declined again (i.e., at time +20 min; t(1229.13)=1.27, p=.71) and eventually ended below the pre-stress baseline (i.e., time 0; t(1229.44)=3.74, p<.005).

Cortisol-related FC changes of RSNs

Following acute stress induction, whole-brain analyses revealed both increased and decreased connectivity patterns for all four RSNs with wide-spread regions (*Supplemental Results; Figure S2; Table S1*). To investigate the functional implications of these connectivity changes, we linked the observed delta-FC to the stress response marker cortisol. Our voxel-wise analyses identified an increased overall connectivity of the SN with a cluster in the right dACC predictive of individual cortisol increase (Bonferroni correction adjusted p_{FWE}<.0167; *Figure 2*). Additional control tests further confirmed that this effect was not associated with head motion change, defined as the difference in the mean value of relative frame-wise displacement between RS1 and RS2. (Rs=-.07, p=.22). No other networks showed connectivity increases or decreases related to the cortisol stress response in the voxel-wise analysis.

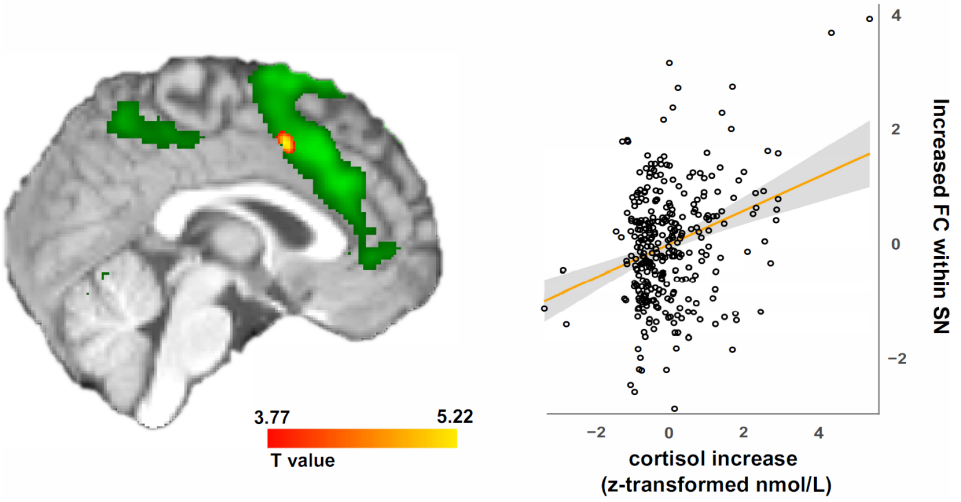

***Figure 2**. Increased overall SN connectivity with dorsal ACC (red-yellow, a core SN subregion) was associated with cortisol increase in response to acute stress induction. Results shown on the left panel are whole brain corrected without additional correction for the number of networks for visualization purpose (P_{fwe}<.05) and imposed on our ICA-derived SN template that was used to restrict the search space (green; z>3). Results illustrated on the right panel are individual cortisol increase against mean coefficients extracted from individual increased SN, using the cluster showing significant increases as the mask (Bonferroni adjusted P_{fwe}<.0167). Follow-up tests confirmed that this effect was not driven by extreme values: the association remained significant also when the data of N=3 participants with relatively extreme values (i.e., >3std from the mean) were removed (Rs=.16, p<.005).*

Thereafter, we calculated the average connectivity changes across all regions showing significant increase or decrease, separately, for each of three resting-state networks and correlated them with individual cortisol increases. At this more global level, reductions in DMN connectivity with the regions also outside the network was significantly correlated with cortisol responses (Rs=-.16, Bonferroni correction adjusted p<.0167, boot.CI=(0.050, 0.266); *Figure 3A*). Further investigation revealed a trend of correlation between this globally decreased DMN connectivity and the head motion changes (Rs=.10, p=.06). However, results from a multiple regression model confirmed the association between DMN connectivity decrease and cortisol increase when effects of head motion were controlled (t(315)=2.58, p<.05).

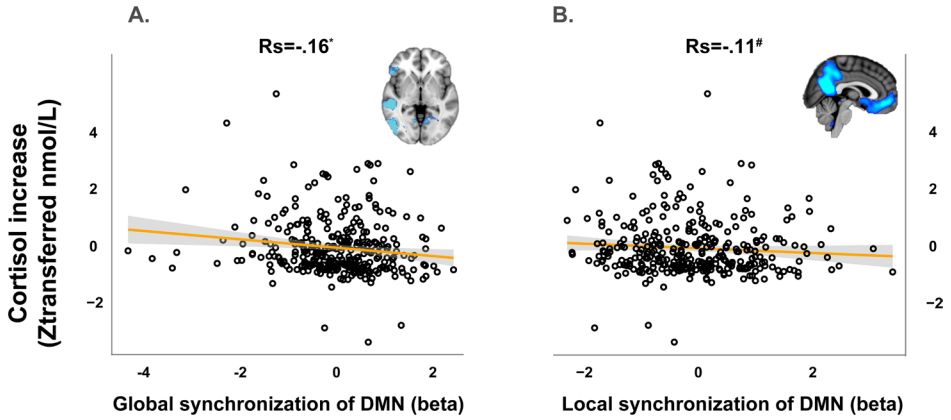

Figure 3. *Stress-induced cortisol increases are correlated with reduced synchronization at a more global level between DMN and brain regions also outside of the network, such as frontal gyrus and temporal gyrus[a] (A) and at a local level within the DMN (B). Stress-induced connectivity changes are indexed by mean coefficients at the x-axis, extracted from each participant using a connectivity map that contains all brain regions showing a significantly reduced synchronization with DMN (A), and using the ICA-derived DMN group template (B), respectively. Brain images depicted the masks that were used to extract aforementioned coefficients.*

 # p<.05

** p<.0167 (Bonferroni corrected)*

[a] full list can be found in Supplementary Table S1

Concerning the connectivity changes within networks as a function of individual differences in cortisol responses, we found an association between the decreased delta-FC within the DMN and larger cortisol increases (FIND atlas vDMN mask, Rs=-.16, Bonferroni correction adjusted p<.0167, boot.CI=(-.27, -.05); ICA-derived DMN group template, Rs=-.11, p=.047, boot.CI=(-.22, -.0007); *Figure 3B*). None of those RSN changes showed correlations with the head motion changes (p's>.11) and none of the other RSNs showed such a linkage with cortisol increase (p's>.05).

Discussion

The current study investigated rapid, stress-induced connectivity-changes *within* major resting-state networks (SN, CEN, DMN), as well as *between* these networks and other brain regions as a function of individual stress-response magnitude, measured by the stress-hormone cortisol. Specifically, cortisol stress response levels were associated with increased connectivity within SN, the network that is critical for detecting behaviorally relevant stimuli and for coordinating neural resources in response to these stimuli. Interestingly, the results also show that the reduction in local (i.e., within network) and global synchronization of DMN, known for its involvement in internal processing and homeostasis, was linked to individual differences in stress-induced cortisol levels. These findings match with the idea of a stress-induced network reorganization and suggest that increased SN and decreased DMN connectivity may function as relevant neural indicators for stress responsiveness.

In line with previous findings, we observed connectivity changes of large-scale networks following stress induction (*Figure S2; Table S1*). Given our interest in RSN connectivity changes in relation to the individual stress-responses, we specifically linked the observed delta-FC to cortisol increase at the individual level. Concerning within-network delta-FC (i.e., local changes), our voxel-wise results demonstrate that cortisol-stress responses were associated with connectivity increases within the SN even when there is limited external input (i.e. during a resting-state scan). This extends previous observations of increased SN connectivity in response to acute stress induction during task-positive conditions (Hermans et al., 2011; Young et al., 2016; van Oort et al., 2017). Specifically, we identified increased connectivity between the SN as a whole and its subregion, the dACC in participants with high cortisol stress responses. As a crucial node of the SN, the dACC has been implicated in diverse functions at the intersection of cognition and emotion including interoceptive-autonomic processing (Craig, 2002; Critchley, Wiens, Rotshtein, Öhman, & Dolan, 2004), pain and negative affect processing (Rotge et al., 2015) and integrating information relevant for cognitive control (Shenhav, Botvinick, & Cohen, 2013), suggesting potential involvement of this region in responding to challenging conditions and the appraisal and expression of anxiety (Etkin, Egner, & Kalisch, 2011). Abnormalities in dACC and more generally in SN connectivity have been implicated as the neurobiological correlate of enhanced salience or threat processing, a major characteristic of stress-related psychiatric disorders (Etkin & Wager, 2007; Koch et al., 2016; Vaisvaser et al., 2013).

With respect to changes in global synchronization, we found that higher cortisol increases after stress induction were associated with larger reductions in global synchronization of DMN (i.e., reductions in the interaction between the whole DMN and widespread brain regions also outside the DMN, as listed in Table S1 “decreased

FC with DMN"). Interestingly, a similar association was also identified for the overall connectivity decrease within the DMN, indicated by the reduced mean coefficient of delta-FC from the FIND atlas-defined network core regions. These results suggests the involvement of the DMN in the processing of acute stress induction without ongoing task demands that was not captured in the previous investigations (Young et al., 2016; Hermans et al., 2011). The DMN has largely been linked to self-referential processes (Andrews-Hanna, Reidler, Sepulcre, Poulin, & Buckner, 2010; Buckner, Andrews-Hanna, & Schacter, 2008). Alterations in the DMN connectivity have consistently been implicated in various psychiatric disorders and particularly in stress-related disorders. For example, reduced baseline DMN connectivity has been linked to PTSD patients, while insufficient suppression of DMN has been implicated in remitted major depression (Admon et al., 2013; Bartova et al., 2015; Koch et al., 2016).

With enhanced SN connectivity on the one hand, yet reduced DMN connectivity on the other, our findings are generally in line with previous investigations that demonstrated a stress-induced network shift towards the SN (Hermans et al., 2011; Hermans et al., 2014). In the current study, however, such a reallocation of neural resources appears to occur between the SN and DMN rather than CEN, when no external stimuli (i.e., ongoing stressors) are present. Our findings of an opposite impact of stress on connectivity of the DMN and SN appear compatible with theories of a neural resource reassignment from the DMN to the SN in the interest of processing more relevant information under a stressful state (Maron-Katz, Vaisvaser, Lin, Hendler, & Shamir, 2016; Quaedflieg et al., 2015; Vaisvaser et al., 2013, 2016). Nevertheless, the current study extends the literature by showing SN and DMN fluctuations in the absence of external task demands that might be dependent on the magnitude of the individual cortisol stress responses. Similar alterations in the SN and DMN connectivity have been implicated in a wide range of psychiatric disorders and particularly in stress-related disorders (Admon et al., 2013; Bartova et al., 2015; Etkin & Wager, 2007; Koch et al., 2016; Sripada et al., 2012; Vaisvaser et al., 2013). On the other hand, however, studies in animals as well as in human suggest that the HPA-axis is highly relevant for fast adaptation to stressful situations (De Kloet et al., 2005; Joëls & Baram, 2009). It will be of interest for future investigations to examine longitudinally whether the increased SN connectivity and decreased DMN connectivity indicate individual adaptation or vulnerability to acute stress induction, and whether those stress-induced neural network responses can predict the development of psychopathology after trauma exposure.

Several limitations of the present study should be mentioned. Firstly, although we recruited an independent group to derive the group network templates for imaging analysis in a non-biased fashion, it was of an insufficient sample size (N=23) to serve as a direct control group for validating stress-induced neural effects observed in a sample of N=335. It is possible that the lack of such a control group could potentially

confound the observed stress effects at neural level with scanning order. However, this concern is mitigated by the fact that our participants were not scanner-naïve (i.e., had previously been tested in the same scanner twice on the same testing day) and showed no cortisol increases before the RS1 and stress induction. Most importantly, within our experimental group, we confirmed that both enhanced SN connectivity and reduced DMN connectivity correlated significantly with individual cortisol responsiveness. These results together strongly suggest that the observed neural effects are stress related. Secondly, the current acquisition length of 6.5 minutes is shorter than the recommended acquisition length (i.e., 9-12 min) of resting-state imaging data (Birn et al., 2013). However, together with our large sample size, the fast multi-band imaging protocol (TR=735ms) enabled us to obtain a relatively large number of scans (N=500) in each session, which increases the reliability of our results. Thirdly, the effect size of the observed correlations could be arguably considered small by traditional standards (i.e., coefficient between 0.1-0.15). Recent meta-analyses however show that traditional guidelines for interpreting correlation coefficients may have been too stringent (Gignac & Szodorai, 2016; Hemphill, 2003) because observed correlations are practically dampened by the imperfect measurement reliability of two variables in the correlation almost in any studies (Hedge, Powell, & Sumner, 2017; Vul, Harris, Winkielman, & Pashler, 2009). In the current study, it is very well conceivable that factors beyond our experimental control (e.g. sleep quality before the experiment day) might have influenced both the cortisol and neural responses, and thus diluted correlation effect sizes. Furthermore, evidence from simulations show that increasing sample size is generally associated with decreasing correlation coefficients and that a large sample size (e.g., N>250) entails more stable effect size (Schönbrodt & Perugini, 2013). The small effect size of the correlations resulting from our large sample size therefore likely reflected a meaningful and robust underlying association between neural network processing and stress responses. Fourthly, it could be considered as a limitation that physiological recordings (e.g., respiration) were not included to further clean up the imaging data. However, acute stress induction has been shown to influence physiological responses. Regressing out physiological parameters further will enhance the risk of only investigating the neural processes that are independent of stress-induced sympathetic and parasympathetic activities (Murphy, Birn, & Bandettini, 2013). To control for potential non-neural physiology, we followed the common practice in the literature to removing the mean intensity of the WM and CSF from the imaging data (Henckens et al., 2012; Hermans et al., 2011; Maron-Katz et al., 2016; Vaisvaser et al., 2013, 2016). More importantly, we went above and beyond this common practice by acquiring imaging data with a fast sampling sequence (i.e., multiband 8), which in combination of ICA has been shown to facilitate the identification and elimination of physiological components (Boubela, Kalcher, Nasel, & Moser, 2014; Parkes, Fulcher, Yücel, & Fornito, 2018; Pruim et al., 2015). Finally, it is worth mentioning that our current resting-state connectivity measurement in the immediate aftermath of a stressor likely contains

a mixture of both acute stress reactions and stress recovery processes. For future studies, including scans during stress recovery (i.e. after acute stress subsides) would be of interest in order to more systematically study the temporal dynamics of the stress-induced network changes observed here (Hermans et al., 2014; Vaisvaser et al., 2013).

In conclusion, our results demonstrate distributed connectivity changes in large-scale RSNs after stress induction. More importantly, the strengthened coupling within the SN, as well as the degree of decoupling within the DMN, and between the DMN and other brain regions, was associated with individual cortisol stress-responsiveness. These results suggest that acute stress induction alters default brain processing and that such an alteration might potentially function as a neural mechanism determining individual stress reactivity.

References

Admon, R., Milad, M. R., & Hendler, T. (2013). A causal model of post-traumatic stress disorder: Disentangling predisposed from acquired neural abnormalities. *Trends in Cognitive Sciences*, *17*(7), 337–347.

Andersson, J. L. R., Jenkinson, M., & Smith, S. (2007). *Non-linear registration, aka spatial normalisation. FMRIB Technial Report TR07JA2. Oxford Centre for Functional Magnetic Resonance Imaging of the Brain, Department of Clinical Neurology, Oxford University, Oxford, UK*.

Andrews-Hanna, J. R., Reidler, J. S., Sepulcre, J., Poulin, R., & Buckner, R. L. (2010). Functional-Anatomic Fractionation of the Brain's Default Network. *Neuron*, *65*(4), 550–562.

Bartova, L., Meyer, B. M., Diers, K., Rabl, U., Scharinger, C., Popovic, A., … Pezawas, L. (2015). Reduced default mode network suppression during a working memory task in remitted major depression. *Journal of Psychiatric Research*, *64*, 9–18.

Beckmann, C. F., & Smith, S. M. (2005). Tensorial extensions of independent component analysis for multisubject FMRI analysis. *NeuroImage*, *25*(1), 294–311.

Birn, R. M., Molloy, E. K., Patriat, R., Parker, T., Meier, T. B., Kirk, G. R., … Prabhakaran, V. (2013). The effect of scan length on the reliability of resting-state fMRI connectivity estimates. *NeuroImage*, *83*, 550–558.

Boubela, R. N., Kalcher, K., Nasel, C., & Moser, E. (2014). Scanning fast and slow: current limitations of 3 Tesla functional MRI and future potential. *Frontiers in Physics*, *2*.

Bozovic, D., Racic, M., & Ivkovic, N. (2013). Salivary Cortisol Levels as a Biological Marker of Stress Reaction. *Medical Archives*, *67*, 374.

Buckner, R. L., Andrews-Hanna, J. R., & Schacter, D. L. (2008). The brain's default network: Anatomy, function, and relevance to disease. *Annals of the New York Academy of Sciences*.

Caballero-Gaudes, C., & Reynolds, R. C. (2017). Methods for cleaning the BOLD fMRI signal. *NeuroImage*, *154*, 128–149.

Cole, M. W., Anticevic, A., Repovs, G., & Barch, D. (2011). Variable global dysconnectivity and individual differences in schizophrenia. *Biological Psychiatry*, *70*(1), 43–50.

Cole, M. W., Yarkoni, T., Repovs, G., Anticevic, A., & Braver, T. S. (2012). Global Connectivity of Prefrontal Cortex Predicts Cognitive Control and Intelligence. *Journal of Neuroscience*, *32*(26), 8988–8999.

Cousijn, H., Rijpkema, M., Qin, S., van Marle, H. J. F., Franke, B., Hermans, E. J., … Fernandez, G. (2010). Acute stress modulates genotype effects on amygdala processing in humans. *Proceedings of the National Academy of Sciences*, *107*(21), 9867–9872.

Craig, a. D. (2002). How do you feel? Interoception: the sense of the physiological condition of the body. *Nature Reviews Neuroscience*, *3*(8), 655–666.

Critchley, H. D., Wiens, S., Rotshtein, P., Öhman, A., & Dolan, R. J. (2004). Neural systems supporting interoceptive awareness. *Nature Neuroscience*, *7*(2), 189–195.

De Kloet, E. R., Joëls, M., & Holsboer, F. (2005). Stress and the brain: From adaptation to disease. *Nature Reviews Neuroscience*.

Dosenbach, N. U. F., Fair, D. A., Miezin, F. M., Cohen, A. L., Wenger, K. K., Dosenbach, R. A. T., … Petersen, S. E. (2007). Distinct brain networks for adaptive and stable task control in humans. *Proceedings of the National Academy of Sciences*, *104*(26), 11073–11078.

Etkin, A., Egner, T., & Kalisch, R. (2011). Emotional processing in anterior cingulate and medial prefrontal cortex. *Trends in Cognitive Sciences*.

Etkin, A., & Wager, T. D. (2007). Functional neuroimaging of anxiety: a meta-analysis of emotional processing in PTSD, social anxiety disorder, and specific phobia. *The American Journal of Psychiatry*, *164*(10), 1476–1488.

Finn, E. S., Scheinost, D., Finn, D. M., Shen, X., Papademetris, X., & Constable, R. T. (2017). Can brain state be manipulated to emphasize individual differences in functional connectivity? *NeuroImage*.

Friston, K. J., Williams, S., Howard, R., Frackowiak, R. S. J., & Turner, R. (1996). Movement-Related effects in fMRI time-series. *Magnetic Resonance in Medicine*, *35*(3), 346–355.

Gignac, G. E., & Szodorai, E. T. (2016). Effect size guidelines for individual differences researchers. *Personality and Individual Differences*, *102*, 74–78.

Gonzalez-Castillo, J., Hoy, C. W., Handwerker, D. A., Robinson, M. E., Buchanan, L. C., Saad, Z. S., & Bandettini, P. A. (2015). Tracking ongoing cognition in individuals using brief, whole-brain functional connectivity patterns. *Proceedings of the National Academy of Sciences*, *112*(28), 8762–8767.

Greve, D. N., & Fischl, B. (2009). Accurate and robust brain image alignment using boundary-based registration. *NeuroImage*, *48*(1), 63–72.

Hedge, C., Powell, G., & Sumner, P. (2017). The reliability paradox: Why robust cognitive tasks do not produce reliable individual differences. *Behavior Research Methods*, 1–21.

Hellhammer, D. H., Wüst, S., & Kudielka, B. M. (2009). Salivary cortisol as a biomarker in stress research. *Psychoneuroendocrinology*, *34*(2), 163–171.

Hemphill, J. F. (2003). Interpreting the Magnitudes of Correlation Coefficients. *American Psychologist*.

Henckens, M. J. a G., van Wingen, G. a, Joëls, M., & Fernández, G. (2012). Corticosteroid induced decoupling of the amygdala in men. *Cerebral Cortex (New York, N.Y. : 1991)*, *22*(10), 2336–2345.

Hermans, E. J., Henckens, M. J. A. G., Joëls, M., & Fernández, G. (2014). Dynamic adaptation of large-scale brain networks in response to acute stressors. *Trends in Neurosciences*, *37*(6), 304–314.

Hermans, E. J., van Marle, H. J. F., Ossewaarde, L., Henckens, M. J. a. G., Qin, S., van Kesteren, M. T. R., … Fernandez, G. (2011). Stress-Related Noradrenergic Activity Prompts Large-Scale Neural Network Reconfiguration. *Science*, *334*(6059), 1151–1153.

Jenkinson, M., Bannister, P., Brady, M., & Smith, S. (2002). Improved optimization for the robust and accurate linear registration and motion correction of brain images. *NeuroImage*, *17*(2), 825–841.

Jenkinson, M., & Smith, S. (2001). A global optimisation method for robust affine registration of brain images. *Medical Image Analysis*, *5*(2), 143–156.

Joëls, M., & Baram, T. Z. (2009). The neuro-symphony of stress. *Nature Reviews. Neuroscience*, *10*(6), 459–466.

Kirschbaum, C., & Hellhammer, D. H. (1994). Salivary cortisol in psychoneuroendocrine research: recent developments and applications. *Psychoneuroendocrinology*, *19*(4), 313–333.

Koch, S. B. J., Klumpers, F., Zhang, W., Hashemi, M. M., Kaldewaij, R., van Ast, V. A., … Roelofs, K. (2017). The role of automatic defensive responses in the development of posttraumatic stress symptoms in police recruits: protocol of a prospective study. *European Journal of Psychotraumatology*, *8*(1), 1412226.

Koch, S. B. J., van Zuiden, M., Nawijn, L., Frijling, J. L., Veltman, D. J., & Olff, M. (2016). Aberrant resting-state brain activity in posttraumatic stress disorder: A meta-analysis

and systematic review. *Depression and Anxiety*, *33*(7), 592–605.

Kudielka, B., & Kirschbaum, C. (2005). Sex differences in HPA axis responses to stress: a review. *Biological Psychology*, *69*, 113–132.

Luo, Y., Fernández, G., Hermans, E., Vogel, S., Zhang, Y., Li, H., & Klumpers, F. (2018). How acute stress may enhance subsequent memory for threat stimuli outside the focus of attention: DLPFC-amygdala decoupling. *NeuroImage*.

Maron-Katz, A., Vaisvaser, S., Lin, T., Hendler, T., & Shamir, R. (2016). A large-scale perspective on stress-induced alterations in resting-state networks. *Scientific Reports*, *6*(February), 21503.

Marquand, A. F., Haak, K. V., & Beckmann, C. F. (2017). Functional corticostriatal connection topographies predict goal-directed behaviour in humans. *Nature Human Behaviour*, *1*(8).

McEwen, B. S. (1998). Stress, Adaptation, and Disease: Allostasis and Allostatic Load. *Annals of the New York Academy of Sciences*, *840*(1), 33–44.

McMenamin, B. W., & Pessoa, L. (2015). Discovering networks altered by potential threat ("anxiety") using quadratic discriminant analysis. *NeuroImage*, *116*, 1–9.

Menon, V. (2011). Large-scale brain networks and psychopathology: A unifying triple network model. *Trends in Cognitive Sciences*, *15*(10), 483–506.

Miller, R., Stalder, T., Jarczok, M., Almeida, D. M., Badrick, E., Bartels, M., … Kirschbaum, C. (2016). The CIRCORT database: Reference ranges and seasonal changes in diurnal salivary cortisol derived from a meta-dataset comprised of 15 field studies. *Psychoneuroendocrinology*, *73*(8), 16–23.

Murphy, K., Birn, R. M., & Bandettini, P. A. (2013). Resting-state fMRI confounds and cleanup. *NeuroImage*, *80*, 349–359.

Nicholson, A. A., Densmore, M., Frewen, P. A., Théberge, J., Neufeld, R. W. J., McKinnon, M. C., & Lanius, R. A. (2015). The Dissociative Subtype of Posttraumatic Stress Disorder: Unique Resting-State Functional Connectivity of Basolateral and Centromedial Amygdala Complexes. *Neuropsychopharmacology*, *40*(10), 2317–2326.

Oathes, D. J., Patenaude, B., Schatzberg, A. F., & Etkin, A. (2015). Neurobiological signatures of anxiety and depression in resting-state functional magnetic resonance imaging. *Biological Psychiatry*, *77*(4), 385–393.

Parkes, L., Fulcher, B., Yücel, M., & Fornito, A. (2018). NeuroImage An evaluation of the ef fi cacy , reliability , and sensitivity of motion correction strategies for resting-state functional MRI. *NeuroImage*, *171*(July 2017), 415–436.

Pruim, R. H. R., Mennes, M., van Rooij, D., Llera, A., Buitelaar, J. K., & Beckmann, C. F. (2015). ICA-AROMA: A robust ICA-based strategy for removing motion artifacts from fMRI data. *NeuroImage*, *112*, 267–277.

Quaedflieg, C. W. E. M., van de Ven, V., Meyer, T., Siep, N., Merckelbach, H., & Smeets, T. (2015). Temporal Dynamics of Stress-Induced Alternations of Intrinsic Amygdala Connectivity and Neuroendocrine Levels. *PLOS ONE*, *10*(5), e0124141.

Reschke-Hernández, A. E., Okerstrom, K. L., Bowles Edwards, A., & Tranel, D. (2017). Sex and stress: Men and women show different cortisol responses to psychological stress induced by the Trier social stress test and the Iowa singing social stress test. *Journal of Neuroscience Research*, *95*(1–2), 106–114.

Rotge, J. Y., Lemogne, C., Hinfray, S., Huguet, P., Grynszpan, O., Tartour, E., … Fossati, P. (2015). A meta-analysis of the anterior cingulate contribution to social pain. *Social Cognitive and Affective Neuroscience*, *10*(1), 19–27.

Satterthwaite, T. D., Elliott, M. A., Gerraty, R. T., Ruparel, K., Loughead, J., Calkins, M. E., … Wolf, D. H. (2013). An improved framework for confound regression and filtering for control of motion artifact in the preprocessing of resting-state functional connectivity data. *NeuroImage*, *64*(1), 240–256.

Schönbrodt, F. D., & Perugini, M. (2013). At what sample size do correlations stabilize? *Journal of Research in Personality*, *47*(5), 609–612.

Schwabe, L., Haddad, L., & Schachinger, H. (2008). HPA axis activation by a socially evaluated cold-pressor test. *Psychoneuroendocrinology*, *33*(6), 890–895.

Seeley, W. W., Menon, V., Schatzberg, A. F., Keller, J., Glover, G. H., Kenna, H., … Greicius, M. D. (2007). Dissociable Intrinsic Connectivity Networks for Salience Processing and Executive Control. *Journal of Neuroscience*, *27*(9), 2349–2356.

Shenhav, A., Botvinick, M. M., & Cohen, J. D. (2013). The expected value of control: An integrative theory of anterior cingulate cortex function. *Neuron*.

Shirer, W. R., Ryali, S., Rykhlevskaia, E., Menon, V., & Greicius, M. D. (2012). Decoding Subject-Driven Cognitive States with Whole-Brain Connectivity Patterns. *Cerebral Cortex*, *22*(1), 158–165.

Smith, S. M., & Nichols, T. E. (2009). Threshold-free cluster enhancement: Addressing problems of smoothing, threshold dependence and localisation in cluster inference. *NeuroImage*, *44*(1), 83–98.

Sripada, R. K., King, A. P., Welsh, R. C., Garfinkel, S. N., Wang, X., Sripada, C. S., & Liberzon, I. (2012). Neural dysregulation in posttraumatic stress disorder: evidence for disrupted equilibrium between salience and default mode brain networks. *Psychosomatic Medicine*, *74*(9), 904–911.

Vaisvaser, S., Lin, T., Admon, R., Podlipsky, I., Greenman, Y., Stern, N., … Hendler, T. (2013). Neural traces of stress: cortisol related sustained enhancement of amygdala-hippocampal functional connectivity. *Frontiers in Human Neuroscience*, *7*, 313.

Vaisvaser, S., Modai, S., Farberov, L., Lin, T., Sharon, H., Gilam, A., … Hendler, T. (2016). Neuro-epigenetic indications of acute stress response in humans: The case of microRNA-29c. *PLoS ONE*, *11*(1), 1–17.

van Marle, H. J. F., Hermans, E. J., Qin, S., & Fernández, G. (2010). Enhanced resting-state connectivity of amygdala in the immediate aftermath of acute psychological stress. *NeuroImage*, *53*(1), 348–354.

van Oort, J., Tendolkar, I., Hermans, E. J., Mulders, P. C., Beckmann, C. F., Schene, A. H., … van Eijndhoven, P. F. (2017). How the brain connects in response to acute stress: A review at the human brain systems level. *Neuroscience & Biobehavioral Reviews*, *83*(April), 281–297.

Vogel, S., Klumpers, F., Krugers, H. J., Fang, Z., Oplaat, K. T., Oitzl, M. S., … Fernández, G. (2015). Blocking the Mineralocorticoid Receptor in Humans Prevents the Stress-Induced Enhancement of Centromedial Amygdala Connectivity with the Dorsal Striatum. *Neuropsychopharmacology*, *40*(4), 947–956.

Vul, E., Harris, C., Winkielman, P., & Pashler, H. (2009). Puzzlingly High Correlations in fMRI Studies of Emotion, Personality, and Social Cognition1. *Perspectives on Psychological Science*, *4*(3), 274–290.

Watson, D., Clark, L. a., & Tellegan, a. (1988). Worksheet 3.1 The Positive and Negative Affect Schedule (PANAS; Watson et al., 1988) PANAS Questionnaire. *Journal of Personality and Social Psychology*, *54*, 1063–1070.

Winkler, A. M., Ridgway, G. R., Webster, M. A., Smith, S. M., & Nichols, T. E. (2014).

Permutation inference for the general linear model. *NeuroImage*, *92*, 381–397.
Young, C. B., Raz, G., Everaerd, D., Beckmann, C. F., Tendolkar, I., Hendler, T., … Hermans, E. J. (2016). Dynamic shifts in large-scale brain network balance as a function of arousal. *Journal of Neuroscience*.
Zu Eulenburg, P., Caspers, S., Roski, C., & Eickhoff, S. B. (2012). Meta-analytical definition and functional connectivity of the human vestibular cortex. *NeuroImage*, *60*(1), 162–169.

Supplemental Methods and Materials

Participants

After exclusion (see details in the main manuscript), data from a total of 335 participants, including 276 police students were analyzed. While the police students had a slightly higher mean age (M=24.22) than the remaining participants (M=23.05; t(106.8)=2.04, p<.05), gender ratio and education level were comparable (X^2_{gender}=.41, p=.52; X^2_{edu}=.98, p=.61).

Stress induction

Stress was induced by sequential administration of a socially evaluated cold pressor task (SECPT) and a mental arithmetic (MA) task. During stress induction, two experimenters were present. The primary experimenter was new to the participants (e.g., had no contact with the participants throughout the day) and wore a white lab coat. The assistant experimenter was familiar to the participant as he/she was hosting the participant for the whole afternoon. The gender of at least one of the experimenters was opposite to the gender of the participants to ensure maximal social stress (Allen, Kennedy, Cryan, Dinan, & Clarke, 2014; Duchesne, Tessera, Dedovic, Engert, & Pruessner, 2012). Data from an independent group of participants (N=23) that completed the same procedure with a non-stressful setup were also collected to generate unbiased resting-state network templates. Participants in this group were instructed to immerse their right foot in lukewarm water (35-37°C), and then to count forward from 10 in steps of 10 at their own pace. Each task lasted for three minutes. Only one experimenter was present, acting in a friendly way in normal casual clothing.

Data acquisition and analysis
Stress measures

Collection of full saliva samples and subjective affect reports (i.e., a total of five samples) was not obtained from a small group of participants, resulting in a sample of N=311 participants with complete stress measurements.

To ensure sufficient saliva material for the analyses of interest, participants were instructed to use their tongue to roll the cotton swab within their mouth for one minute without chewing or biting it (Luo et al., 2018). The saliva samples were stored at -24°C until they were analyzed by Dresden LabService (Germany) using a commercially available chemiluminescence immunoassay with high sensitivity (IBL Inc.). Self-reported ratings of PANAS were collected via either a paper questionnaire (i.e., for measurement at +30 min outside the scanner) or digitally on a screen in the MRI scanner (using Presentation® software Version 16.0, Neurobehavioral Systems,

Inc., Berkeley, CA, www.neurobs.com).

Statistical analyses on stress measures were carried out separately on the sample with complete measurements (reported in the main texts) and the full sample (N=372). Linear mixed models via the *lme4* package (Bates, Maechler, Bolker, & Walker, 2015) in software R (R Core Team, 2017) were used. The effects of sampling time (different time points) were tested in both samples, separately, and the results for the full sample are reported below.

As cortisol, α-amylase and negative rating scores were all positively skewed, log transformation was carried out for those measures before running the aforementioned analyses. P-values were derived using a Type III test with Kenward-Roger approximation for degrees of freedom, as implemented in the Anova function (Fox & Weisberg, 2011). Multivariate t-distribution (mvt) adjustment was used to correct multiple comparison for the follow-up tests via *lsmeans* package in R (Lenth, 2016).

Supplementary Results

Full-sample stress measures

Within the stressed participants (N=372), we found significant main effect of the sampling time on all stress measures, namely the cortisol level ($F(4,1372.5)=169.43$, $p<.0001$), α-amylase level ($F(3,1008.1,)=11.23$, $p<.0001$) and negative affect ratings ($F(4,1415.3)=112.94$, $p<.0001$). Follow-up tests on pair-wise comparison revealed similar patterns of stress measure changes in the full sample as identified in the subsample, with cortisol level significantly increased approximately 20 and 30 minutes after stress induction onset in contrast to pre-stress baseline (all p's<.0001; no difference between two samples at +20 min and at +30 min (p=.07), while α-amylase level and negative affect rating peaked immediate after stress induction (i.e., 10 min after the onset; all p's<.0001). In contrast to α-amylase level that remained high at 20 min after the onset (p<.0005), negative affect rating declined quickly back to the baseline level (p=.78).

Gender and group effects

The typical gender and potential group (i.e., police students vs. remaining participants) effects on cortisol were evaluated in our experimental sample (N=335). As expected, we observed typical effects of gender, with males showing higher cortisol stress-responses as compared to females ($t(210.04)=5.60$, $p<.0001$). Furthermore, the mean cortisol increases were comparable between police students and the remaining participants ($t(61.74)=1.08$, $p=0.28$) that had similar gender ratio ($X^2=.41$, $p=.52$).

Additional analyses show that the observed correlations between network delta-FC (i.e., in the SN and DMN) and cortisol stress-responses did not differ between males and females (p's > .48), suggesting the neural mechanisms associated with individual stress responsiveness are similar for males and females.

Delta-FC of RSNs

Following acute stress induction, whole-brain analyses revealed both increased and decreased connectivity patterns for all RSNs with wide-spread regions (*Figure S2*). As for the DMN, decreased FC was observed not only within the core regions of the network (i.e., angular gyrus, temporal gyrus), but also with other brain regions such as the frontal lobe, putamen, and occipital cortex. On the other hand, the DMN also exhibited increased FC within core DMN regions, such as the precuneus. With respect to the CEN, we observed increased FC within the network, as well as between the network and several regions that are not typically included in this network, such as the caudate. Lastly, the SN also showed enhanced as well as reduced connectivity with brain regions also outside the network (full results in *Table S1*). These results suggest that in general, functional connectivity changes (i.e., delta-FC) occurred not only at a local level (i.e., within the network of interest), but also at a more global level (i.e., in synchronization with brain regions also outside the network).

With regard to the averaged coefficients of delta-FC within each network (i.e., masked by ICA group template), we observed strengthened delta-FC in the CEN ($t(334)=3.47$, $p<.001$). However, this delta-FC was not correlated with cortisol stress-responses and we observed similar CEN increases in the non-stressed participants ($t(20)=3.29$, $p<.005$; Figure S3). A further control test revealed a correlation between the overall CEN connectivity changes and motion artifacts (i.e., averaged relative frame-wise displacement) for the stressed participants ($Rs=.11$, $p<.05$), further suggesting the observed changes in connectivity strength of the CEN might not be specific to stress induction (*Figure S3*). None of the other RSNs showed changes in the delta-FC strength (all p's>.05).

Supplementary Figures

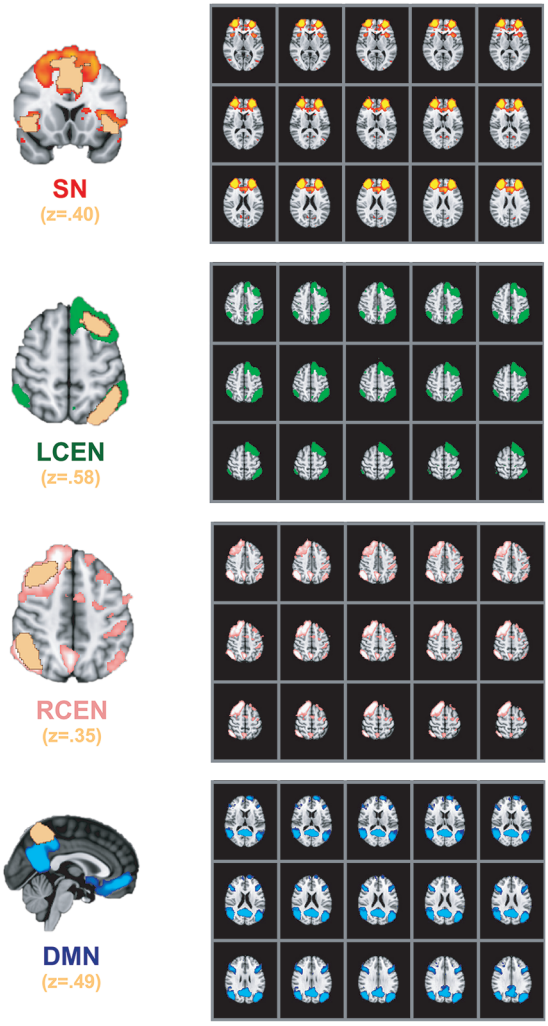

Figure S1. *Resting-state networks (RSNs) including the salience network (SN), left and right central executive networks (LCEN/RCEN) and default mode network (DMN) derived from the group ICA templates (z>3 for illustration purpose). Binarised ROIs of Stanford FIND Atlas (copper brown) were imposed on four RSNs. Z-scores refer to Fisher's Z-transformation of correlation coefficients between the time-series of each RSN and corresponding FIND ROI, respectively.*

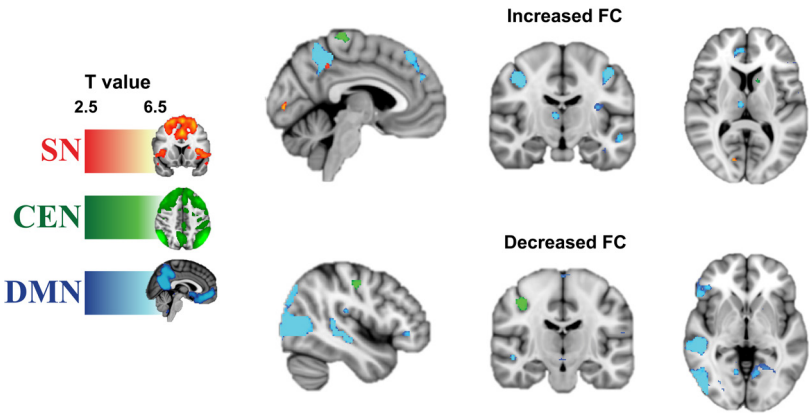

Figure S2. *Whole-brain functional connectivity changes following stress induction.*
Both increases and decreases were observed in our resting-state networks: the salience network (SN), left and right central executive networks (LCEN/RCEN), and default mode network (DMN). Results are whole-brain FWE corrected with P_{fwe}*<.0125 to account for the number of networks and connectivity directionality in the analyses. ICA-derived network templates that were used to assess these network changes are shown in the legends (z>3 for illustration purpose).*

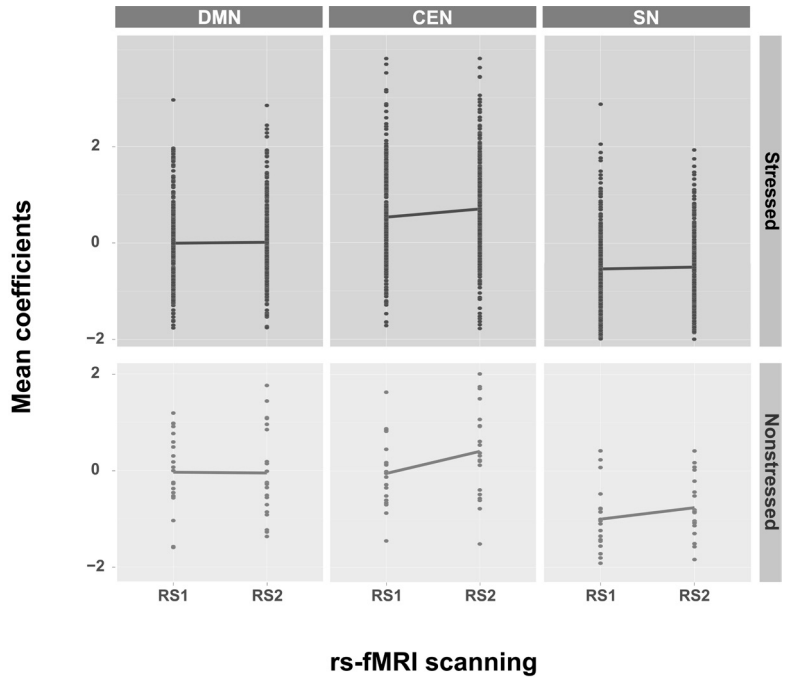

Figure S3. *Mean coefficients of within-network connectivity, extracted from resting-state networks, including the default mode network (DMN), bilateral central executive network (CEN) and salience network (SN) for each resting-state fMRI (rs-fMRI) scanning session (i.e., RS1, RS2). While there was an overall increase in connectivity strength observed after stress induction for the bilateral CEN, data from the non-stressed participants exhibited similar increase patterns in delta-FC coefficients of the CEN. These results suggest that across all participants there were no stress-specific changes in connectivity within the CEN.*

Table S1. Functional connectivity increases (left) and decreases (right) of three resting-state networks following stress induction

RSNs	Increased Functional Connectivity							Decreased Functional Connectivity						
	index	Cluster (voxels)	anatomical label	Max. T	coordinates			index	Cluster (voxels)	anatomical label	Max. T	coordinates		
					X	Y	Z					X	Y	Z
DMN	1	2399	Right parietal lobe	3.09	82	-56	34	1	2167	Right lateral occipital cortex	3.02	54	-70	-8
	2	646	Right paracingulate gyrus	3.83	10	46	34	2	850	Right superior lateral occipital cortex	3.59	26	-76	44
	3	405	Right precuneus cortex	3.93	40	-18	10	3	840	Right superior temporal gyurs	3.28	52	-30	-10
	4	389	Left angular gyrus	3.93	-54	-56	20	4	248	Left parietal lobe	4.53	-8	-48	64
	5	336	Left lateral occipital cortex	4.16	-14	-88	18	5	197	Cerebellum	3.97	30	-54	-54
	6	254	Left precentral gyrus	4.09	-36	-20	18	6	162	Cerebellum	5.28	-20	-86	-40
	7	232	Left temporal lobe	4.68	-54	-6	36	7	135	Right inferior frontal gyrus	4.73	54	26	-4
	8	131	Left interior frontal gyrus	5.20	-54	30	16	8	117	Left precentral gyrus	4.20	0	-32	66
	9	109	Right frontal lobe	4.59	30	42	46	9	100	Left parietal lobe	4.58	-10	-70	38

10	104	Left temporal lobe	3.89	-36	-38	-22	10	72	Right frontal lobe	4.48	10	12	70
11	47	Left frontal lobe	4.23	-56	-2	12	11	62	Left angular gyrus	4.72	-48	-60	54
12	47	Cerebellum	5.07	-44	-46	-34	12	34	Left lateral occipital cortex	4.52	-34	-70	48
13	42	Right thalamus	6.40	8	-16	8	13	21	Left parietal lobe	4.36	-58	-18	16
14	40	Cerebellum	4.48	14	-86	8	14	20	Right parietal lobe	5.37	48	-24	20
15	39	Right occipital lobe	4.49	4	-90	14	15	19	Left paracingulate gyrus	4.36	-2	22	42
16	23	Left insula	4.38	-32	-14	16	16	12	Right cerebral white matter	2.65	2	-16	-10
17	16	Left cerebral white matter	3.95	-34	-20	26	17	7	Cerebellum	3.24	40	-58	-10
18	13	Brain stem	4.95	10	-44	-44	18	6	Left postcentral gyrus	4.74	-62	-12	32
19	8	Left temporal lobe	3.49	-36	-14	-44	19	2	Left superior frontal gyrus	4.11	-18	2	66
20	6	Left temporal lobe	3.92	-68	-32	-4	20	1	Right postcentral gyrus	4.88	56	-8	32
21	1	Left frontal lobe	3.86	-64	6	16	21	1	Left putamen	3.85	-18	10	-2
							22	1	Brain stem	3.11	10	-30	-14

SN	1	216	Right occipital lobe	4.41	6	-90	-4	1	5	Cerebellum	4.99	-8	-68	-18
	2	32	Left posterior cingulate gyrus /precuneus	4.29	-6	-46	38							
	3	8	Right postcentral gyrus	4.54	62	-18	24							
CEN	1	258	Left middle frontal lobe	4.18	-42	28	40	1	236	Left occipital lobe	4.53	-36	-74	24
	2	93	Left precentral gyrus	4.11	0	-32	66	2	138	Right postcentral gyrus	4.33	42	-16	38
	3	21	Left caudate	5.10	-12	12	10	3	15	Left cerebral white matter	3.69	-32	-54	28
	4	2	Left middle frontal lobe	3.91	-40	16	56	4	13	Left parietal lobe	4.30	-26	-50	48
								5	12	Left superior lateral occipital cortex	5.05	-12	-96	24

RSNs = resting-state networks
DMN = default mode network
SN = salience network
CEN = central executive network

Anatomical labeling was based on Harvard-Oxford Cortical/ Subcortical Structural Atlas and MNI Structural Atlas.

Supplementary References

Allen, A. P., Kennedy, P. J., Cryan, J. F., Dinan, T. G., & Clarke, G. (2014). Biological and psychological markers of stress in humans: Focus on the Trier Social Stress Test. *Neuroscience and Biobehavioral Reviews*, *38*, 94–124.

Bates, D., Maechler, M., Bolker, B., & Walker, S. (2015). Fitting linear mixed-effects models using lme4. *Journal of Statistical Software*.

Duchesne, A., Tessera, E., Dedovic, K., Engert, V., & Pruessner, J. C. (2012). Effects of panel sex composition on the physiological stress responses to psychosocial stress in healthy young men and women. *Biol Psychol*, *89*(1), 99–106.

Fox, J., & Weisberg, S. (2011). An {R} Companion to Applied Regression, Second Edition. Retrieved from http://socserv.socsci.mcmaster.ca/jfox/Books/Companion

Lenth, R. V. (2016). Least-Squares Means: The R Package lsmeans. *Journal of Statistical Software*, *69*(1), 1–33.

Luo, Y., Fernández, G., Hermans, E., Vogel, S., Zhang, Y., Li, H., & Klumpers, F. (2018). How acute stress may enhance subsequent memory for threat stimuli outside the focus of attention: DLPFC-amygdala decoupling. *NeuroImage*.

R Core Team. (2017). R: A Language and Environment for Statistical Computing. *R Foundation for Statistical Computing, Vienna, Austria*.

CHAPTER III

DISCRIMINATING STRESS FROM REST BASED ON RESTING-STATE CONNECTIVITY OF THE HUMAN BRAIN: A SUPERVISED MACHINE LEARNING STUDY

This chapter is submitted to Journal of Neuroscience as Wei Zhang, Alberto Llera*, Mahur Hashemi, Reinoud Kaldewaij, Saskia Koch, Christian Beckmann, Floris Klumpers** and Karin Roelofs**. Discriminating stress from rest based on resting-state connectivity of the human brain: A supervised machine learning study.*

* *Equal contributions*

** *Equal contributions*

Abstract

Acute stress induces large-scale neural reorganization with relevance for stress-related psychopathology. Here we applied a novel supervised machine learning method, combining the strengths of a-priori theoretical insights with a data-driven approach, to identify which connectivity changes are most prominently associated with a state of acute stress and individual differences therein.

Resting-state fMRI scans were taken from 334 healthy participants (79 females) before and after a formal stress-induction. For each individual scan, mean time-series were extracted from 46 functional parcels of three major brain networks previously shown to be potentially sensitive to stress effects (default mode, salience and executive control networks). A data-driven approach was then used to obtain discriminative spatial linear filters that classified the pre- and post-stress scans. To assess potential relevance for understanding individual differences, probability of classification using the most discriminative filters was linked to individual cortisol stress-responses.

Our model correctly classified pre- vs. post-stress states with highly significant accuracy (above 75%; Z=13.53; leave-one-out validation relative to chance performance). Discrimination between pre- and post-stress states was mainly based on connectivity changes in regions from the salience and default mode networks, including the dorsal ACC, amygdala, PCC and precuneus. Interestingly, the probability of classification using these connectivity changes were associated with individual cortisol increases (Rs=-0.10).

Our results confirm the involvement of DMN and SN using a data-driven approach, and specifically single out key regions which might receive additional attention in future studies for their relevance also for individual differences.

Introduction

Acute stress as well as stress-related psychopathologies have been proposed to involve abnormalities in three major brain networks, namely the salience (SN), default mode (DMN) and central executive networks (CEN; Hermans et al., 2011; Menon, 2011; Zhang et al., 2019). However, few studies empirically tested how stress affects brain architecture at the network level (Hermans et al., 2011; Maron-Katz et al., 2016; Young et al., 2016; Zhang et al., 2019). The vast majority of research on functional connections has focused on a limited number of core regions from those major networks regarding stress effects and related psychopathologies (Koch et al., 2016; van Oort et al., 2017). The commonly used seed-based analyses in these studies is hypothesis-driven, and thus enables direct testing with straightforward interpretations (Cole, 2010). However, this approach relies heavily on strong a-priori knowledge about the critical brain regions responsive to stress, and the seed-region selection could very well be biased. In contrast, current network-level approaches consider distributed circuits or regions as a unified piece. This leaves it unacknowledged that human behavior and cognition are associated with not only integrated, but also segregated neural circuits that vary dynamically under different contextual demands (Cohen and D'Esposito, 2016; Keerativittayayut et al., 2018; Shine et al., 2018). The difficulty in defining networks, as well as lack of specificity of inter-regional connectivity patterns has therefore been key critiques of this type of analyses. An intermediate approach that takes a data-driven perspective with the guidance from a-priori knowledge about major brain networks may solve the aforementioned issues and allow for investigations into neural network-level stress responses with enriched information about regional connectivity patterns. Here, we applied a novel analysis in a relatively large sample to balance the strength and drawbacks of analyses described above.

Previously, acute stress has been shown to induce connectivity changes in SN, DMN and CEN at the network level (Hermans et al., 2011; Zhang et al., 2019), as well as in specific core regions particularly the amygdala, dorsal anterior cingulate cortex (dACC), medial prefrontal cortex (mPFC), posterior cingulate cortex (PCC) and precuneus (PCu) in particular (Li, Weerda, Milde, Wolf, & Thiel, 2014; Maron-Katz et al., 2016; Vaisvaser et al., 2013; see comprehensive review by van Oort et al., 2017). In order to test the relevance of these regions in stress reactivity, we set out to investigate whether their functional connections can substantially drive the classification between pre-stress and post-stress brain states. In specific, this study tests connectivity changes in resting-state fMRI (rs-fMRI) scans taken before and after a formal stress-induction. In contrast to previous studies investigating stress-induced connectivity changes as a whole in SN, DMN and CEN (Hermans et al., 2011; Zhang et al., 2019), here we aim to elucidate which functional parcels within these networks will exhibit altered functional connections after stress induction. Further, to explore the neural origins of individual differences in acute stress-responses,

characteristics of the classifiers (i.e., the discriminant features between pre- and post-stress states) will be linked to acute stress-induced cortisol levels.

To better characterize functional architectures of interest, here we employed a machine-learning algorithm to linearly index potential classes of interest (i.e., pre- vs. post-stress), using the average fMRI BOLD signals from the functional connectivity-based brain parcels (or functional regions of interest, fROI) from the aforementioned SN, DMN and CEN. This technique has been recently applied for the first time to fMRI data to discriminate different mental states (Llera et al., 2019). Taking the information from multiple functional parcels with the restrictions of three major brain networks, our approach bridges macro network-level analysis that allows for quantifying the neural substrates of stress reactivity as a system, with more micro parcel or cluster-level analysis that enables the disclosure of local spatial characteristics of these networks. This intermediate meso-level approach therefore offers an opportunity to identify stress-responses at a refined neural level.

Methods and Materials

Participants

We used data from 372 participants that were acquired in accordance with the principles of the Declaration of Helsinki and approved by the Independent Review Board Nijmegen (IRBN), the Netherlands. All participants gave their written informed consent before the study and all data were collected at the Donders Institute for Brain, Cognition and Behavior in Nijmegen, The Netherlands. Exclusion criteria included any current psychiatric or neurological disorder, a history of, or current endocrine or neurological treatment, current use of psychotropic medication, and current drug or alcohol abuse (full details in Koch et al., 2017). Further exclusion included data with signal artifacts and excessive head movements, resulting in a final sample of 334 participants (including 79 females; mean age=24.01; full exclusion details in Zhang et al., 2019).

These data were previously used to identify stress-related connectivity changes at the network level, using a-priori hypotheses (Zhang et al., 2019). Here we used the same large dataset, with a novel data-driven approach to pinpoint which specific subdivisions from the networks of interest are most prominently affected by acute stress.

Experimental Design

Acute stress induction took place in the late afternoon (i.e., between 4-7pm) when the diurnal rhythm of cortisol allows for a relatively stable level (Miller et al., 2016). Two sessions of rs-fMRI scanning were carried out, one before stress induction (RS1)

and one after (RS2). All participants were acquainted with the scanning procedure before the acquisition of RS1 (full details of experiment protocols in Koch et al., 2017).

Stress responses were induced by sequential administration of a socially evaluated cold pressor task (SECPT) and a mental arithmetic (MA) task, a procedure that has been shown to successfully induce psychophysiological and subjective stress responses (Schwabe et al., 2008; Luo et al., 2018). As has been implemented in previous studies (Luo et al., 2018; Vogel et al., 2015), participants were instructed to immerse their right foot in icy-cold (0-3°C) water for three minutes and to count back out loud from 2053 in steps of 17 as quickly and accurately as possible (MA task) immediately after the SECPT.

Data acquisition

Imaging data acquisition

Each session of rs-fMRI scan lasted for approximately six minutes, during which participants were instructed to lie still and to look at a small white cross at the screen center. All images were collected using a 3T Siemens Magnetom Prisma^{fit} MRI scanner (Erlangen, Germany) with a 32-channel head coil. A T2*-weighted multi-band EPI sequence with acceleration factor 8 (MB8) was used to acquire BOLD-fMRI whole-brain covered images (TR=735ms, TE=39ms, flip angle=52°, voxel size=2.4×2.4×2.4mm^3, slice gap=0mm, FOV=210mm). This state-of-the-art sequencing protocol was optimized from the recommended imaging protocols for the Human Connectome Project (http://protocols.humanconnectome.org/HCP/3T/imaging-protocols.html), with the fast acquisition speed facilitating the detection and removal of non-neuronal contributions to BOLD changes (Boubela et al., 2014). High-resolution structural images (1×1×1mm^3) were also acquired, using a T1-weighted MP-RAGE sequence (TR=2300ms, TE=3.03ms, flip angle=8°, FOV=256×256×192mm^3).

Stress measurement collection

Salivary samples, as well as self-reported ratings of positive and negative affect (PANAS; Watson et al., 1988) were collected in a total of five times around acute stress induction -10, 0, +10, +20, and +30 minutes with respect to the onset time (at 0 minute) of stress induction. In addition to salivary cortisol levels, subjective ratings on negative affect were calculated using the sum scores of the 10 negative affect items for each participant.

Statistical Analysis

Analyses on stress measures

Increases in salivary cortisol and negative affect ratings were calculated for each participant as the indication of stress level. Specifically, whereas cortisol increase was defined as cortisol level at time 20 minutes after stress induction onset (i.e., peak level) subtracted from time 0 (baseline level), negative affect increase was calculated as the difference in ratings between the baseline and at time 10 minutes after stress induction onset (i.e., peak level for negative affect). Main effect of sampling time and significant increases were observed in cortisol level (i.e., differences between peak level at +20 min. and baseline 0 min.) and subjective report on negative affect (i.e., differences between peak level at +10 min. and baseline 0 min.), indicating a successful stress induction (see *Figure 1* in Zhang et al., 2019).

fMRI preprocessing and analysis
Preprocessing

Analysis of fMRI data was performed with FSL5.0.9 (FMRIB, Oxford, UK). The first five images of each resting-state scan were discarded to allow for $T2^*$ equilibration effects. Further preprocessing included motion correction, spatial smoothing with a 5mm FWHM kernel, denoising using ICA-AROMA (Pruim et al., 2015), and high-pass filtering with a cut-off of 100 seconds. To further minimize motion and psychophysiological confounds after the denoising procedure, the six realignment parameters, their temporal derivatives and the quadratic terms of both the original parameters and derivatives were used as motion parameters in a multiple linear regression model (Friston et al., 1996; Zu Eulenburg et al., 2012; Caballero-Gaudes and Reynolds, 2017). Additionally, each individual T1 image was segmented for subject-specific white matter and CSF masks that were subsequently thresholded with a 95% probability and registered with the functional image. Mean signal intensities of white matter and CSF were extracted and included in the regression model (Satterthwaite et al., 2013; Caballero-Gaudes and Reynolds, 2017). The resulting residuals of the imaging data were used for further analyses, with each participant having one pre- and one post-stress rs-fMRI recording.

Identifying spatial characteristics of pre- and post-stress states from rs-fMRI data

In a previous study by Llera et al. (Llera et al., 2019), the algorithm of Spatial Patterns for Discriminative Estimation (SPADE) was introduced and validated to achieve optimal discriminative linear filtering between two fMRI conditions (i.e., task vs. resting state). Specifically, the algorithm is based on characterization of covariance matrices from each condition to simultaneously extract linear filters that maximize the explained variance for one condition while minimize it for the other (Fukunaga,

1990). In essence, this algorithm is a generalized eigenvalue decomposition for optimal linear discrimination that provides on one side of the eigenspectrum (i.e., top eigenvectors) high variance for one condition and low for the other, and vice versa on the other side of the same eigenspectrum (i.e., bottom eigenvectors). Consequently, discrimination between conditions can be achieved by selecting pairs of linear spatial filters from the top (i.e., first eigenvectors) and bottom (i.e., last eigenvectors) of the eigenspectrum, which represent the best features for discrimination (full details can be found in (Ramoser et al., 2000; Blankertz et al., 2003; Llera et al., 2012).

Here for the first time, we used SPADE to identify resting-state connectivity patterns that best discriminate between stressed and non-stressed states. Given the number of data-points from the rs-fMRI data (see section Imaging data acquisition), a reduction in fMRI spatial dimensionality is required to compute full-ranked spatial covariance matrices. Accordingly, a total of 40 functional parcels from the Stanford FIND atlas (Shirer et al., 2012) that are all considered part of the intrinsic networks of interest (i.e., DMN, SN and CEN) were selected as the functional units of interest (fROIs). Since the amygdala is not included in the FIND atlas while mounting evidence suggests its engagement in stress-related processing (Janak & Tye, 2015; Ressler, 2010; Zhang et al., 2018; also see review by McEwen & Gianaros, 2010), we further augmented the set of functional units with three amygdala subnuclei of each hemisphere from Jülich cytoarchitectonic probability map. A minimum probability of 25% was set to ensure the full coverage of the amygdala structure (Zilles & Amunts, 2010). The resulting 46 fROIs (*Figure 1*) were subsequently registered with the individual functional images for each participant, and mean time-series were extracted from each subject-specific fROI (see full list of fROI in *Table 1*).

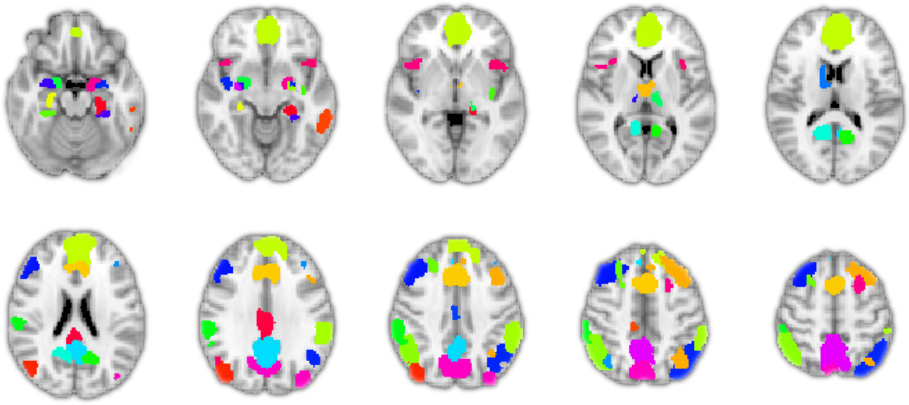

Figure 1. *The selected 46 functional parcels from the salience network, the default mode network and the central executive network. Forty parcels were from the Stanford FIND atlas (i.e., including the medial prefrontal cortex, dorsal anterior cingulate cortex, anterior and posterior insula, posterior cingulate cortex, precuneus) and the remaining six (i.e., bilateral amygdala subnuclei) from Jülich Cytoarchitectonic probability atlas. Full list of included parcels can be found in Table 1.*

Table 1. Forty-six functional parcels from the SN, DMN and CEN

Network	Subsystem Region (parcel counts)	Hemisphere	
		Left	Right
		Bilateral	
Salience Network	Amygdala (6)	centromedial nucleus	centromedial nucleus
		laterobasal nucleus	laterobasal nucleus
		superfical nucleus	superfical nucleus
	Anterior SN (3)	anterior insula	anterior insula
		dorsal anterior cingulate gyrus	
	Posterior SN (10)	middle frontal gyrus	
		angular gyrus	
		precuneus	
			posterior cingulate cortex
			precuneus
			angular gyrus
		thalamus	thalamus
		posterior insula	posterior insula
Default Mode Network	Ventral DMN (9)	posterior cingulate cortex	
		angular gyrus	
		parahippocampal gyrus	
		inferior parietal lobule	
			PCC/precunous
		PCC/precunous	
			middle frontal gyrus
			parahippocampal gyrus
			inferior parietal lobule
	Dorsal DMN (7)	medial prefrontal cortex	
		PCC/precunous	
			posterior cingulate gyrus
			angular gyrus
		thalamus	
		hippocampal gyrus	hippocampal gyrus
	Precunous (4)	posterior cingulate cortex	
		precunous	
		angular gyrus	angular gyrus
Central Executive Network	Left CEN (3)	middle frontal lobe	
		angular gyrus	
		inferior temporal gyrus	
	Right CEN (4)		middle frontal lobe
			angular gyrus
			superior frontal gyrus
			caudate

Next, we constructed within-subject covariance matrices between all parcel-specific time-courses for pre- and post-stress datasets, separately and subsequently averaged them across all participants. We then used the SPADE analysis to learn spatial filters that represent most discriminative features between pre- and post-stress scans. Importantly, the learned spatial filters from each covariance matrix maximized the explained variances either in the pre- or post-stress datasets (*Figure 2*). A leave-one-out cross validation approach was used to validate the robustness of the learned filters, by using the data from N-1 participants at each fold for learning spatial filters, extracting features and training a linear discriminant analyses classifier (Bishop, 2007). Notably, the features are obtained from log-transformed variances of the data projected onto the spatial filters and the quality of the classifier is assessed using the averaged ratio of correctly classified samples (i.e., classification accuracy) across folds. Critically, we trained the model at different dimensionalities (i.e., using different number of filters) and selected the number of spatial filters that achieved the maximal classification accuracy. Wilcoxon signed-rank tests were then conducted to test the classification accuracy of our model against a random chance of 50%, and to test accuracy improvements with increasing dimensionality. In order to locate crucial functional parcels (i.e., fROIs) from the SN, DMN and CEN that are responsive to acute stress induction, the most discriminative spatial filters were transformed into anatomical spatial maps in the brain (Haufe et al., 2014). A cut-off of Z>1.96 was used for these interpretable spatial maps.

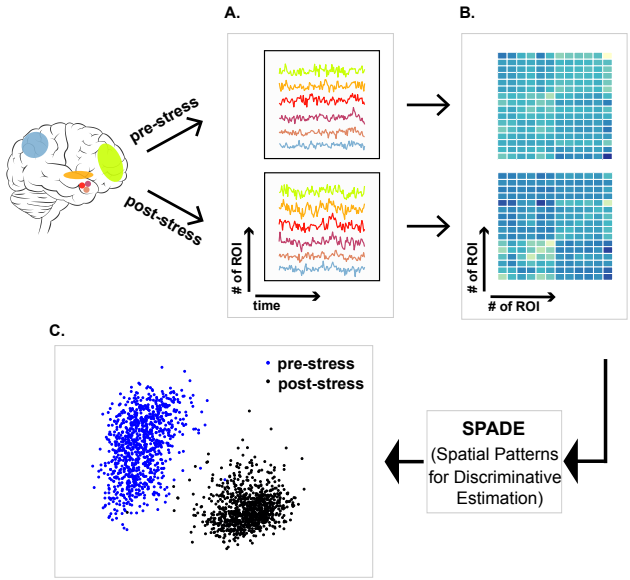

Figure 2. *Illustration of analysis steps. Mean time-courses were extracted from all N participants for pre- and post-stress scans, respectively (A). Thereafter, within-subject covariance matrices were constructed for pre- and post-stress data and concatenated across N-1 (i.e., leave-one-out) participants (B), which were further fed into SPADE for obtaining discriminative spatial filters. These spatial filters can discriminate the pre- from the post-stress data at individual subject level (C). The observed spatial filters that reached the maximal classification accuracy were further located in the brain as interpretable spatial maps (see Figure 4).*

Linking CSP features to individual stress responses

To further explore whether the most discriminative spatial filters we observed were predictive of the intensity of individual stress responses, we correlated the acute stress-induced cortisol increases (i.e., difference between the peak and baseline levels) with the odds ratio of correctly classifying a given rs-fMRI scan as being from the post-stress in contrast to pre-stress dataset. For this correlation analysis, we partialled out the potential influence of cortisol baseline level (assessed just before the pre-stress scan acquisition) to precisely investigate the association between brain activity and cortisol reactivity (i.e., using semi-partial Spearman correlation analyses). In case the spatial filter showed a significant correlation with cortisol increases (i.e., $p<0.05$), a follow-up test was carried out to visualize the involved functional parcels that together substantiated the discriminant effect of selected spatial filters. To do so , we first calculated the differential covariance matrix (i.e., normalized differences between post-stress and pre-stress covariance matrices) for the selected filters. Thereafter, covariance values were converted into Z-statistics and a 95% percentile was used to select the most relevant parcels for illustration.

Results

The maximal discrimination accuracy of our model was 77.99%, highly significant above a chance-level random performance ($Z=13.53$, $p<0.00001$). This maximum was achieved using four pairs of filters. However, this accuracy was statistically comparable to the accuracy achieved by using either two (75.9% accuracy; $Z=0.39$, $p=0.70$) or three pairs of filters (77.84% accuracy; $Z=1.31$, $p=0.19$). As the accuracy of using two pairs was still significantly higher than using only one ($Z=1.96$, one-sided $p=0.0248$) and a random chance-level performance ($Z=12.79$, $p<0.00001$), further analyses only focused on the first two pairs of filters (i.e., two spatial filters from each of the top and the bottom of the eigenspectrum; *Figure 3*). Thereafter, we checked whether the discriminative strength of these filters was specific for distinguishing pre- versus post-stress states. To this end, a control analysis was conducted to test if the observed discrimination was due to scanning order effects instead of stress-induced brain structure reorganization. The results show that our model could not distinguish the sequential rs-fMRI scans in an independent sample ($N=26$) that underwent a non-stressful control procedure in between two rs-fMRI scans (i.e., with a maximal accuracy of 61.5% not different from a random performance, $p>0.07$), thereby suggesting that the selected features (i.e., spatial filters) in the experimental sample are stress-specific.

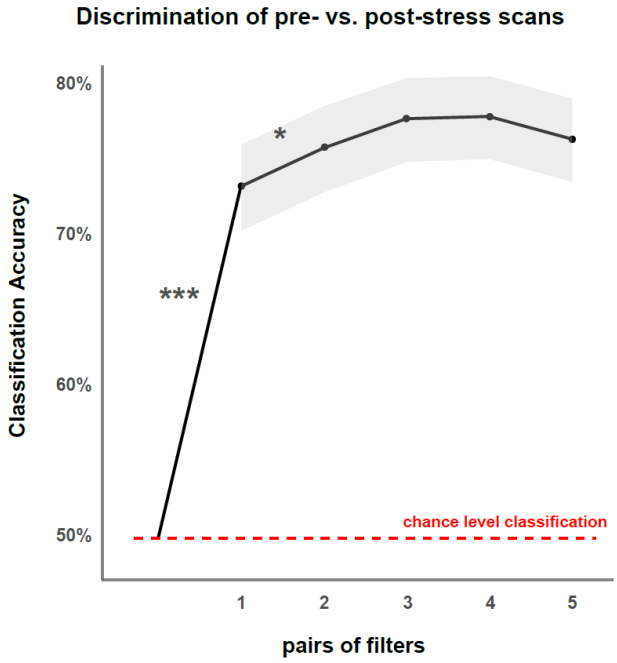

Figure 3. *Classification accuracy for pre- vs. post-stress states with 1-5 pairs of spatial filters. Classification accuracy was significantly higher than chance level (i.e. 50% indicated by the red dashed line) when using only one pair of spatial filters, and further significantly increased when using two pairs of spatial filters with asterisk indicating statistical significance (i.e., *** p<.0001; * p<.05) and gray shading indicating the 95% confidence interval.*

Hereafter, we mapped the fROIs in the brain that have predominantly substantiated the discrimination of the first two pairs of filters. The anatomical mapping revealed that connectivity patterns involving the core regions from the SN (i.e., amygdala, dorsal anterior cingulate cortex (dACC), thalamus (THA), and DMN (i.e., precunous (PCu), posterior cingulate cortex (PCC), inferior parietal lobule (IPL) provided the most crucial information for accurate classification of pre- vs. post-stress states.

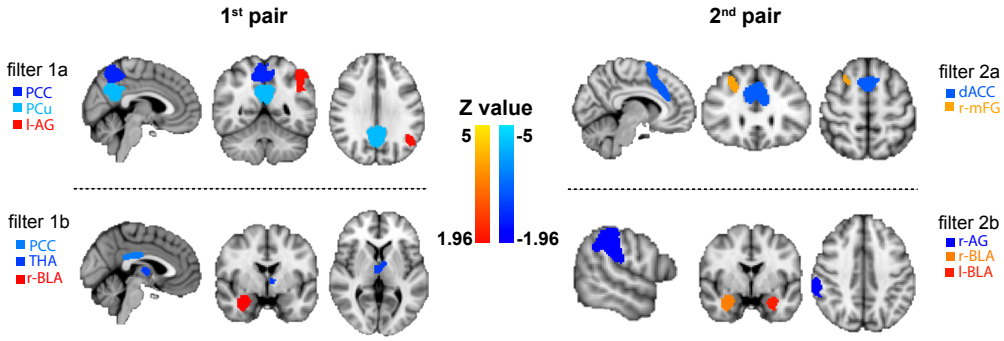

Figure 4. *Functional parcels associated with statistically maximal classification accuracy for pre- and post-stress scans in the brain. The filters were selected from the top (i.e., 1a, 2a) and the bottom (i.e., 1b, 2b) of the*

eigenspectrum. Together in pairs (i.e., 1st pair and 2nd pairs) they represent the most discriminative features of post- and pre-stress states. Within each individual spatial filter, color-coding (reddish or blueish) indicates the relative directionality of correlation, with the same color (i.e., all blueish) indicating positive correlations between parcels and different colors (i.e., blueish versus reddish) representing anti-correlation of the demonstrated parcels. For example, PCu and PCC exhibited a positive correlation whereas PCu and l-AG an anti-correlation in spatial filter 1a. dACC: bilateral dorsal anterior cingulate cortex; PCC: bilateral posterior cingulate cortex; PCu: bilateral precuneus; THA: bilateral thalamus; l-AG: left angular gyrus; r-AG: right angular gyrus; l-BLA: left basolateral amygdala; r-BLA: right basolateral amygdala; r-mFG: right middle frontal gyrus

To relate the observed fROIs to stress processing, we linked the individual cortisol stress-responses (i.e., absolute cortisol increase corrected for baseline level) to the odds ratio of classification, which represented the most discriminant features. Again, we focused on the first two pairs of spatial filters (as shown in *Figure 4*) that had achieved the maximal classification accuracy in the current sample. We observed a significant correlation between the odds ratio calculated for BLA-AG filter (i.e., filter with most detectable connectivity changes from bilateral BLA and right AG; depicted as filter 2b in *Figure 4*) with cortisol increases (Rs=-0.10, p=0.046; *Figure 5*). No such effect was observed for any other spatial filters (all p's>0.05).

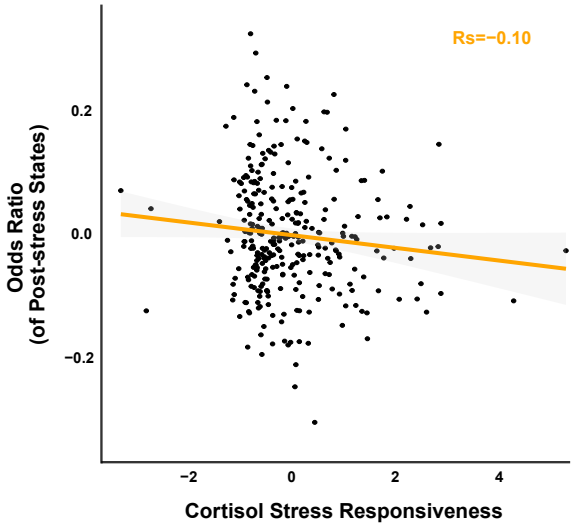

Figure 5. *Individual cortisol responsiveness to acute stress was correlated with odds ratio of post-stress brain states for BLA-AG filter (i.e., filter 2b in Figure 4). Note, Spearman rank correlation was performed to minimize the impact of potential outliers and removing the apparent outliers (i.e., >3SD) resulted in similar effect (RS=-0.09) with only slightly changed p-value (p=0.087).*

Subsequently, we explored which brain structures exhibited most notable correlations with BLA-AG filter under stress. To do so, we identified the functional parcels that had interacted with left and right BLA, as well as with r-AG, respectively. Interestingly, we found left and right BLA to exhibit strongest correlations with a set of (almost) identical functional parcels stemming predominantly from subcortical regions, including the hippocampus, caudate and thalamus. Additionally, we found

r-AG mainly covariated with parcels from the same DMN network (*Figure 6*). Follow-up tests show that bilateral BLA-based correlations were positive for all parcels except the right caudate and right thalamus, whereas right AG showed positive correlations with both DMN parcels (i.e., PCC and IPL) but was anti-correlated with right aIN from the SN.

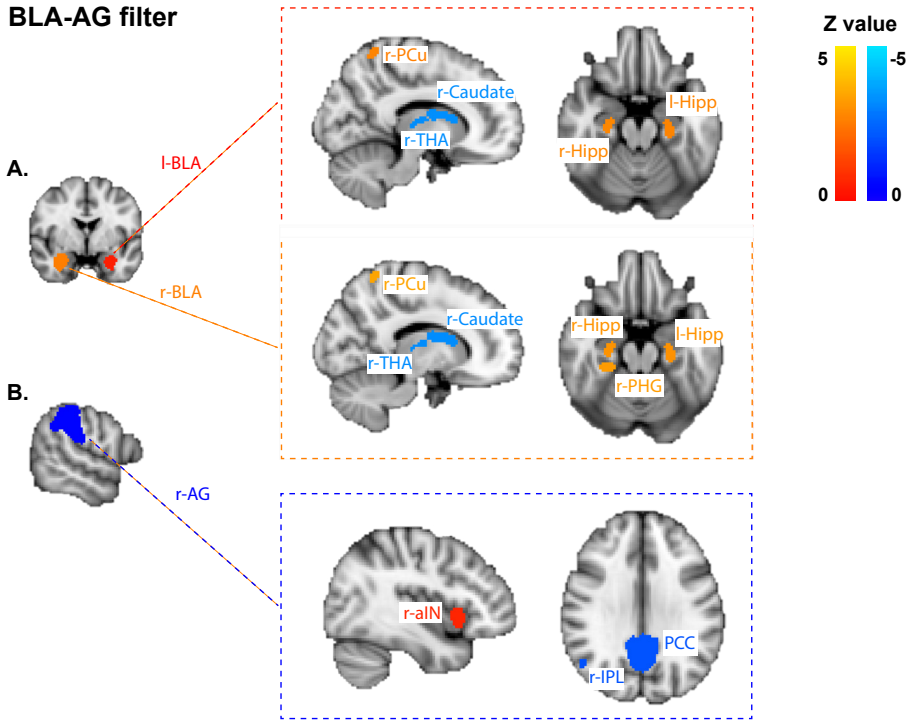

Figure 6. *Functional parcels involved in most notable correlations with A. the left and right basolateral amygdala (l-BLA / r-BLA) and B. right angular gyrus (r-AG), respectively. Together, these correlations substantiated the discriminative strength of BLA-AG filter (i.e., the filter 2b in Figure 4) that was associated with individual cortisol stress-responses. Interestingly, the left and right BLA appeared to exhibit significant covariance with a set of almost identical brain structures with similar patterns.*
l-: left ; r-: right
PCu: precuneus; THA: thalamus; Hipp: hippocampus; PHG: parahippocampal gyrus; aIN: anterior insula; IPL: inferior parietal lobule; PCC: bilateral posterior cingulate cortex

Discussion

In the current study, we used a novel approach to investigate the most critical subregions from major resting-state networks (SN, DMN and CEN) that are affected by acute stress induction. Based on the correlations among these functional parcels, our model could successfully classify the pre- and the post-stress states with a maximal classification accuracy above 75%. Our analysis further showed that discriminant features of the BLA-AG filter correlated with the level of a biologically

meaningful stress marker, namely cortisol stress-reactivity. These findings demonstrate that the data-driven approach we used here is able to identify a small number of key structures amongst a large and unbiased initial set of ROIs within large-scale networks previously demonstrated to be associated with stress effects (see review by van Oort et al., 2017).

Specifically, we explored the impact of acute stress induction on a functional connectome generated from BOLD fMRI data acquired under rest within 46 parcels, all from the SN, DMN and CEN. Our approach thus managed to mitigate the potential biases introduced by focusing only on a small number of the ROIs. In line with previous findings that have shown the involvement of the SN and DMN hub regions in stress-related processing (for review see van Oort et al., 2017), here we observed significant changes in connectivity patterns of bilateral dACC and bilateral BLA from the SN, and bilateral PCC/PCu from the DMN after stress induction (*Figure 4*). Importantly, we also observed such changes in bilateral thalamus, right middle frontal gyrus (mFG), left inferior parietal lobule (IPL) and right angular gyrus (AG) that notably contributed to the accurate discrimination between the pre- and post-stress states. As these later structures are not typically considered as the core or hub regions of the DMN, they have been largely overlooked in previous stress studies using a seed-based approach. Nevertheless, there is evidence suggesting the involvement of these structures in stress and more generally emotion-related processing, such as emotion regulation (i.e., the mFG; Fonzo, Huemer, & Etkin, 2016; Grecucci, Giorgetta, Bonini, & Sanfey, 2013), perception with emotional valence (i.e., the IPL; Engelen, de Graaf, Sack, & de Gelder, 2015; Sarkheil, Goebe, Schneider, & Mathiak, 2013), and information-encoding under stress (i.e., the AG; Vogel, Kluen, Fernández, & Schwabe, 2018). These findings indicate potential relevance of these additionally identified brain regions for future investigations into stress-related processes and related disorders.

In line with existing findings that link key structures of the SN and DMN to stress-related processes (Admon et al., 2013; Koch et al., 2016; van Oort et al., 2017), we observed connectivity patterns that substantiated accurate discrimination in core regions from the SN (i.e., dACC and amygdala) and DMN (i.e., PCC and PCu). However, in contrast to previous studies that considered these key structures as being functionally homogenous, here we investigated their inter-regional covariances with enhanced specificity of subdivisions. For example, the amygdala or amygdaloid complex is known as a group of multiple subnuclei with distinguishable cytoarchitectonic and connectional features (Sah et al., 2003). However, most human studies have investigated acute stress effects on the amygdala as a whole (see review by van Oort et al., 2017). Here, we divided the bilateral amygdala into six subnuclei (i.e., basolateral, centromedial and superficial nuclei from each hemisphere), and only left and right BLA nuclei showed noteworthy changes in their connectivity profile for discriminating pre- vs. post-stress states. Similarly, although

PCC and PCu have often been used as seed-regions to investigate stress effects on DMN connectivity, very rarely these hub regions were tested with specified subdivisions that are known to function distinctively (Zhang and Li, 2012; Leech and Sharp, 2014; Bzdok et al., 2015). Here again, we show that acute stress only affected limited parts (i.e., a few subdivisions) of the entire structure, thereby suggesting a potential relevance to shift the focus on more local-level functional characteristics for these hub regions in respect to stress effects.

Further, our follow-up tests revealed a correlation between individual cortisol reactivity to acute stress induction and the odds ratio of correctly classifying the acutely stressed brain state from the rs-fMRI scans for BLA-AG filter (*Figure 5*). This result validates the biological meaning of the spatial filters that emerged in distinguishing the stressed from the non-stressed brain states. Our follow-up test demonstrated a similar connectivity pattern for the left and right BLA not only with regard to the almost identical set of parcels they interacted with, but also regarding the direction of connectivity patterns they formed with these parcels. Additionally, we observed stress effects on the connectivity profile of the AG with PCC, PCu and aIN. Given the opposite connectivity directions with PCC, PCu from the same DMN, and aIN from the SN, the observed AG-connectivity profile may reflect a potential inter-network crosstalk, that is generally in line with the idea of brain network reconfiguration under stress (Hermans, et al 2014).

It is important to consider the limitations of the current study when interpreting the results. Firstly, the machine-learning algorithm used here does not allow for simple detection of the exact directionality of the connectivity changes (i.e., increases or decreases) following acute stress induction. Instead, it focused on the detection of changes per se that could yield maximal discriminative strength to tell the stressed from the non-stressed neutral states. Importantly, this approach does allow for inferring relative changing directions (i.e., the color coding in *Figure 4* quantifies the correlation within each spatial filter but not indicates the overall correlations). Based on these findings, it would be interesting for future investigations to identify the directionality of stress-induced connectivity changes in specific brain structures of interest (i.e., positive or negative correlation between parcels as have been done for BLA-AG filter). Therefore, the approach used here can serve as a crucial step to unbiasedly curtail a large number of brain structures, enabling subsequent investigation of the most relevant ones for connectivity directionality. Secondly, although we observed an association between the cortisol increases and the discriminative feature (i.e., odds ratio), this pattern was only present for one individual filter. This is likely due to the fact that the trained spatial filters here might have reflected the aggregated information from multiple neural and hormonal systems in a time-frame arguably capturing a mixture of stress reactivity and stress recovery processes. On the other hand, the cortisol levels we measured here (i.e., increases from baseline to the peak level) predominantly indicated the HPA-axis

reactivity to stressors. For future studies, acquiring additional imaging scans after acute stress subsides (i.e., stress recovery) may help elucidate the implications of the brain spatial patterns observed here. Nevertheless, it is important to note that our model was trained on the functional imaging data and was not designed to predict cortisol stress-responses. The fact that it could still explain variances in cortisol data suggests that the observed connectivity patterns discriminative of pre- and post-stress scans are driven, to a certain degree, by the neurobiological processes also giving rise to cortisol responses.

In conclusion, the current study used an unbiased data-driven approach to detect the most relevant brain structures from the SN, DMN and CEN in response to acute stress. By combining our a-priori knowledge -of stress-sensitive neural networks- with data-driven modeling, our results show that acute stress substantially affects the intermediate meso-scale connectivity patterns of the hub regions from the SN and DMN, as well as a number of regions not typically predefined as stress-sensitive.

References

Admon R, Milad MR, Hendler T (2013) A causal model of post-traumatic stress disorder: Disentangling predisposed from acquired neural abnormalities. Trends Cogn Sci 17:337–347.

Bishop C (2007) Pattern Recognition and Machine Learning. Technometrics 49:366–366.

Blankertz B, Dornhege G, Schäfer C, Krepki R, Kohlmorgen J, Müller KR, Kunzmann V, Losch F, Curio G (2003) Boosting bit rates and error detection for the classification of fast-paced motor commands based on single-trial EEG analysis. IEEE Trans Neural Syst Rehabil Eng 11:127–131.

Boubela RN, Kalcher K, Nasel C, Moser E (2014) Scanning fast and slow: current limitations of 3 Tesla functional MRI and future potential. Front Phys 2.

Bzdok D, Heeger A, Langner R, Laird AR, Fox PT, Palomero-Gallagher N, Vogt BA, Zilles K, Eickhoff SB (2015) Subspecialization in the human posterior medial cortex. Neuroimage 106:55–71.

Caballero-Gaudes C, Reynolds RC (2017) Methods for cleaning the BOLD fMRI signal. Neuroimage 154:128–149.

Cohen JR, D'Esposito M (2016) The Segregation and Integration of Distinct Brain Networks and Their Relationship to Cognition. J Neurosci 36:12083–12094.

Cole (2010) Advances and pitfalls in the analysis and interpretation of resting-state FMRI data. Front Syst Neurosci.

Engelen T, de Graaf TA, Sack AT, de Gelder B (2015) A causal role for inferior parietal lobule in emotion body perception. Cortex 73:195–202.

Fonzo GA, Huemer J, Etkin A (2016) History of childhood maltreatment augments dorsolateral prefrontal processing of emotional valence in PTSD. J Psychiatr Res 74:45–54.

Friston KJ, Williams S, Howard R, Frackowiak RSJ, Turner R (1996) Movement-Related effects in fMRI time-series. Magn Reson Med 35:346–355.

Fukunaga K (1990) Statistical Pattern Statistical Pattern Recognition. Pattern Recognit 22:833–834.

Grecucci A, Giorgetta C, Bonini N, Sanfey AG (2013) Reappraising social emotions: the role of inferior frontal gyrus, temporo-parietal junction and insula in interpersonal emotion regulation. Front Hum Neurosci 7.

Haufe S, Meinecke F, Görgen K, Dähne S, Haynes JD, Blankertz B, Bießmann F (2014) On the interpretation of weight vectors of linear models in multivariate neuroimaging. Neuroimage 87:96–110.

Hermans EJ, Henckens MJAG, Joëls M, Fernández G (2014) Dynamic adaptation of large-scale brain networks in response to acute stressors. Trends Neurosci 37:304–314.

Hermans EJ, van Marle HJF, Ossewaarde L, Henckens MJ a. G, Qin S, van Kesteren MTR, Schoots VC, Cousijn H, Rijpkema M, Oostenveld R, Fernandez G (2011) Stress-Related Noradrenergic Activity Prompts Large-Scale Neural Network Reconfiguration. Science (80-) 334:1151–1153.

Janak PH, Tye KM (2015) From circuits to behaviour in the amygdala. Nature 517:284–292.

Keerativittayayut R, Aoki R, Sarabi MT, Jimura K, Nakahara K (2018) Large-scale network integration in the human brain tracks temporal fluctuations in memory encoding performance. Elife 7.

Koch SBJ, Klumpers F, Zhang W, Hashemi MM, Kaldewaij R, van Ast VA, Smit AS, Roelofs K (2017) The role of automatic defensive responses in the development of

posttraumatic stress symptoms in police recruits: protocol of a prospective study. Eur J Psychotraumatol 8:1412226.
Koch SBJ, van Zuiden M, Nawijn L, Frijling JL, Veltman DJ, Olff M (2016) Aberant resting-state brain activity in posttraumatic stress disorder: A meta-analysis and systematic review. Depress Anxiety 33:592–605.
Leech R, Sharp DJ (2014) The role of the posterior cingulate cortex in cognition and disease. Brain 137:12–32.
Li S, Weerda R, Milde C, Wolf OT, Thiel CM (2014) Effects of acute psychosocial stress on neural activity to emotional and neutral faces in a face recognition memory paradigm. Brain Imaging Behav 8:598–610.
Llera A, Chauvin R, Mulders P, Naaijen J, Mennes M, Beckmann CF (2019) Spatial Patterns for Discriminative Estimation (SP ♠ DE). bioRxiv:746891.
Llera A, Gómez V, Kappen HJ (2012) Adaptive classification on brain-computer interfaces using reinforcement signals. Neural Comput 24:2900–2923.
Luo Y, Fernández G, Hermans E, Vogel S, Zhang Y, Li H, Klumpers F (2018) How acute stress may enhance subsequent memory for threat stimuli outside the focus of attention: DLPFC-amygdala decoupling. Neuroimage.
Maron-Katz A, Vaisvaser S, Lin T, Hendler T, Shamir R (2016) A large-scale perspective on stress-induced alterations in resting-state networks. Sci Rep 6:21503.
McEwen BS, Gianaros PJ (2010) Stress- and Allostasis-Induced Brain Plasticity. Annu Rev Med 62:431–445.
Menon V (2011) Large-scale brain networks and psychopathology: A unifying triple network model. Trends Cogn Sci 15:483–506.
Miller R et al. (2016) The CIRCORT database: Reference ranges and seasonal changes in diurnal salivary cortisol derived from a meta-dataset comprised of 15 field studies. Psychoneuroendocrinology 73:16–23.
Pruim RHR, Mennes M, van Rooij D, Llera A, Buitelaar JK, Beckmann CF (2015) ICA-AROMA: A robust ICA-based strategy for removing motion artifacts from fMRI data. Neuroimage 112:267–277.
Ramoser H, Müller-Gerking J, Pfurtscheller G (2000) Optimal spatial filtering of single trial EEG during imagined hand movement. IEEE Trans Rehabil Eng 8:441–446.
Ressler KJ (2010) Amygdala Activity, Fear, and Anxiety: Modulation by Stress. Biol Psychiatry 67:1117–1119.
Sah P, Faber ESL, Lopez De Armentia M, Power J (2003) The amygdaloid complex: anatomy and physiology. Physiol Rev 83:803–834.
Sarkheil P, Goebe R, Schneider F, Mathiak K (2013) Emotion unfolded by motion: A role for parietal lobe in decoding dynamic facial expressions. Soc Cogn Affect Neurosci 8:950–957.
Satterthwaite TD, Elliott MA, Gerraty RT, Ruparel K, Loughead J, Calkins ME, Eickhoff SB, Hakonarson H, Gur RC, Gur RE, Wolf DH (2013) An improved framework for confound regression and filtering for control of motion artifact in the preprocessing of resting-state functional connectivity data. Neuroimage 64:240–256.
Schwabe L, Haddad L, Schachinger H (2008) HPA axis activation by a socially evaluated cold-pressor test. Psychoneuroendocrinology 33:890–895.
Shine JM, van den Brink RL, Hernaus D, Nieuwenhuis S, Poldrack RA (2018) Catecholaminergic manipulation alters dynamic network topology across cognitive states. Netw Neurosci 2:381–396.

Shirer WR, Ryali S, Rykhlevskaia E, Menon V, Greicius MD (2012) Decoding Subject-Driven Cognitive States with Whole-Brain Connectivity Patterns. Cereb Cortex 22:158–165.

Vaisvaser S, Lin T, Admon R, Podlipsky I, Greenman Y, Stern N, Fruchter E, Wald I, Pine DS, Tarrasch R, Bar-Haim Y, Hendler T (2013) Neural traces of stress: cortisol related sustained enhancement of amygdala-hippocampal functional connectivity. Front Hum Neurosci 7:313.

van Oort J, Tendolkar I, Hermans EJ, Mulders PC, Beckmann CF, Schene AH, Fernández G, van Eijndhoven PF (2017) How the brain connects in response to acute stress: A review at the human brain systems level. Neurosci Biobehav Rev 83:281–297.

Vogel S, Kluen LM, Fernández G, Schwabe L (2018) Stress affects the neural ensemble for integrating new information and prior knowledge. Neuroimage 173:176–187.

Vogel S, Klumpers F, Krugers HJ, Fang Z, Oplaat KT, Oitzl MS, Joëls M, Fernández G (2015) Blocking the Mineralocorticoid Receptor in Humans Prevents the Stress-Induced Enhancement of Centromedial Amygdala Connectivity with the Dorsal Striatum. Neuropsychopharmacology 40:947–956.

Watson D, Clark L a., Tellegan a. (1988) Worksheet 3.1 The Positive and Negative Affect Schedule (PANAS; Watson et al., 1988) PANAS Questionnaire. J Pers Soc Psychol 54:1063–1070.

Young CB, Raz G, Everaerd D, Beckmann CF, Tendolkar I, Hendler T, Fernandez G, Hermans EJ (2016) Dynamic shifts in large-scale brain network balance as a function of arousal. J Neurosci.

Zhang S, Li C shan R (2012) Functional connectivity mapping of the human precuneus by resting state fMRI. Neuroimage 59:3548–3562.

Zhang W, Hashemi MM, Kaldewaij R, Koch SBJ, Beckmann C, Klumpers F, Roelofs K (2019) Acute stress alters the 'default' brain processing. Neuroimage 189:870–877.

Zhang X, Ge TT, Yin G, Cui R, Zhao G, Yang W (2018) Stress-induced functional alterations in amygdala: Implications for neuropsychiatric diseases. Front Neurosci 12.

Zilles K, Amunts K (2010) Centenary of Brodmann's map conception and fate. Nat Rev Neurosci 11:139–145.

Zu Eulenburg P, Caspers S, Roski C, Eickhoff SB (2012) Meta-analytical definition and functional connectivity of the human vestibular cortex. Neuroimage 60:162–169.

CHAPTER IV

STRESS-INDUCED SALIENCE NETWORK RECONFIGURATION PREDICTS TRAUMA-RELATED SYMPTOMS: A LONGITUDINAL STUDY

This chapter is under preparation for journal submission as Wei Zhang, Reinoud Kaldewaij, Mahur Hashemi, Saskia Koch, Vanessa van Ast, Christian Beckmann, Floris Klumpers and Karin Roelofs*. Stress-induced salience network reconfiguration predicts trauma-related symptoms: A longitudinal study*

**Equal contributions*

Abstract

There are substantial individual differences in how stress affects responses of Salience (SN), Default Mode (DMN) and Central Executive Networks (CEN). Here, we investigate whether stress-induced connectivity changes (i.e., delta-FC) of these large-scale networks represent a resilience factor, or an acquired effect of posttraumatic stress disorder (PTSD) symptoms. We linked stress-induced delta-FC of these three networks to symptom development. Specifically, we measured acute stress-induced delta-FC before (Wave1) and after 16 months of potential trauma exposure during repeated emergency aid services (Wave2). Neural markers were used to predict changes in perceived stress levels (PSS) and post-traumatic stress symptoms (PCL and CAPS) in 190 participants that experienced their core traumas between Wave1 and Wave2 assessments.

Results from prediction analyses show that weakened synchronization between the SN and DMN core regions at Wave1 predicted longitudinal increases from Wave 1 to Wave 2 in perceived stress level (R_s=-0.19, $p<0.01$; adjusted $p<0.05$) but not in post-traumatic stress symptoms. These effects remained when controlling for trauma severity and cortisol reactivity. Interestingly, increased coupling between the overall SN and anterior cerebellum was acquired in participants with higher clinician-rated PTSD symptoms, particularly intrusion symptoms at Wave2 (R_s=-0.22, $p<0.005$; adjusted $p<0.05$). These results suggest that SN synchronization after acute stress is a biomarker for predictive as well as acquired stress symptoms. Particularly, weak acute stress-induced SN synchronization with DMN may function as a vulnerability factor for posttraumatic stress symptoms even in relatively resilient individuals, like police officers. These findings provide a stepping-stone towards improved assessment and early detection of risk versus resilience factors.

Introduction

Acute stress has been shown to induce a re-allocation of resources from the three large-scale neural networks: the salience (SN), default mode (DMN) and central executive network (CEN; Hermans et al., 2011; Zhang et al., 2019). It has been speculated that in health this neural network reconfiguration prioritizes resources to facilitate processing of challenging situations (Hermans et al., 2011; Hermans, Henckens, Joëls, & Fernández, 2014; Zhang et al., 2019). However, frequent and chronic exposure to stressors may lead to unfavorable consequences, for instance in stress-related disorders that have been associated with alterations in SN and DMN (Admon, Milad, & Hendler, 2013; Koch et al., 2016; Menon, 2011). To date it remains unclear whether stress-induced network reorganizations can function as a resilience factor, protecting individuals against the negative consequences of trauma exposure. It requires measuring reorganization of large-scale networks in response to acute stress in a well-powered prospective longitudinal design to answer this question. Here, we set out to test these effects in 321 Dutch police recruits who in the line of duty experienced a variety of potentially traumatic events.

So far, the vast majority of investigations on the neural mechanisms underlying stress-related psychopathology has used cross-sectional designs. Mounting evidence from these investigations links altered functions of the three major large-scale brain networks, particularly the SN and DMN to stress-related disorders. In a recent study to investigate the relevance of resting-state network connectivity to individual stress responses, we found an association between stress-induced network reorganization and individual cortisol responsivity (Zhang et al., 2019). In specific, we defined the networks of interest using ICA (independent component analysis; Beckmann & Smith, 2005) and found connectivity changes of the SN (including dorsal cingulate cortex, anterior insula and amygdala) and DMN (including posterior cingulate cortex, precuneus and ventromedial prefrontal cortex) were correlated with cortisol increases after stress induction, respectively. As cortisol is known to aid in inhibiting sympathetic stress responses and regaining physiological homeostasis following acute stressors (De Kloet, Joëls, & Holsboer, 2005; McEwen, 1998), these results suggested an adaptive reorganization of brain structures in face of a challenge. On the other hand, some studies suggest that abnormal hyper-connectivity of the SN (i.e., between core regions of the network such as amygdala-insula and amygdala-dACC) and hypo-connectivity of the DMN(i.e., between network regions such as vmPFC-PCC, as well as between network components and regions of SN, such as amygdala-vmPFC) are associated with PTSD symptoms (Akiki, Averill, & Abdallah, 2017; Bremner, Elzinga, Schmahl, & Vermetten, 2007; Shin & Liberzon, 2010; Wang et al., 2016). Due to the nature of cross-sectional designs, however, these studies cannot tell whether the observed abnormalities already existed before or were acquired as a consequence of trauma exposure. Based on the few available longitudinal studies (for example, van Wingen, Geuze, Vermetten, & Fernández,

2012; Van Wingen, Geuze, Vermetten, & Fernández, 2011), Admon and colleagues proposed predisposing markers and acquired effects in brain activation for PTSD (Admon et al., 2013). A more recent review proposed a neurobiological model of PTSD based on dysfunction of large-scale networks. In specific, hyperactive SN and hypoactive DMN, CEN, together with inefficient modulation of SN over DMN and CEN are suggested to characterize PTSD (Akiki et al., 2017). Yet, dynamics within and between these network under challenges have not been prospectively tested in relation to long-term consequences after trauma exposure.

Using a longitudinal design, the current study aimed to elucidate this question. Specifically, we used stress-induced connectivity changes (i.e., delta-FC) of the SN and DMN, as well as CEN at baseline to predict the perceived stress and PTSD symptoms after 16-month exposure to police-training related trauma. Neuroimaging data collected at the follow-up allowed us to also investigate potentially acquired abnormalities after trauma exposure

Based on the studies reviewed above, we hypothesized the *predictive* effects of acute stress-induced delta-FC for trauma symptom development to involve SN and DMN. Specifically, we expected to find SN connectivity decreases, either within the network (i.e., local connectivity) or in communication with regions also outside the network (i.e., global connectivity) following stress induction predictive of higher levels of post-trauma stress vulnerability. In contrast, we expected to observe the opposite pattern for the delta-FC of DMN, with increased DMN global or local connectivity predicting higher post-trauma stress levels. Although CEN connectivity changes after stress induction was not associated with individual stress responses in our previous study (Zhang et al., 2019), there has been evidence for decreased CEN connectivity in response to stress under task conditions (Hermans et al., 2011), as well as evidence for the involvement of CEN connectivity in stress-related processing and psychopathology (Daniels et al., 2010; Liu et al., 2017; Menon, 2011; Miller et al., 2018). Hence, we also explored whether stress-induced changes in the CEN resting-state connectivity could predict post-trauma stress levels.

Concerning acquired abnormalities, we based our hypotheses on the previous findings that suggested hyper-connectivity of the SN and hypo-connectivity of the DMN underlying PTSD symptoms (Akiki et al., 2017; Bremner et al., 2007; Shin & Liberzon, 2010; Wang et al., 2016). Accordingly, we expected trauma exposure to sensitize acute stress responses at the network level, resulting in strengthened SN connectivity and reduced DMN connectivity after stress induction in individuals with higher post-trauma stress levels. For completeness, we also explored the acquired connectivity changes after stress induction in the CEN.

Methods and Materials

Participants

Out of a total number of N=427 participants (including 85 non-police students), 321 police students from Dutch Police Academy participated in the current experiment in accordance with the principles of the Declaration of Helsinki and with the approval from the Independent Review Board Nijmegen (IRBN), the Netherlands. All participants gave their written informed consent before the study upon their first lab visit (Wave 1). Exclusion criteria included any current psychiatric or neurological disorder, history of, or current endocrine or neurological treatment, current use of psychotropic medication, and current drug or alcohol abuse (full details in Koch et al., 2017). Further exclusion was carried out to ensure data quality (see below for specifics). For the current research question aiming to predict posttraumatic stress symptoms in police recruits after experiencing traumatic events during their training, we *included* data from all participants who reported core trauma experiences between wave1 and wave2 and *excluded* data from those officers who reported core trauma before wave1. Consequently, the final sample consisted of N=190 participants that had complete data from all measurements (see *Figure 1* for detailed sample selection).

Procedure

The baseline lab visit (i.e., Wave 1) took place, in parallel with the early police curriculum mostly consisting of in-class theoretical trainings. During this visit, participants filled out questionnaires in the morning to investigate their baseline-level of perceived stress (i.e., PSS), stress-related symptoms (i.e., PCL). After a variety of other experimental assessments (described in Koch et al., 2017), the experiment of acute stress induction was conducted in the late afternoon (i.e., between 4-7pm) to ensure stable salivary cortisol levels. Two sessions of resting-state fMRI (rs-fMRI) data were acquired directly before and after stress induction, respectively to assess stress-induced functional connectivity changes (i.e., delta-FC). Hormonal and subjective measurements of acute stress responses were collected for a total number of five times (see *Figure 2*). After an average of 16 months (SD=1.9), participants came in for their second lab visit (i.e., Wave 2). During this visit, the perceived stress level and stress-related symptoms were measured again to assess consequences of exposure to trauma-like events during their on-street emergency aid training, and PLES (Police Life Event Scale) was measured to indicate experienced trauma intensity. Around this visit, participants also went through a telephone interview comprising the Clinician-Administered PTSD Scale (CAPS; see full details about all measurements in Koch et al., 2017).

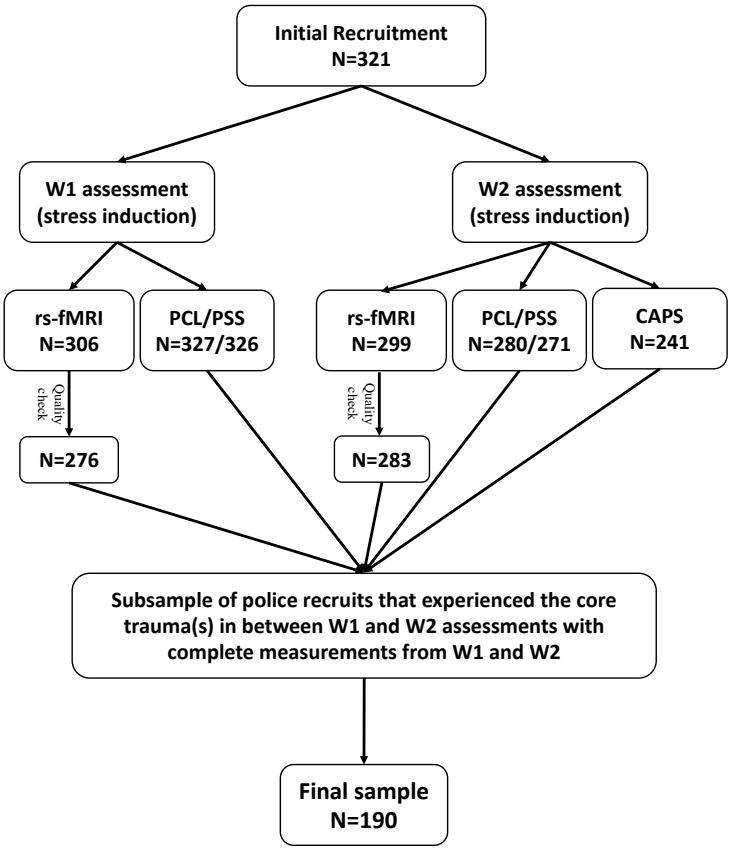

Figure 1. *A total number of 321 police recruits participated in the current study. Data from a subsample were acquired for resting-state functional MRI (rs-fMRI) and stress level-related questionnaires (i.e., PTSD Checklist, PCL; Perceived Stress Scale, PSS) or interviews (i.e., Clinician-Administered PTSD Scale, CAPS), at both Wave 1 and Wave 2 assessments, respectively. After data quality check and the screening of core trauma experiences (i.e., occurrence in between two assessments), data from a final sample of 190 participants were used for further analyses.*

Data acquisition and analysis

Imaging data acquisition

During both the pre- and post-stress induction acquisition in Wave 1 and Wave 2, participants were instructed to lie still and watch a small white cross at the screen center. All images were acquired using a 3T Siemens Magnetom Prisma^{fit} MRI scanner (Erlangen, Germany) with a 32-channel head coil. A multi-band T2*-weighted EPI sequence with eight acceleration factors was used to acquire BOLD-fMRI images (TR=735ms, TE=39ms, flip angle=52°, voxel size=2.4×2.4×2.4mm^3, slice gap=0mm, FOV=210mm), which has been shown to facilitate the identification and elimination of motion artefacts, as well as physiological components, together with the use

of independent component analysis-based noise detection methods (i.e., ICA-AROMA; Boubela, Kalcher, Nasel, & Moser, 2014; Parkes, Fulcher, Yücel, & Fornito, 2018; Pruim et al., 2015). High-resolution structural images (1×1×1mm^3) were also acquired, using a T1-weighted MP-RAGE sequence *(TR=2300ms, TE=3.03ms, flip angle=8°, FOV=256×256×192mm^3)*.

Assessment of stress-related measures

To index acute endocrine and subjective stress responses, salivary samples and self-reported ratings of negative affect both in Wave1 and Wave 2 were measured throughout a formal stress induction that consisted of a SECPT (Socially Evaluated Cold Pressure Task) and MA (mental arithmetic) task (see detailed procedure in Zhang et al., 2019). Perceived stress and PTSD symptom levels were also measured at both waves, using PSS and PCL respectively. CAPS, a widely used and accepted clinical criterion measure of PTSD (Weathers, Keane, & Davidson, 2001; Weathers, Ruscio, & Keane, 1999) was conducted at Wave 2 by trained psychologists. In addition, intensity of trauma experiences was measured using PLES.

Following our previous practice (Zhang et al., 2019), increases in salivary cortisol and negative affect ratings were calculated for each participant as the indication of acute stress responses at Wave 1 and Wave 2, separately. In specific, cortisol increase was defined as cortisol level 20 minutes after stress induction onset (i.e., at time +20 min. when response level peaked) subtracted from baseline level just before stress induction (i.e., at time 0 min.). Negative affect increase was calculated as the difference in ratings between the baseline (time 0 min.) and 10 minutes after the onset of stress induction (time +10 min.; *Figure 2*). In order to investigate trauma-related development of symptoms between waves, the differences in sum scores of perceived stress level (PSS) and PTSD symptoms (PCL) were calculated (i.e., Wave 2 minus Wave 1 scores resulting in delta-PSS and delta-PCL, respectively). Sum score of CAPS was also calculated (only available for Wave 2). The number of traumatic events reported in PLES was used to indicate trauma intensity for each participant.

fMRI preprocessing and analysis
Preprocessing

Preprocessing of rs-fMRI data included motion correction, spatial smoothing (5mm FWHM kernel), ICA-AROMA based denoising (Pruim et al., 2015), and high-pass filtering with a cut-off of 100 seconds. Mean signal intensity of white matter and cerebrospinal fluid, as well as head motion parameters were regressed out to minimize psychophysiological confounds and motion artefacts (Fox & Raichle, 2007; Parkes et al., 2018; Power, 2017). The resulting residuals were subsequently registered with the MNI atlas and used for statistical analyses. Detailed preprocessing can be found in the *Supplemental Materials and Methods*.

Statistical analyses

As has been described in our previous work (Zhang et al., 2019), changes in acute stress-induced functional connectivity (i.e., delta-FC) of RSNs were defined as the differences in connectivity before and after stress induction in each of three RSNs (i.e., SN, DMN and CEN). Coefficients of delta-FC that indicated acute stress effects on RSNs at both local (i.e., connectivity changes within each RSN) and more global levels (i.e., connectivity changes of RSNs with the brain regions also outside the network) were used to *predict* stress-related symptom development, respectively. Specifically, thresholded (Z>3) group network templates from our previous study was used to extract local-level connectivity coefficient, whereas thresholded ($p<0.167$) delta-FC mask of each network was used to extract more global-level connectivity coefficient (see details in Zhang et al., 2019). In line with previous findings about cortisol stress reactivity predictive of subsequent PTSD symptom development after trauma exposure (Galatzer-Levy, Ma, Statnikov, Yehuda, & Shalev, 2017; Isaac R. Galatzer-Levy et al., 2014), we also tested whether acute stress-induced cortisol increases could predict stress-related symptomatology. In addition to predictive effects, changes in acute stress responses were further examined as acquired effects of stress-related symptom development. Specifically, differences in acute stress responses at neural level (i.e., both local and global level delta-FC), as well as at hormonal and behavioral levels were calculated between Wave 1 and Wave 2. Thereafter, these changes in stress reactivity were linked to trauma-related symptom scores.

To index the development of posttraumatic stress levels, we calculated the change scores of PSS (i.e., Wave 1 score subtracted from Wave 2 score, delta-PSS) and PCL (delta-PSS), respectively. We further used the scores of CAPS to explore whether acute stress responses at the baseline assessment could predict the PTSD symptom level measured by clinical interview. To explore development of specific symptom clusters, sum scores of each sub-cluster in delta-PCL and CAPS were further linked to acute stress responses.

Spearman rank correlation was used for all correlation analyses in this study to mitigate the influences from extreme values and reduce the chance of false positives. Concerning the results for our a-priori hypotheses (i.e., regarding the delta-FC of SN and DMN), FDR corrections were applied to account for the number of analyses involving three outcome measurements (i.e., delta-PCL, delta-PSS and CAPS scores), whereas for more exploratory analyses concerning the delta-FC of CEN, FDR corrections were conducted to account for two levels of network connectivity (i.e., local and more global levels) and three outcome measurements. Follow-up tests on sub-cluster symptom scores were carried out when the sum score was predicted by baseline acute stress responses at Wave 1 (i.e., for predictive effects analyses) or associated with the changes in acute stress responses between two

waves (i.e., for acquired effects analyses). Concerning these exploratory analyses, FDR corrections were conducted to account for the number of analyses involving all four sub-cluster symptom scores, for the local and more global level connectivity, separately. In case of significant results concerning delta-PCL or delta-PSS (either the sum score or the sub-cluster score), semi-partial Spearman correlation was further conducted to control for the influences of baseline stress levels in Wave 1 assessment. Additionally, we used a Generalized Additive Model (GAM) to explore whether the significant predictive effects of neural measures remain present when taking into account the potential influences of stress reactivity at hormonal and behavioral levels from baseline assessment (i.e., from Wave 1), as well as individual differences in trauma intensity. Unlike multiple linear regression that estimates a single parameter for each predictor, GAM finds unspecified (non-parametric) functions that relate the predicted Y (dependent variable) values to the predictor values, and thus allows non-parametric fit (Hastie, 2008; Tibshirani & Hastie, 1986).

All statistical analyses were conducted using R (R Core Team, 2018), with pcor function from RVAideMemoire package (Hervé, 2018) and gam function from mgcv package (Wood, 2011) specifically for running semi-partial correlation and GAM analyses, respectively.

Results

Manipulation Checks - Acute stress responses

Successful acute stress induction was observed in both Wave 1 (i.e., baseline) and Wave 2 (i.e., after trauma) assessments. Specifically, increases in salivary cortisol and reported negative affect were observed in Wave 1 following stress induction, as reflected in main effects of sampling time ($F_{cortisol}$ (4, 677.36)=76.82, p<0.0001; F_{affect} (4,719.87)=51.50, p<0.005). The same significant effects were observed in Wave 2 ($F_{cortisol}$ (4,644.18)=123.4, F_{affect} (4,675.06)=51.03, p's<0.0001). Follow-up tests indicated that the temporal pattern of stress effects matched previous investigations with immediate changes in negative affect and cortisol responses that peaked after 20 minutes (see *Figure 2*).

Manipulation Checks - Traumatic experiences and posttraumatic stress measures

In between our two waves of data collection, the police recruits on average experienced 6.63 potentially traumatic events (SD=3.78) as measured by the Police Life Events Schedule (PLES) with a range between 0 and 17. Most frequently experienced trauma were encountering suicide (including attempt), severe (traffic) accidents and physical assault, which occurred in 31.4% 23.6% and 17.8% of the total cases, respectively (see *Figure S1* in *Supplemental Results* for a detailed overview of reported events).

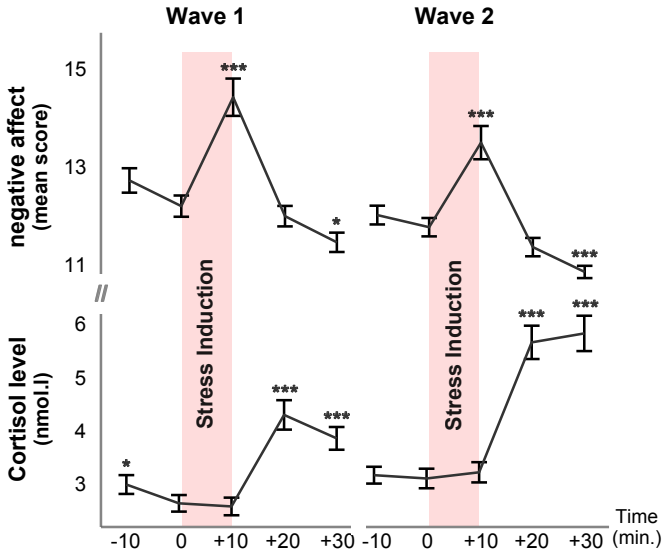

Figure 2. *Hormonal and behavioral responses to acute stress induction in Wave 1 and Wave 2, respectively. Acute stress induction has led to comparable response patterns in hormonal and behavioral measures. Whereas cortisol levels peaked 20 minutes after the onset of stress induction and remained high, negative affect peaked immediately after the onset of stress induction and declined thereafter until eventually below the pre-stress baseline level. Error bars represent SEM (standard error of measurement) and asterisks indicate significant differences relative to the pre-stress baseline level at time 0 min. ***p<0.0001; *p<0.05.*

From Wave 1 to Wave 2, average stress symptom levels increased numerically. However, due to a large variance in individual trajectories (see *Figure 3*), no significant changes at the group level were observed in perceived stress (PSS: t(182)=1.48, p=0.14), nor in overall symptom levels (PCL: t(189)=0.77, p=0.44). However, when inspecting symptom-clusters, a significant increase in intrusion symptoms was observed (t(189)=2.22, p<0.05). At wave 2, clinical interview (CAPS) scores of overall PTSD symptoms were averaged to 1.79 (SD=4.01; sum score range: 0-27) and only three participants meeting the criteria for full-blown PTSD according to DSM-5 criteria (*Figure S2*). These results demonstrate that the police recruits were overall resilient to the potentially traumatic experiences as expected, yet a large proportion of recruits did exhibit clinically relevant (i.e., reported at least one symptom in each cluster in Wave 2 PCL) increases in symptom levels. We subsequently tested whether changes in neural network connectivity after stress induction could explain variability in stress-symptom development.

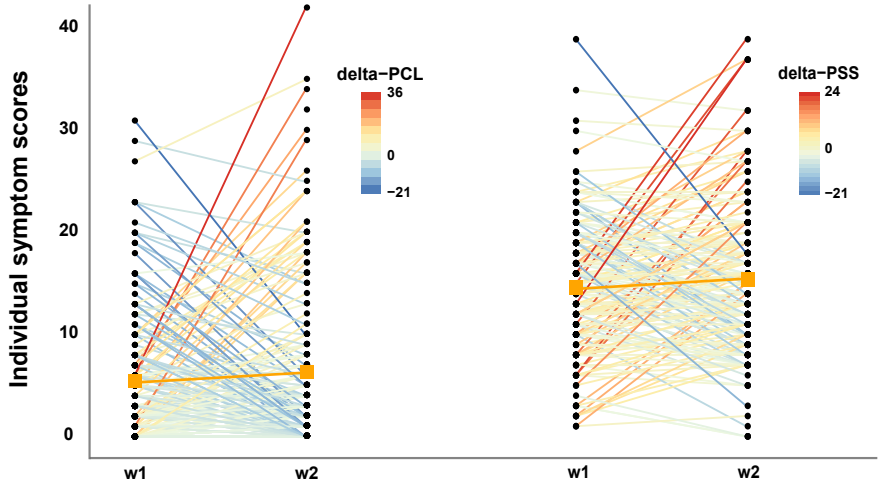

Figure 3. *Development of PTSD symptom levels (assessed by PCL-5) and perceived stress levels (assessed by PSS) from Wave 1 (w1) to Wave 2 (w2). Large individual differences were observed for change scores in PCL (i.e., delta-PCL, left panel; range: -21 to +36), and in PSS (i.e., delta-PSS, right panel; range -21 to +24). Each line represents the change of individuals in stress symptoms from w1 to w2. Group means for both PCL and PSS from each wave assessment are illustrated with the orange squares and orange lines.*

Predictive effects of baseline (Wave 1) acute stress responses

As expected, we found decreased synchronization of SN with DMN core regions (i.e., posterior cingulate cortex/Precuneus) following stress induction at Wave 1 predictive of larger increases in perceived stress level after trauma exposure (PSS: Rs=-0.19, p=0.0094; *Figure 4*). This effect remained significant after FDR correction (adjusted p=0.0167) and when baseline level PSS (at Wave 1) was statistically controlled for (Rs=-0.19, p=0.0039). This predictive effect of SN-DMN synchronization remained as the only significant predictor in our follow-up analysis using Generalized Additive Model (GAM), where influences of baseline (i.e., Wave 1) cortisol, subjective reactivity, as well as trauma intensity were considered (F=7.20, p=0.008). We observed no predictive effects for delta-PCL or CAPS scores, nor with respect to hypothesized DMN connectivity changes after stress induction. (all uncorrected p's>0.08).

Subsequent exploratory analyses for CEN revealed that increased delta-FC was predictive of higher PTSD symptom levels at both a local (i.e., delta-FC within the CEN; Rs=0.21, p=0.0031) and more global level (i.e., delta-FC of CEN with brain regions also outside the network; Rs=0.19, p=0.0089). After FDR corrections, the effect of local delta-FC of CEN remained significant (adjusted p=0.019), while that of the global delta-FC became trend significant (adjusted p=0.053).

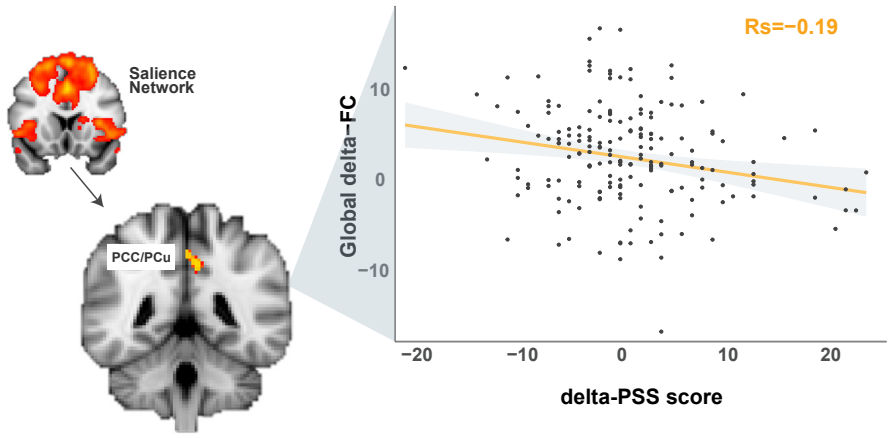

***Figure 4**. Decreases in the coupling between the overall SN and regions from the DMN (i.e. posterior cingulate cortex (PCC)/precuneus (PCu), as well as from postcentral gyrus and intracalcarine cortex) in response to acute stress induction predicted the higher levels of perceived stress after exposure to police-related traumas. The arrow indicates functional connectivity changes between the overall salience network (i.e., coefficients extracted using the depicted network mask thresholded at Z>3) and clusters in PCC/PCu, visual cortex and somatosensory cortex.*

Follow-up tests zooming in the sub-cluster symptoms revealed that both local and global-level CEN connectivity changes after stress induction most strongly predicted levels of alteration in mood and cognition (local: Rs=0.19, p=0.0085; global: Rs=0.17, p=0.017), as well as hyper-arousal symptoms (local: Rs=0.25, p=0.00058; global: Rs=0.18, p=0.015). Although the more global-level effects disappeared after FDR corrections (all adjusted p's>0.05), the local effects remained significant after multiple comparison correction (adjusted p<0.035; *Figure S3*).

Interestingly, we did not find predictive effects of cortisol reactivity on the development of stress-related symptomology that have been reported in previous investigations (all p's>0.05; Galatzer-Levy et al., 2017; Galatzer-Levy et al., 2014). Additionally, stress-induced increases in negative affect from Wave 1 assessment could not predict posttraumatic stress measures either (all p's>0.05).

Acquired effects after trauma exposure

Thereafter, we tested how *changes* from Wave 1 to Wave 2 at hormonal, behavioral and neural levels were related to increases in symptomology (potential acquired effects). The results show that cortisol stress-responsiveness and negative affect increases were not associated with symptom changes after trauma exposure (all p's>0.05). At the neural level, increased connectivity between the overall SN and anterior cerebellum was associated with higher PTSD symptom levels indicated by the CAPS total score (Rs=0.-18, p=0.019). No such effects were observed for delta-PCL, nor delta-PSS scores. When considering all three outcome measures, the effect on the CAPS total score remained trend significant (FDR adjusted p=0.057). Follow-

up tests examining sub-cluster symptoms revealed a significant correlation between this reduced decoupling effect and intrusion symptoms (Rs=-0.22, p=0.0038), with the greater acute stress-induced coupling in SN-anterior cerebellum, the higher intrusion symptom scores (*Figure 5*). This effect remained significant after FDR correction accounting for all four sub-cluster symptoms (adjusted p=0.015), as well as for the development of cortisol and subjective stress reactivity measures ((i.e., differential cortisol and subjective stress reactivity between Wave 1 and Wave 2 assessments; F=6.05, p=0.015). We did not find similar effects for delta-PCL, nor for delta-PSS scores.

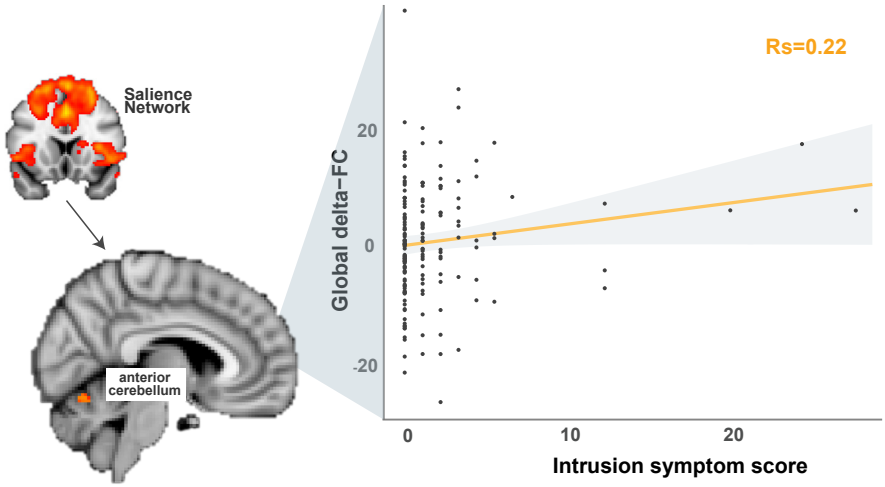

Figure 5. *Increased coupling (stemming from reduced decoupling) between the overall SN and anterior cerebellum (as depicted in the brain image) in response to acute stress induction was associated with higher levels of intrusion symptom, measured by CAPS scores. The arrow indicates functional connectivity changes between the overall salience network (i.e., coefficients extracted using the depicted network mask thresholded at Z>3) and clusters in anterior cerebellum.*

Discussion

In the current prospective longitudinal study, we investigated whether acute stress-induced neural network changes could predict increases in stress-related symptomatology after exposure to real-life trauma. Reduced global connectivity of the SN after stress at wave 1, with regions including the PCC and adjacent precuneus (PCu) from the DMN, predicted increased post-trauma stress levels 16 months later. In addition, enhanced within-network connectivity of the CEN was associated with higher PTSD symptom levels (CAPS) at Wave 2 follow-up. A slightly different pattern emerged for neural network changes (Wave 2 versus Wave 1) that followed symptom increases and thus appear acquired rather than a pre-trauma risk factor. In specific, individuals who developed higher PTSD symptom levels, particularly CAPS-intrusions, showed increased coupling between the SN and anterior cerebellum following acute stress induction at Wave 2. Interestingly, hormonal and subjective stress measures had no predictive nor acquired effects and the predictive value of

our neural measures remained when taking into account hormonal and subjective stress measures. Together, the results from this large longitudinal study suggest that SN synchronicity in response to acute stress particularly offers a promising biomarker for trauma symptom development.

As expected, acute stress-induced decreases in overall SN connectivity with several brain regions including PCC and PCu from the DMN predicted higher perceived stress level after exposure to real life traumas. Acute stress has been suggested to engage the SN immediately at the potential cost of neural resources that would otherwise have been allocated to other neural circuits (Hermans et al., 2011; Zhang et al., 2019). This stress-induced reconfiguration of brain function is hypothesized to facilitate the coping with the challenging situations at hand by reallocating neural resource towards the SN for attention direction to important stimuli and integration of top-down appraisal and bottom-up visceral and sensory information (see Uddin, 2015 for review). Insufficient SN involvement in response to stress therefore may signal suboptimal processing and thus result in undesirable consequences. Contrary to our expectations, we did not observe this predictive effect in the connectivity within the SN, which was previously associated with individual differences in cortisol stress responses (Zhang et al., 2019). These findings suggest that overall connectivity within the SN (i.e., interactions between network core regions) may better reflect the magnitude of cortisol stress reactivity but the connectivity between the SN and other neural circuits (i.e., particularly the posterior DMN) may be involved in vulnerability of or resilience to the long-term consequences of real-life stressors. This idea is also in line with the fact that the abnormalities in connectivity between the hub regions of the SN (i.e., amygdala and dACC) and DMN (i.e., PCC/PCu) have been consistently implicated in stress-related psychopathology (Akiki et al., 2017; Lei et al., 2015; D. R. Miller et al., 2017; Mulders, van Eijndhoven, Schene, Beckmann, & Tendolkar, 2015; Sripada et al., 2012).

Importantly, most studies reporting on the SN-DMN involvement in stress-related processing have focused on a single brain region or a few key regions, and have typically used a cross-sectional design to compare abnormalities of regional connectivity patterns observed in PTSD patients against healthy controls. No single study, to our knowledge, so far has used a network-based approach to link stress-induced connectivity patterns of these large-scale networks at baseline to the subsequent symptom development after trauma exposure. The results from this first prospective longitudinal study suing a network-based approach indicates that dys-synchronous SN-DMN communication in response to acute stress induction appeared to enhance the chance of undesired consequences in mental health after trauma exposure, and predicted high stress level 16 months later. Our findings therefore provided concrete evidence that reconfiguration of these large-scale networks upon acute stress exposure is highly relevant for investigating resilience and risk factors for PTSD.

On the other hand, we did not observe predictive effects of acute stress-induced overall DMN connectivity on the subsequent development of stress-related symptoms. In light of SN-DMN interaction that did exhibit a predictive effect, this suggests that the components of the DMN may have functioned in a non-adhesive manner in response to stress (i.e., the posterior parts such as the PCC and PCu interacting with the SN). Hence, the mean coefficient indicating overall cohesion of these components might fail to capture individual variability in symptom development after trauma. This postulation is in line with the existing observations where the DMN components demonstrated differential disruption patterns or associations with other brain circuits in PTSD (Miller et al., 2017; Sripada et al., 2012; Tursich et al., 2015).

In contrast to a few recent prospective longitudinal studies (Galatzer-Levy et al., 2014; Steudte-Schmiedgen et al., 2015), we did not find evidence for cortisol reactivity to acute stressors that was predictive of PTSD symptom development after trauma. This discrepancy may lie in the fact that our study sample is relatively resilient with subclinical level of symptom scores, whereas the sample in the study by Steudte-Schmiedgen et al. was predominantly clinical (i.e., combat soldiers) with larger variances in symptomology. In contrast to using a latent variable modeling approach for subtyping the tested sample, as has been done by Galatzer-Levy and colleagues, we linked cortisol stress reactivity before trauma exposure to the overall and sub-cluster PTSD symptom scores after trauma. Further investigations are in need to test the predictive value of cortisol stress responses, taking into account aforementioned differences in sample variance, as well as in analytical approaches.

Interestingly, SN reconfiguration to acute stress not only had predictive values in our study, it was also associated with acquired effects of stress-related symptoms. In specific, a reduction in the decoupling between the SN and anterior cerebellum was associated with higher intrusion symptoms after trauma exposure. Interestingly, the cerebellum has been has linked to emotional processing and regulation, particularly also negative emotional memories in a growing number of investigations (Strata, Scelfo, & Sacchetti, 2011; Piergiorgio Strata, 2015; also see review by Schutter & Van Honk, 2005). Recent studies also suggested its involvement in pathophysiology of PTSD (Baldaçara et al., 2011; Holmes et al., 2018; Monti et al., 2018; Rabellino, Densmore, Théberge, McKinnon, & Lanius, 2018; Sussman, Pang, Jetly, Dunkley, & Taylor, 2016; Yin et al., 2011). Our observation of strengthened connectivity between the anterior cerebellum and the overall SN therefore might have indicated the pathological processing of traumatic memories in the current sample.

There are a few limitations in the current study worth mentioning. First, although it is relevant to study stress resilience and vulnerability in a relatively resilient sample, it has the disadvantage of limited variation in stress-related psychopathology. As has been indicated in *Figure 3*, the majority of our participants showed little

changes in PCL and PSS scores between two assessments. Similar pattern was observed in the CAPS (i.e., majority of participants reported no clinical symptoms and only three participants met the criteria for a full-brown PTSD diagnosis). Most studies, predominantly the cross-sectional studies so far investigating the neurobiological correlates of PTSD symptoms have focused on the clinical populations in comparison with healthy controls, which could maximize the variances pertinent to symptomology (see review for Bremner, Elzinga, Schmahl, & Vermetten, 2007; Michopoulos, Norrholm, & Jovanovic, 2015). An advantage of our sample here is that it is not affected by the typical confounds that surround more severe psychopathology (e.g. medication intake), and that we had a good view on the premorbid status. Second, the limited temporal resolution of our assessments, twice with a 16-month interval, might not be sufficient to capture information on symptom evolvement. It would be of interest for future investigations to consider more personalized and time-delineated measurement of trauma experiences and symptom development, with data collection ideally at multiple time-points during and after trauma exposure. Lastly, in this study we found effects for PSS and CAPS, but not for PCL. This may be related to the relatively resilient study sample that showed limited variation in PTSD symptom level. It may imply that PSS is more sensitive to capture individual differences in a subclinical sample than PCL.

In conclusion, the current study used connectivity changes of large-scale neural networks in response to an acute stress challenge to predict subsequent stress-related symptoms after trauma exposure in police recruits. Whereas SN-DMN connectivity prospectively predicted the longitudinal changes in perceived stress level, altered SN-cerebellum connectivity was observed in participants with higher PTSD symptom levels. These findings suggest that acute stress-induced SN connectivity changes may serve as a potential marker of PTSD vulnerability.

References

Admon, R., Milad, M. R., & Hendler, T. (2013). A causal model of post-traumatic stress disorder: Disentangling predisposed from acquired neural abnormalities. *Trends in Cognitive Sciences*, *17*(7), 337–347.

Akiki, T. J., Averill, C. L., & Abdallah, C. G. (2017). A Network-Based Neurobiological Model of PTSD: Evidence From Structural and Functional Neuroimaging Studies. *Current Psychiatry Reports, 19, 81*.

Baldaçara, L., Jackowski, A. P., Schoedl, A., Pupo, M., Andreoli, S. B., Mello, M. F., … Bressan, R. A. (2011). Reduced cerebellar left hemisphere and vermal volume in adults with PTSD from a community sample. *Journal of Psychiatric Research*, *45*(12), 1627–1633.

Beckmann, C. F., & Smith, S. M. (2005). Tensorial extensions of independent component analysis for multisubject FMRI analysis. *NeuroImage*, *25*(1), 294–311.

Boubela, R. N., Kalcher, K., Nasel, C., & Moser, E. (2014). Scanning fast and slow: current limitations of 3 Tesla functional MRI and future potential. *Frontiers in Physics*, *2*.

Bremner, J. D., Elzinga, B., Schmahl, C., & Vermetten, E. (2007). Structural and functional plasticity of the human brain in posttraumatic stress disorder. *Progress in Brain Research, 167, 171-186*.

Caballero-Gaudes, C., & Reynolds, R. C. (2017). Methods for cleaning the BOLD fMRI signal. *NeuroImage*, *154*, 128–149.

Daniels, J. K., Mcfarlane, A. C., Bluhm, R. L., Moores, K. A., Richard Clark, C., Shaw, M. E., … Lanius, R. A. (2010). Switching between executive and default mode networks in posttraumatic stress disorder: Alterations in functional connectivity. *Journal of Psychiatry and Neuroscience*, *35*(4), 258–266.

De Kloet, E. R., Joëls, M., & Holsboer, F. (2005). Stress and the brain: From adaptation to disease. *Nature Reviews Neuroscience, 6, 463-475*.

Fox, M. D., & Raichle, M. E. (2007). Spontaneous fluctuations in brain activity observed with functional magnetic resonance imaging. *Nature Reviews Neuroscience*. https://doi.org/10.1038/nrn2201

Friston, K. J., Williams, S., Howard, R., Frackowiak, R. S. J., & Turner, R. (1996). Movement-Related effects in fMRI time-series. *Magnetic Resonance in Medicine*, *35*(3), 346–355.

Galatzer-Levy, I. R., Ma, S., Statnikov, A., Yehuda, R., & Shalev, A. Y. (2017). Utilization of machine learning for prediction of post-traumatic stress: A re-examination of cortisol in the prediction and pathways to non-remitting PTSD. *Translational Psychiatry*, *7*(3), 1–8.

Galatzer-Levy, I. R., Steenkamp, M. M., Brown, A. D., Qian, M., Inslicht, S., Henn-Haase, C., … Marmar, C. R. (2014). Cortisol response to an experimental stress paradigm prospectively predicts long-term distress and resilience trajectories in response to active police service. *Journal of Psychiatric Research*, *56*(2), 36–42.

Hastie, T. (2008). gam: Generalized Additive Models. R Package.

Hermans, E. J., Henckens, M. J. A. G., Joëls, M., & Fernández, G. (2014). Dynamic adaptation of large-scale brain networks in response to acute stressors. *Trends in Neurosciences*, *37*(6), 304–314.

Hermans, E. J., van Marle, H. J. F., Ossewaarde, L., Henckens, M. J. a. G., Qin, S., van Kesteren, M. T. R., … Fernandez, G. (2011). Stress-Related Noradrenergic Activity Prompts Large-Scale Neural Network Reconfiguration. *Science*, *334*(6059), 1151–1153.

Hervé, M. (2018). RVAideMemoire: Testing and Plotting Procedures for Biostatistics.

Holmes, S. E., Scheinost, D., DellaGioia, N., Davis, M. T., Matuskey, D., Pietrzak, R. H., … Esterlis, I. (2018). Cerebellar and Prefrontal Cortical Alterations in PTSD: Structural and Functional Evidence. *Chronic Stress*, *2*, 247054701878639.

Koch, S. B. J., Klumpers, F., Zhang, W., Hashemi, M. M., Kaldewaij, R., van Ast, V. A., … Roelofs, K. (2017). The role of automatic defensive responses in the development of posttraumatic stress symptoms in police recruits: protocol of a prospective study. *European Journal of Psychotraumatology*, *8*(1), 1412226.

Koch, S. B. J., van Zuiden, M., Nawijn, L., Frijling, J. L., Veltman, D. J., & Olff, M. (2016). Aberrant resting-state brain activity in posttraumatic stress disorder: A meta-analysis and systematic review. *Depression and Anxiety*, *33*(7), 592–605.

Lei, D., Li, K., Li, L., Chen, F., Huang, X., Lui, S., … Gong, Q. (2015). Disrupted Functional Brain Connectome in Patients with Posttraumatic Stress Disorder. *Radiology*, *276*(3), 818–827.

Liu, Y., Li, L., Li, B., Feng, N., Li, L., Zhang, X., … Yin, H. (2017). Decreased Triple Network Connectivity in Patients with Recent Onset Post-Traumatic Stress Disorder after a Single Prolonged Trauma Exposure. *Scientific Reports*, *7*(1).

McEWEN, B. S. (1998). Stress, Adaptation, and Disease: Allostasis and Allostatic Load. *Annals of the New York Academy of Sciences*, *840*(1), 33–44.

Menon, V. (2011). Large-scale brain networks and psychopathology: A unifying triple network model. *Trends in Cognitive Sciences*, *15*(10), 483–506.

Michopoulos, V., Norrholm, S. D., & Jovanovic, T. (2015). Diagnostic Biomarkers for Posttraumatic Stress Disorder: Promising Horizons from Translational Neuroscience Research. *Biological Psychiatry*, *78*(5), 344–353.

Miller, D. R., Hayes, S. M., Hayes, J. P., Spielberg, J. M., Lafleche, G., & Verfaellie, M. (2017). Default Mode Network Subsystems Are Differentially Disrupted in Posttraumatic Stress Disorder. *Biological Psychiatry: Cognitive Neuroscience and Neuroimaging*, *2*(4), 363–371.

Miller, G. E., Chen, E., Armstrong, C. C., Carroll, A. L., Ozturk, S., Rydland, K. J., … Nusslock, R. (2018). Functional connectivity in central executive network protects youth against cardiometabolic risks linked with neighborhood violence. *Proceedings of the National Academy of Sciences*, *115*(47), 12063–12068.

Monti, D. A., Tobia, A., Stoner, M., Wintering, N., Matthews, M., Conklin, C. J., … Newberg, A. B. (2018). Changes in cerebellar functional connectivity and autonomic regulation in cancer patients treated with the Neuro Emotional Technique for traumatic stress symptoms. *Journal of Cancer Survivorship*, *12*(1), 145–153.

Mulders, P. C., van Eijndhoven, P. F., Schene, A. H., Beckmann, C. F., & Tendolkar, I. (2015). Resting-state functional connectivity in major depressive disorder: A review. *Neuroscience & Biobehavioral Reviews*, *56*, 330–344.

Parkes, L., Fulcher, B., Yücel, M., & Fornito, A. (2018). NeuroImage An evaluation of the ef fi cacy , reliability , and sensitivity of motion correction strategies for resting-state functional MRI. *NeuroImage*, *171*, 415–436.

Power, J. D. (2017). A simple but useful way to assess fMRI scan qualities. *NeuroImage*, *154*, 150–158.

Pruim, R. H. R., Mennes, M., van Rooij, D., Llera, A., Buitelaar, J. K., & Beckmann, C. F. (2015). ICA-AROMA: A robust ICA-based strategy for removing motion artifacts from fMRI data. *NeuroImage*, *112*, 267–277.

Rabellino, D., Densmore, M., Théberge, J., McKinnon, M. C., & Lanius, R. A. (2018). The

cerebellum after trauma: Resting-state functional connectivity of the cerebellum in posttraumatic stress disorder and its dissociative subtype. *Human Brain Mapping*, *39*(8), 3354–3374.

R Foundation for Statistical Computing. (2018). *R: a Language and Environment for Statistical Computing. http://www.R-project.org/*.

Satterthwaite, T. D., Elliott, M. A., Gerraty, R. T., Ruparel, K., Loughead, J., Calkins, M. E., … Wolf, D. H. (2013). An improved framework for confound regression and filtering for control of motion artifact in the preprocessing of resting-state functional connectivity data. *NeuroImage*, *64*(1), 240–256.

Schutter, D. J. L. G., & Van Honk, J. (2005). The cerebellum on the rise in human emotion. *Cerebellum*, *4*(4), 290–294.

Shin, L. M., & Liberzon, I. (2010). The neurocircuitry of fear, stress, and anxiety disorders. *Neuropsychopharmacology*.

Sripada, R. K., King, A. P., Welsh, R. C., Garfinkel, S. N., Wang, X., Sripada, C. S., & Liberzon, I. (2012). Neural dysregulation in posttraumatic stress disorder: evidence for disrupted equilibrium between salience and default mode brain networks. *Psychosomatic Medicine*, *74*(9), 904–911.

Steudte-Schmiedgen, S., Stalder, T., Schönfeld, S., Wittchen, H. U., Trautmann, S., Alexander, N., … Kirschbaum, C. (2015). Hair cortisol concentrations and cortisol stress reactivity predict PTSD symptom increase after trauma exposure during military deployment. *Psychoneuroendocrinology*, *59*, 123–133.

Strata, P. (2015). The Emotional Cerebellum. *Cerebellum, 14(5), 570-577*.

Strata, P., Scelfo, B., & Sacchetti, B. (2011). Involvement of cerebellum in emotional behavior. *Physiological Research*, *60 Suppl 1*, S39-48.

Sussman, D., Pang, E. W., Jetly, R., Dunkley, B. T., & Taylor, M. J. (2016). Neuroanatomical features in soldiers with post-traumatic stress disorder. *BMC Neuroscience*, *17*(1).

Trevor Hastie, R. T. (1986). General additive models. *Statistical Science*, *1*(3), 297–318.

Tursich, M., Ros, T., Frewen, P. A., Kluetsch, R. C., Calhoun, V. D., & Lanius, R. A. (2015). Distinct intrinsic network connectivity patterns of post-traumatic stress disorder symptom clusters. *Acta Psychiatrica Scandinavica*, *132*(1), 29–38.

Uddin, L. Q. (2015). Salience processing and insular cortical function and dysfunction. *Nature Reviews Neuroscience, 16:55-16*.

van Wingen, G. A., Geuze, E., Vermetten, E., & Fernández, G. (2012). The neural consequences of combat stress: long-term follow-up. *Molecular Psychiatry*, *17*(2), 116–118.

Van Wingen, G. A., Geuze, E., Vermetten, E., & Fernández, G. (2011). Perceived threat predicts the neural sequelae of combat stress. *Molecular Psychiatry*, *16*(6), 664–671.

Wang, T., Liu, J., Zhang, J., Zhan, W., Li, L., Wu, M., … Gong, Q. (2016). Altered resting-state functional activity in posttraumatic stress disorder: A quantitative meta-analysis. *Scientific Reports*, *6*.

Weathers, F. W., Keane, T. M., & Davidson, J. R. T. (2001). Clinician-administered PTSD scale: A review of the first ten years of research. *Depression and Anxiety*.

Weathers, F. W., Ruscio, A. M., & Keane, T. M. (1999). Psychometric properties of nine scoring rules for the clinician- administered posttraumatic stress disorder scale. *Psychological Assessment*, *11*(2), 124–133.

Wood, S. N. (2011). Fast stable restricted maximum likelihood and marginal likelihood estimation of semiparametric generalized linear models. *Journal of the Royal Statistical Society. Series B: Statistical Methodology*, *73*(1), 3–36.

Yin, Y., Li, L., Jin, C., Hu, X., Duan, L., Eyler, L. T., … Li, W. (2011). Abnormal baseline brain activity in posttraumatic stress disorder: a resting-state functional magnetic resonance imaging study. *Neuroscience Letters*, *498*(3), 185–189.

Zhang, W., Hashemi, M. M., Kaldewaij, R., Koch, S. B. J., Beckmann, C., Klumpers, F., & Roelofs, K. (2019). Acute stress alters the "default" brain processing. *NeuroImage*, *189*, 870–877.

Zu Eulenburg, P., Caspers, S., Roski, C., & Eickhoff, S. B. (2012). Meta-analytical definition and functional connectivity of the human vestibular cortex. *NeuroImage*, *60*(1), 162–169.

Supplemental Materials and Methods

Preprocessing

Analysis of fMRI data was performed with FSL5.0.9 (FMRIB, Oxford, UK). The first five images of each resting-state scan were discarded to allow for $T2^*$ equilibration effects. Further preprocessing included motion correction, spatial smoothing with a 5mm FWHM kernel, denoising using ICA-AROMA (Pruim et al., 2015), and high-pass filtering with a cut-off of 100 seconds. To further minimize motion and psychophysiological confounds after the denoising procedure, the six realignment parameters, their temporal derivatives and the quadratic terms of both the original parameters and derivatives were used as motion parameters in a multiple linear regression model (Caballero-Gaudes et al., 2017; Friston et al., 1996; zu Eulenburg et al., 2012). Additionally, each individual T1 image was segmented for subject-specific white matter and CSF masks that were subsequently thresholded with a 95% probability and registered with functional image. Mean signal intensities of white matter and CSF were extracted and included in the regression model (Caballero-Gaudes & Reynolds, 2017; Satterthwaite et al., 2013). The resulting residuals were normalized with standard MNI atlas and analyzed subsequently. For each participant, one pre- and one post-stress rs-fMRI recording were preprocessed and analyzed.

Supplemental Results

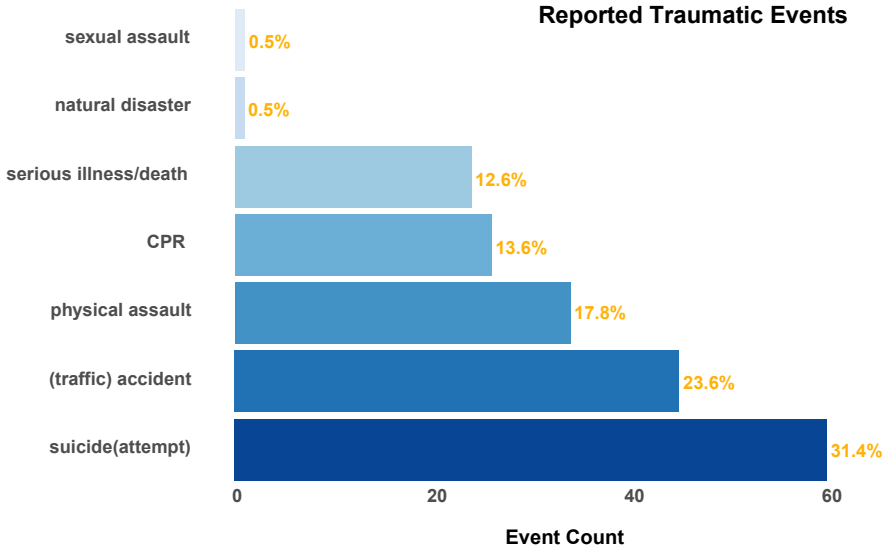

Figure S1. *Counts and frequency (percentage) of reported traumatic events that participants had experienced or witnessed during their emergency aid training (i.e., in between Wave 1 and Wave 2 assessments). Overall, suicide (including attempt) and (traffic) accidents were the most frequently experienced events, followed by physical assault, CPR (cardiopulmonary resuscitation) and serious illness or death. Experiences in natural disasters and sexual assault were most infrequent.*

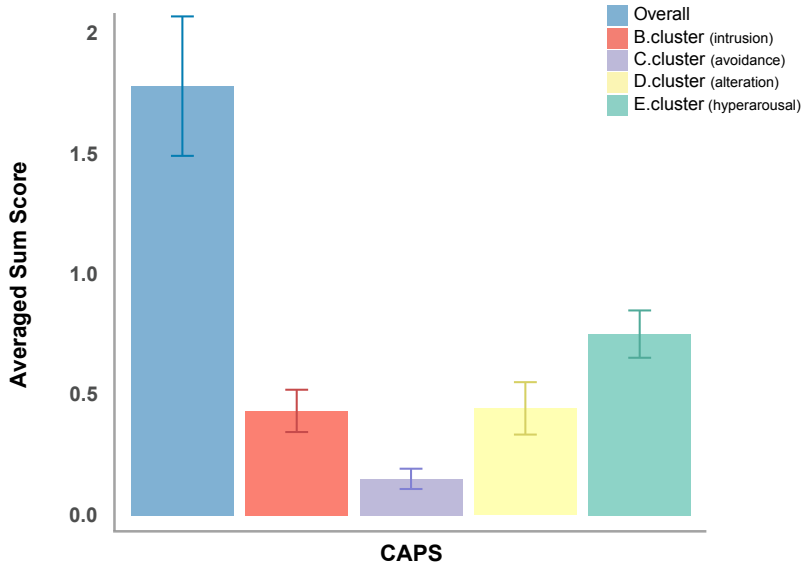

Figure S2. *Averaged sum scores of overall CAPS and each individual sub-cluster symptoms. At group level, overall CAPS scores increased significantly with increases in each individual sub-cluster symptoms.*

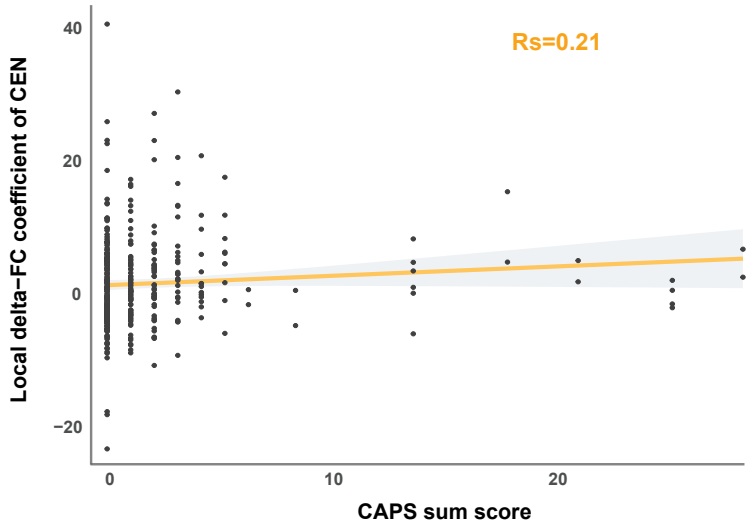

Figure S3. *Increases of connectivity within the CEN predicted higher levels of PTSD symptoms, indicated by CAPS sum scores.*

Supplementary Reference

Caballero-Gaudes, C., & Reynolds, R. C. (2017). Methods for cleaning the BOLD fMRI signal. *NeuroImage*, *154*, 128–149.

Friston, K. J., Williams, S., Howard, R., Frackowiak, R. S. J., & Turner, R. (1996). Movement-Related effects in fMRI time-series. *Magnetic Resonance in Medicine*, *35*(3), 346–355.

Pruim, R. H. R., Mennes, M., van Rooij, D., Llera, A., Buitelaar, J. K., & Beckmann, C. F. (2015). ICA-AROMA: A robust ICA-based strategy for removing motion artifacts from fMRI data. *NeuroImage*, *112*, 267–277.

Satterthwaite, T. D., Elliott, M. A., Gerraty, R. T., Ruparel, K., Loughead, J., Calkins, M. E., … Wolf, D. H. (2013). An improved framework for confound regression and filtering for control of motion artifact in the preprocessing of resting-state functional connectivity data. *NeuroImage*, *64*(1), 240–256.

Zu Eulenburg, P., Caspers, S., Roski, C., & Eickhoff, S. B. (2012). Meta-analytical definition and functional connectivity of the human vestibular cortex. *NeuroImage*, *60*(1), 162–169.

CHAPTER V

MEMORY CONTEXTUALIZATION: THE ROLE OF PREFRONTAL CORTEX IN FUNCTIONAL INTEGRATION ACROSS ITEMS AND CONTEXT REPRESENTATIONAL REGIONS

This chapter has been published as Zhang W, van Ast V, Klumpers F, Roelofs K and Hermans EJ* (2018) Memory contextualization: The role of prefrontal cortex in functional integration across items and context representational regions. Journal of Cognitive Neuroscience 30(4): 579-593.*

**Equal contributions*

Abstract

Memory recall is facilitated when retrieval occurs in the original encoding context. This context dependency effect likely results from the automatic binding of central elements of an experience with contextual features (i.e., memory "contextualization") during encoding. However, despite a vast body of research investigating the neural correlates of explicit associative memory, the neural interactions during encoding that predict implicit context-dependent memory remain unknown. Twenty-six participants underwent fMRI during encoding of salient stimuli (faces), which were overlaid onto unique background images (contexts). To index subsequent context-dependent memory, face recognition was tested either in intact or rearranged contexts, after scanning. Enhanced face recognition in intact relative to rearranged contexts evidenced successful memory contextualization. Overall subsequent memory effects (brain activity predicting whether items were later remembered vs. forgotten) were found in the left inferior frontal gyrus (IFG) and right amygdala. Effective connectivity analyses showed that stronger context-dependent memory was associated with stronger coupling of the left IFG with face- and place-responsive areas, both within and between participants. Our findings indicate an important role for the IFG in integrating information across widespread regions involved in the representation of salient items and contextual features.

Introduction

Context is essential for memory retrieval. It is well established that memories are easier to recall when retrieval occurs in a context that resembles the original encoding context (Godden & Baddeley, 1975; Smith & Vela, 2001; Endel Tulving & Thomson, 1973; van Ast, Cornelisse, Meeter, Joëls, & Kindt, 2013; van Ast, Cornelisse, Meeter, & Kindt, 2014). Memory contextualization, in which an event and its context are automatically bound together into one integrated representation during encoding, is vital for the subsequent retrieval of relevant memories in specific situations (Liberzon & Sripada, 2007; van Ast et al., 2013, 2014). Conversely, the inability to properly contextualize information has been linked to fragmentation of episodic memories and overgeneralization of (fear) memories that are characteristic of, for instance, post-traumatic stress disorder (PTSD) (Acheson, Gresack, & Risbrough, 2012; Brewin, Gregory, Lipton, & Burgess, 2010; Ehlers & Clark, 2000; Liberzon & Sripada, 2007; Meyer et al., 2013; Quaedflieg et al., 2015) or schizophrenia (Talamini, de Haan, Nieman, Linszen, & Meeter, 2010). However, despite its relevance for general healthy memory function and clinical memory overgeneralization, the brain mechanisms underlying memory contextualization – the process whereby automatic encoding of an item-in-context results in subsequent *implicit* context effects on memory – are just beginning to be explored.

Evidence from rodents shows that selective hippocampal damage results in deficits in forming a memory of the context (or location) where items were previously experienced (Eichenbaum, 2004). For instance, rats with hippocampal lesions fail to recognize a previously encountered object when contextual information relative to encoding has been changed (Mumby, Gaskin, Glenn, Schramek, & Lehmann, 2002). Other evidence for a role of the hippocampus in implicit context effects on memory for cues comes from fear conditioning studies: in addition to conditioned freezing to an auditory cue, rats also exhibit freezing behavior when placed in the training context, but hippocampal lesions eliminate such contextual fear responses without affecting conditioned responses to the tone (Phillips & LeDoux, 1992). Recently, using large-scale neuronal population recordings, new insights into the nature of hippocampal context representations have emerged. Such studies show that hippocampal ensemble context codes become associated with the memories and behaviors that are appropriate for that context. When confronted with a familiar context, the hippocampal context code is automatically re-expressed, thereby priming the relevant memories and reducing the interference from memories associated with other contexts (for a review see Smith & Bulkin, 2014).

Analogous to this animal work, implicit context dependency of memories has been demonstrated consistently in human studies where context similarity between the original encoding and retrieval context enhanced both recognition and recollection (Cox, Tijdens, Meeter, Sweegers, & Talamini, 2014; Talamini et al., 2010; Talamini

& Gorree, 2012; Tsivilis, Otten, & Rugg, 2001; van Ast et al., 2013, 2014). The consistent observation of highly context dependent memories across this wide range of studies underscores context-dependent memory as one of the hallmarks of human episodic memory (Tulving, 1972). With respect to the neural correlates of such context-dependent memories, one study using magnetoencephalography (MEG) has shown that with an intact encoding-retrieval context, high theta power during encoding predicted successful recognition, whereas high theta power was detrimental when the retrieval context was rearranged relative to encoding. In addition, cross-frequency coupling analysis revealed a context-dependent theta-to-gamma memory effect which was assigned to the left hippocampus using source localization (Staudigl & Hanslmayr, 2013). An intracranial electroencephalography (iEEG) study furthermore implicated the prefrontal cortex (PFC) in successful item in context (temporal, in this case) binding during implicit memory encoding (Long & Kahana, 2015). However, given inherent uncertainty of (deep) source localization of EEG and MEG signals, and limited coverage of iEEG, an extension of these findings using techniques that allow for stronger spatial inferences, such as functional MRI (fMRI), is needed.

In contrast with such studies assessing (neural) encoding mechanisms that can subsequently modulate implicit context effects on recognition, previous fMRI studies have almost exclusively focused on how subsequent *explicit* memory of relations among cues is accomplished during encoding (Davachi, 2006). 'Context' in these studies refers to scenes that were explicitly associated with objects: the corresponding retrieval tests directly probed associative memory among these cues. These studies converge on the idea that explicit encoding of items versus context memories rely on distinct operations within the medial temporal lobe, in which "what" and "where" processing streams function in parallel and converge within the hippocampus (Davachi, 2006; Diana, Yonelinas, & Ranganath, 2007; Eichenbaum, Sauvage, Fortin, Komorowski, & Lipton, 2012; Ranganath, 2010b). In addition to the hippocampus, the PFC has been shown to play an equally important role in relational memory encoding when the integration of contextual information with specific item features is required (Murray & Ranganath, 2007; Prince, 2005; Summerfield et al., 2006). Indeed, lateral areas of the PFC might be involved in selecting task-relevant information and in strategy implementation to find associations among items during memory encoding(Ranganath, 2010a). When an event is encoded in a particular context, the PFC is therefore likely to contribute to the process of integrating relevant elements together. In agreement with this line of reasoning, some fMRI studies documented the involvement of both the hippocampus and the PFC in enhanced item (i.e., word) memory in semantic versus non-semantic contexts (Kapur et al., 1994; Wagner, 1998), or maintaining a representation of temporal context (Davachi & DuBrow, 2015; Jenkins & Ranganath, 2010). However, as these studies employed either explicit encoding instructions with subsequent associative recognition, or very broad context manipulations, such observations do

not necessarily imply that the same brain regions are involved when no explicit instructions are given to memorize the relevant items (i.e., incidental encoding), or when subsequent recognition is putatively modulated by implicit context effects. Indeed, a patient study suggests that the neural structures underlying explicit binding versus implicit contextual probing may differ (Chun & Phelps, 1999; Graf & Schacter, 1985). Thus, previous fMRI studies did not unequivocally address the question, which neural processes during encoding contribute to subsequent implicit context effects on memory.

Only two studies so far used an implicit context manipulation during recognition (Hayes, Baena, Truong, & Cabeza, 2010; Hayes, Nadel, & Ryan, 2007). In those studies, faces during encoding were presented against a naturalistic scene (Hayes et al., 2007; 2010) or a monocolored white (Hayes et al., 2007) and black (Hayes et al., 2010) background. Both studies found a decrement in recognition when a face encoded in a scene-context was presented against the monocolored background during recognition, as compared to faces that were presented against the monocolored background both during encoding and recognition. This effect was associated with a larger subsequent memory effect (SME), for example, in the hippocampus as well as enhanced connectivity between the hippocampus and visual association areas for the face in scene-context (Hayes et al., 2010). However, the stronger involvement of the hippocampus and its associated connectivity with face-responsive areas can be explained by the more complex and visually richer scene processing during encoding, as simply perceiving visually rich scenes has been associated with extensive hippocampal activation (Zeidman, Mullally, & Maguire, 2015). Therefore, it remains to be convincingly shown that PFC and hippocampus are involved in memory contextualization during encoding, resulting in subsequent implicit context effects on memory.

In the current study, we investigated the hypothesis that information across neural circuits involved in item and context representations would be integrated by the hippocampus and prefrontal regions to subserve memory contextualization, subsequently resulting in context-dependent memories. To investigate this, we implemented a memory task using neutral face images as items and scene images as contexts. Crucially, we manipulated context similarity during recognition relative to encoding, by presenting faces against either identical (intact) or different (rearranged) scenes. By doing so, we ensured the presence of visually rich background images at all time. Further, any modulation in memory performance by a shift in context cannot be driven by a change in familiarity, as all items and contexts have already been presented during encoding. Behaviorally, we expected to observe enhanced face recognition in intact contexts versus rearranged contexts (Cox et al., 2014; Meyer, Krans, van Ast, & Smeets, 2017; Talamini et al., 2010; van Ast et al., 2013, 2014). Since stronger context-dependent memory is observed with “deeper” encoding strategies (De Beni & Pazzaglia, 1995; Graf & Schacter,

1985; Richardson, 1980), we explicitly instructed our participants to actively form a vivid mental image of the face in context, and to indicate on a trial-by-trial basis how well they did in forming this mental face-in-context image. We expected that this 'subjective memory contextualization index' during encoding would predict subsequent context-dependent face memory. At the neural level, regardless of context, we expected to find subsequent memory effects for the faces in the face-responsive region of the fusiform gyrus (FG) (i.e., fusiform face area; FFA) and/or the amygdala, in line with previous research (Kanwisher, McDermott, & Chun, 1997; Kanwisher & Yovel, 2006). In response to the presented contexts, we expected activity in the place-responsive region in the parahippocampal gyrus (i.e., parahippocampal place area; PPA), as this region has been linked to the representation of contextual features (Epstein, Harris, Stanley, & Kanwisher, 1999). Most importantly, we predicted that the integration of face (FFA/amygdala) and context (PPA) representations during effective memory contextualization would be associated with stronger neural activity in the PFC and hippocampus. Finally, as actively integrating information likely requires functional connections among these brain regions, we also expected to find stronger neural coupling between the PFC/hippocampus and distributed areas involved in representations of face (FFA/amygdala) and context (PPA) to support memory contextualization.

Methods and Materials

Participants

Thirty-four right-handed university students (mean age=23.65) with no history of neurological or psychiatric disease gave written informed consent. Due to technical failure (e.g., MR scanner malfunction), data of eight participants were lost. Also, in line with previous memory research (Rimmele, Davachi, & Phelps, 2012), participants were excluded from the analyses in case their memory performance did not exceed chance level, leading to exclusion of an additional 5 participants (see 2.3.2). Consequently, current analyses are based on 21 participants (mean age=24.24, SD=2.86; N_{female}=15). All study procedures were approved by the local institutional review board (Commissie Mensgebonden Onderzoek Regio Arnhem-Nijmegen).

Experimental tasks and procedure

A localizer task and encoding part of the memory contextualization task (MCT-encoding) were administered during fMRI scanning. Recognition (MCT-recognition) was assessed outside the scanner. In total, 280 color images of faces from three databases (Langner et al., 2010; Lundqvist, Flykt, & Ohman, 1998; Tottenham et al., 2009) and 160 color images from various sources that depict indoor scenes, city landscapes, or natural scenes were selected for these two tasks. All tasks were

administered using Presentation® software (Version 16.4, www.neurobs.com).

Localizer task

A functional localizer task was used to identify brain activation elicited specifically by faces and contexts. Forty face images (out of total 280), forty context images (out of total 160) and an equal number of those images that were phase scrambled were presented in the task. Scrambling was accomplished within MATLAB (The MathWorks Inc., 2012) by randomizing the Fourier-transformed phase of R, G and B layers of each stimulus image, which was then added to the existing RGB phase structures in the original images. Thereby, the relative phase of the RGB layers in the scrambled images was identical to that in the original images, and the color composition was kept the same as in the original images as well.

During the task, the four categories (face, context, scrambled face and scrambled context) of image stimuli were presented with a blocked design. The order of the sixteen blocks was mirrored to avoid co-variation of task effects with linear trends. Within each block, 20 images from one specific category (e.g., face) were continuously presented in 20 trials of 1-s duration, without inter-trial interval (ITI). In each trial, the face or scrambled face stimuli were presented within an oval shape in the middle of the screen while the context or scrambled context stimuli were presented full-screen. All images used in the localizer task were presented twice, resulting in a total of 320 trials. To keep participants engaged, a small red dot was presented in half of the trials that were randomly selected. Participants were instructed to indicate their detection of the red dot using a button press.

Memory contextualizatin task

During the memory contextualization task (MCT), faces served as to-be recognized items, while background scenes served as context. A total number of 240 face images and 120 context images were used in MCT. The face images were divided into two sets, each of which was randomly selected as either the target stimuli (i.e., used in both the encoding (MCT-encoding) and recognition (MCT-recognition) phases) or as the lures (i.e., used only in MCT-recognition phase). The 120 context images used in the MCT-encoding were used again in the MCT-recognition.

MCT-encoding

In order to pair the face and context images and to assign the paired face-context combinations to different conditions that were later presented in the MCT-recognition as either intact or rearranged, the randomly selected 120 face images for encoding were divided into two subsets with 60 gender-matched face images in each subset. Similarly, all context stimuli were also divided into two subsets that

were matched on location (indoors vs. outdoors) of contexts. For each participant, the face and the context stimuli subsets were randomly assigned to intact or rearranged condition of MCT-recognition and those faces and contexts were then randomly paired up (i.e., face-context combination), resulting in randomized pairing of face-context combinations within each condition. Furthermore, restrictions were made so that no trials from one condition (i.e., intact) were presented more than twice consecutively for each participant (see 2.2.2.2). All stimuli were presented in 120 trials with a jittered ITI (average duration = 2 sec).

It is worth mentioning that the terms "intact" and "re-arranged" have previously been used to refer to explicit knowledge of item–item associations in some studies (e.g., Litman & Davachi, 2008; Giovanello, Schnyer, & Verfaellie, 2004; Jackson & Schacter, 2004). Here, we follow other recent studies that used the same terms to investigate implicit context effects (Meyer et al., 2017; van Ast et al., 2013, 2014; Hayes et al., 2010; Tsivilis, Otten, & Rugg, 2001).

The MCT-encoding task was introduced as a test of imagination ability to induce deep incidental encoding (van Ast et al., 2013) since deeper or more vivid encoding strategies have been shown to strengthen context-dependent memory (De Beni & Pazzaglia, 1995; Richardson, 1980). Specifically, participants were instructed to imagine a scene where the person (face) interacts with the place (context) as vividly as possible in each trial. We reasoned that these instructions would aid deep encoding and thereby promote the formation of an association between faces and their unique contexts (De Beni & Pazzaglia, 1995; Richardson, 1980).

A 6-minute long practice session, using the same face and context stimuli as in the localizer task was carried out before the MCT-encoding task (*Figure 1A*). This practice session allowed the participants to become familiarized with the task and helped to attenuate primacy effects. To further balance remaining primacy effects across participants, ten trials from each condition (i.e., to-be intact or to-be rearranged) were randomly selected and presented in an intermixed way in the first 20 trials and the same items were tested at the beginning of the MCT-recognition task (see below). Note that these 20 trials were not removed from analyses. We aimed to minimize primacy effects because the current study focused on the encoding process, primacy effects are mainly due to, for example, novelty effects during encoding. We did not make specific restrictions to control recency effects, but because trials were presented in a random order, no systematic influence on recency effects can be expected.

Within each trial, a one-second presentation of a context stimulus was followed by a three-second overlaid presentation of an oval-shaped face stimulus to allow the encoding of context alone without the interference from centrally-presented face stimuli. Participants then reported how well they could imagine the person

being part of this scene within one second, using a four-item scale (i.e., from "not vivid at all" to "perfectly vivid"). This trial-by-trial index was used as subjective contextualization ability. Total duration of the MCT-encoding task was 14 minutes (7 sec x 120 trials).

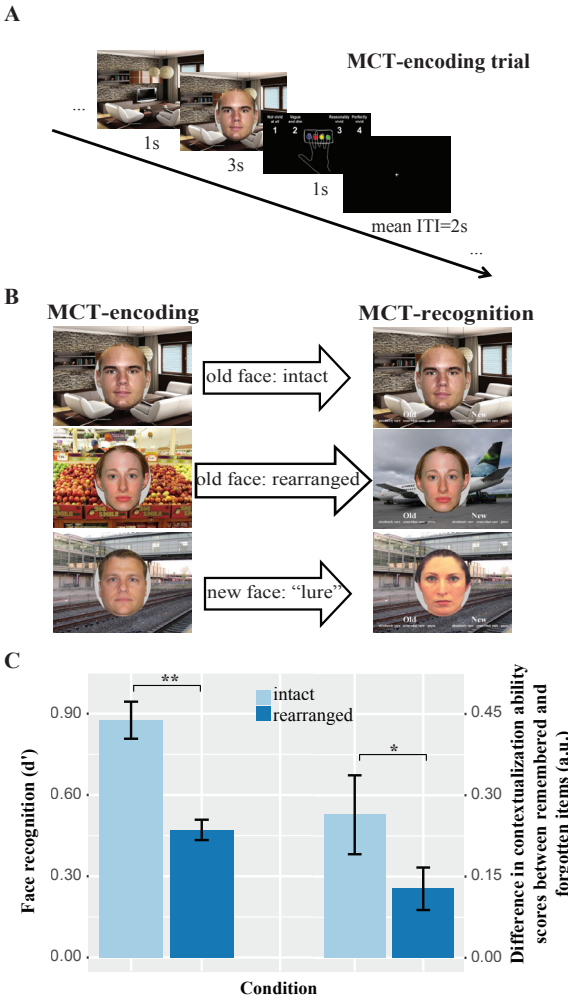

Figure 1. *Experimental paradigm of MCT and the validation of the experiment. (A) MCT-encoding trial: For each trial of the encoding task, the context stimulus was presented for 1 sec, followed by the combined presentation of the face and context stimuli for 3 sec. Participants were instructed to imagine the person interacting with the context. Participants then reported how well they could imagine this interactive scene on a 4-point scale (1 = not vivid at all, 4 = perfectly vivid) presented for 1 sec. Trials were separated by a jittered ITI with an average of 2 sec. (B) MCT-encoding and recognition: During recognition, previously presented face stimuli from the encoding task (left) were presented against either their original encoding context stimuli ("intact") or against different ones ("rearranged"). New face stimuli (not seen during encoding) were presented in "lure" trials against context stimuli (seen during encoding and recognition; bottom right). The presentation of face and context stimuli in the recognition task was self-paced. Participants were instructed to indicate if the presented face was old or new and to what extent they were confident about their judgment based on a 6-point scale. (C) A significant difference in d' was found between intact and rearranged trials, which validated the experimental manipulation of context dependency of face memory*

*(left); higher subjective contextualization ability scores were found for remembered versus forgotten items in intact versus rearranged conditions (right). Error bars represent standard errors of the mean. **p < .001, two-tailed; *p < .05, one-tailed.*

MCT-recognition

Face recognition took place outside the scanner approximately 20 minutes, with a range of 18 to 22 minutes, after participants had finished the encoding task. The 120 old faces from encoding were intermixed with 120 new faces (i.e., "lures"). Crucially, to assess context-dependent memory, half of the old faces was presented against the same context stimuli as in the encoding task (intact condition), while the other half was reshuffled and presented in different face-context combinations (rearranged condition). New faces were randomly combined with the 120 old contexts. Thus, during recognition each context was presented twice in total. As explained above, the first 20 trials from the encoding phase were intermixed with 20 trials containing new faces (i.e. not presented in the encoding task) and presented at the beginning of recognition for each participant. The number of trials for each condition out of those 40 trials was counterbalanced: 10 trials from the intact condition, 10 trials from the rearranged condition (thus in total 20 trials with old faces) as well as 20 trials from the "lure" condition. During the entire task, the trial sequence was pseudo-randomized individually, whereby neither old nor new faces, nor the trials from the same condition were presented on more than two trials consecutively.

For each trial, the face stimulus was presented overlaid onto the context. A 6-point confidence rating scale was presented at the bottom of the screen (*Figure 1B*), with which participants indicated if the face was old or new and to what extent they were confident about their judgment (1=absolutely sure it was a new face; 2=somewhat sure it was a new face; 3=guessing it was a new face; 4=guessing it was an old face; 5=somewhat sure it was an old face; 6=absolutely sure it was an old face). Trials were self-paced, and a fixed two-second inter-trial interval was used. On average, the MCT-recognition task took 22 minutes (5.5 sec * 240 trials).

Data acquisition and analysis

fMRI data acquisition

All images were acquired using a 3 Tesla Siemens Magnetom Skyra (Erlangen, Germany) MRI scanner with a 32-channel head coil at the Donders Institute for Brain, Cognition and Behavior in Nijmegen, the Netherlands. High-resolution structural images ($1\times1\times1mm^3$) were acquired using a T1-weighted MP-RAGE sequence (TR=2300 ms, TE=3.03 ms, flip angle=8°, FOV=256×256×192 mm^3). During both localizer and encoding tasks, $T2^*$-weighted dual-echo EPI BOLD-fMRI images were acquired using an interleaved ascending slice acquisition sequence (slices=40,

TR=2570 ms, TEs=15/35.7 ms, flip angle=90°, voxel size =2×2×2mm^3, slice gap=0.34 mm, FOV=212×212 mm^2). Gradient-echo field-map data were also acquired for EPI off-resonance distortion correction (slices=64, TR=1020 ms, TEs=10/12.46 ms, flip angle=90°, FOV=224×224 mm^2, slice thickness=2 mm).

Behavioral data analysis

Participants were tested in a within-subjects factorial design with subsequent memory (later remembered versus later forgotten) and retrieval context (intact versus rearranged) as main experimental factors. To ensure memory performance was above chance level, we conducted binomial tests to investigate the statistical significance of the observed deviations (number of remembered vs. forgotten trials) from the null distribution (i.e., random performance). We defined above- chance level performance as a number of correct trials. that has a chance of $p < .05$ of arising from this null distribution. This criterion led to a threshold of 134 correct trials ($p = .041$) out of 240 faces presented in the recognition task. Based on this procedure, data from five participants were excluded from all analyses.

To assess memory recognition, hit rates (i.e., proportion of correct responses to "old" faces) and false alarm rates (i.e., proportion of incorrect responses to "new" faces) were calculated and then converted to d-prime (d'; the sensitivity index used in signal detection theory that takes into account response bias (Emmerich, 1967) as a function of retrieval context, and of subjective contextualization ability. The difference of d' between intact and rearranged conditions (i.e., delta d') quantified context dependency of memory, with a larger delta d' indicating a stronger contextualization effect.

Subjective contextualization ability was derived from the trail-by-trail vividness scores that participants reported for their imagined scenarios involving the face-in-context stimuli. These contextualization ability scores were analyzed using a repeated-measures ANOVA with Subsequent memory performance (i.e., hits vs. misses) and Retrieval conditions (i.e., intact vs. rearranged) as within-subject factors. When the analysis returned a significant inter- action effect, we used a (one-tailed) t test to test our prediction that the difference between contextualization ability scores for hits and misses would be larger in intact than in rearranged trials. Furthermore, hit rates corrected for false alarm rates (i.e., hit rates minus false alarm rates) were modeled as a function of confidence level (i.e., low, middle and high) and retrieval conditions (i.e., intact vs. rearranged) to investigate the association between memory performance and confidence rating-based memory strength (Kirwan, Wixted, & Squire, 2008; Slotnick & Dodson, 2005). A repeated-measures ANOVA was used for these models.

fMRI data analysis

Data preprocessing and statistical analyses were carried out using Statistical Parametric Mapping Software (SPM8, Wellcome Trust Centre for Neuroimaging). Prior to preprocessing, dual-echo images were corrected for geometric distortions caused by magnetic field inhomogeneity (Hutton et al., 2002) separately for each echo, using field map images. The corrected single-echo images were then recombined using the parallel-acquired inhomogeneity-desensitized (PAID) method (Poser, Versluis, Hoogduin, & Norris, 2006). Preprocessing and further analyses were carried out on the combined images. The first five recombined EPI volumes were discarded to allow for T1 equilibration. Preprocessing of the fMRI data included coregistration of functional and structural images using mutual information maximization, spatial normalization with the Montreal Neurological Institute (MNI) template using non-linear warping, and spatial smoothing using an 8mm FWHM Gaussian kernel.

Functional localizer

To localize the brain regions responsive to faces and contexts respectively, brain activation in response to faces in contrast to scrambled faces, and to contexts in contrast to scrambled contexts, were estimated using a GLM model with 24 additional motion parameters as nuisance regressors (six realignment parameters, six squared realignment parameters, six first derivatives of realignment parameters and six squared first derivatives of realignment parameters). Voxel-level whole-brain FWE corrections were used as multiple comparison correction. Since the fusiform gyrus (FG; including fusiform face area, FFA) and the amygdala have been implicated in facial feature processing (Mende-siedlecki, Said, & Todorov, 2013; Todorov, 2012), while the parahippocampal gyrus (PHG; including parahippocampal place area, PPA) has been associated with context representations, we a-priori hypothesized that these regions would be involved in face and context processing, respectively. In line with these hypotheses, we then created three spherical ROIs with an 8mm radius centered at the peak voxels of aforementioned regions.

Memory contextualization

To investigate brain mechanisms underlying memory contextualization, all trials during encoding were sorted based on whether faces were later remembered or forgotten (i.e., subsequent memory effects, SMEs; Brewer, Zhao, Desmond, Glover, & Gabrieli, 1998; Gabrieli, Brewer, Desmond, & Glover, 1997; Kirchhoff, Wagner, Maril, & Stern, 2000; Nyberg, Cabeza, & Tulving, 1996; Paller & Wagner, 2002; A. Wagner, 1998) To ensure that neural correlates truly related to successful memory formation, we checked whether the subjective confidence levels as assessed during memory recognition related to successful subsequent memory. Hit rates

differed from false alarm rates for high ($t(18) = 5.45$, $p < 0.001$), middle ($t(19) = 10.23$, $p < 0.001$) and low confidence levels ($t(19) = 2.15$, $p = 0.045$). However, a closer examination revealed that at the lowest confidence level, participants on average recognized old faces correctly in 21 out of a total 38 of trials (hit rate=55%), whereas they misjudged new faces as "old" (i.e. false alarm) in 19 trials out of a total of 40 (false alarm rate=48%). Based on the observed false alarm rate (19/40), one can estimate the number of correct guesses as (38*19/40=) 18 trials out of a total of 38 low-confidence trials. Therefore, only (21-18=) three additional correct recognitions on average can be attributed to a performance benefit due to memory. We therefore excluded all low-confidence correct trials from the SME analyses. The "remembered" trials for the SME analyses therefore only included trials where participants recognized faces with middle to high confidence level. Consequently, the average trial number for each regressor (i.e., hits/misses in intact/rearranged conditions) in the fMRI statistical model ranged from 23 to 37 across participants.

For statistical analysis of the encoding task, event-related trial responses were modeled with 4-second box-car functions in a 1st-level GLM analysis and separate regressors were created for "remembered" and "forgotten" trials in intact versus rearranged conditions. Additionally, subjective contextualization ability scores were added in the model as linear parametric modulators to remembered and forgotten trials, respectively, which we expected to predict the subsequent memory of faces. Mean time series of white matter and CSF, as well as 24 motion parameters were included as nuisance regressors. The main effects of SM and their interactions with retrieval context (i.e., memory contextualization where SMEs differ between conditions) were tested at the group level. A-priori ROIs including the amygdala, face- and context-responsive regions were used for small volume correction (SVC). In addition to those functional ROI masks derived from the localizer task, we used the standardized bilateral hippocampus parcellation from the Automated Anatomical Labeling template (AAL; Tzourio-Mazoyer et al., 2002).

Finally, a psychophysiological interaction (PPI) analysis (Gitelman, Penny, Ashburner, & Friston, 2003) was conducted to investigate functional connectivity associated with memory contextualization. The brain regions that not only activated in response to the overall SME contrast (remembered vs. forgotten trials), but also were associated with the subjective contextualization ability score, were taken as the seed region for the analysis. We first extracted the BOLD time courses of the seed region and calculated the first eigenvariate. We then deconvolved this time course using the canonical HRF to obtain the estimated time course of neural activity, which was used as physiological component. The interaction of the subsequent memory (remembered versus forgotten) and retrieval context (intact versus rearranged) was used to define the psychological component. We then created the psychophysiological interaction (PPI) term by multiplying the psychological and physiological components. This interaction time course, which is

used to test for stronger connectivity associated with subsequent memory in intact versus rearranged trials, was reconvolved with the canonical HRF and then included in new first-level models alongside the first eigenvariate of the seed-region time course. We then calculated the parameter estimate maps for the PPI regressor for each participant, and used a one-sample t-test at second level to test this interaction at the group level. We further used the effective connectivity coefficients of this PPI analysis to behaviorally predict context dependency of memories that was indicated by the delta d' between intact and rearranged conditions across all participants via an ANCOVA. We further checked the distribution of delta d' based on the calculation of Mahalanobis distance for potential outliers, and then used non-parametric permutation tests (Nichols & Holmes, 2001) for verification of results if any data point deviated from the mean more than two standard deviations.

All statistical analyses of fMRI data have used voxel-level whole-brain FWE corrections or SVCs for a-priori ROIs with $p<0.05$.

Results

Memory Performance

As expected, we found stronger context dependency of memory for faces, indicated by higher d0 in intact versus rearranged trials, $F(1, 20) = 64.59$, $\eta 2p = .76$, $p < .001$ (see Figure 1C; also see hits/misses per condition, per confidence level in Table 1). Confidence ratings during recognition, which can be seen as a measure of memory strength (Kirwan et al., 2008; Slotnick & Dodson, 2005), were associated with memory performance, $F(2, 26) = 156.11$, $\eta 2p = .92$, $p < .001$, as indicated by a main effect of Confidence level on memory performance, with better memory performance (i.e., higher hit rate minus false alarm rate) at higher confidence levels: high level > middle level, $t(14) = 11.7$, $p < .001$; middle level > low level, $t(16) = 7.99$, $p < .001$. This effect was also modulated by context, $F(1, 13) = 7.84$, $\eta 2p = .38$, $p < .005$, as indicated by an interaction effect of Confidence level and Retrieval condition, with all three levels of confidence ratings associated with better memory performance in intact versus rearranged trials: $intact_{high} > rearranged_{high}$, $t(15) = 6.14$, $p < .001$; $intact_{mid} > rearranged_{mid}$, $t(17) = 3.84$, $p < .005$; $intact_{low} > rearranged_{low}$, $t(16) = 2.29$, $p < .05$ (also see *Table 1*).

Table 1. Descriptives [Mean Number of Trials and Accuracy (*SEM*)] of Memory Performance

Stimulus	*Target*						*Lure*	
Retrieval Context	*Intact*			*Rearranged*			*n.a.*	
Memory Performance	*Hit*	*Miss*	*HR-FAR*	*Hit*	*Miss*	*HR-FAR*	*CR*	*FA*
Confidence level								
Overall	39.57 (1.41)	20.86 (1.43)	0.16 (0.03)	30.05 (1.08)	29.52 (1.04)	0.03 (0.02)	80.86(2.18)	39.14(2.18)
High	16.67 (2.14)	5.71 (1.36)	0.54(0.03)	8.19(1.28)	7.57 (1.69)	0.33 (0.05)	24.71(4.63)	6.95(1.33)
Middle	13.14 (1.43)	8.24 (0.79)	0.10 (0.03)	11.57 (1.13)	11.76 (1.14)	0 (0.03)	35.62(3.10)	13.38(1.52)
Low	9.76 (1.28)	6.90 (1.08)	−0.17 (0.04)	10.29 (1.08)	10.19 (1.28)	−0.24 (0.03)	20.52(2.29)	18.81(1.83)
d^0	0.88(0.07)		*n.a.*	0.47(0.04)		*n.a.*	*n.a.*	

Note that false alarm rates are assessed in lure trials and can therefore not be calculated separately for intact versus rearranged trials. CR = correct rejection; FA = false alarm; HR-FAR = hit rate minus false alarm rate; n.a. = not applicable.

Higher subjective contextualization ability scores during encoding were associated with trials that were later re- membered versus forgotten, $F(1, 20) = 19.55$, $\eta 2p = .49$, $p < .001$ (mHit = 2.84, SEM = 0.44; mMiss = 2.64, SEM = 0.46). In agreement with our expectations, this difference in subjective contextualization ability score for remembered versus forgotten items was enhanced by context similarity, $t(20) = 1.79$, $p = .045$, one-tailed (see *Figure 1C* and *Table 2*), suggesting a predictive effect of contextualization ability on the degree to which context aids retrieval.

These behavioral results demonstrate that the MCT resulted in context-dependent memories, allowing to then investigate the neural mechanisms of these effects.

Table 2. Descriptives [Mean Scores (*SEM*)] of Subjective Contextualization Ability

Retrieval Context	*Intact*		*Rearranged*	
Memory Performance	*Hit*	*Miss*	*Hit*	*Miss*
Overall	2.90 (.075)	2.70 (.087)	2.88 (.080)	2.75 (.087)
High confidence level	3.09 (.11)	2.13 (.33)	2.79 (.18)	2.31 (.25)
Middle confidence level	2.65 (.17)	2.54 (.17)	2.65 (.17)	2.47 (.18)
Low confidence level	2.41 (.20)	2.42 (.20)	2.67 (.18)	2.67 (.18)

Note that subjective contextualization ability score was not tested statistically as a function of confidence level.

Definition of regions of interest

Brain activity during the localizer task was investigated using the [face>scrambled face] and [context>scrambled context] contrasts. Among other regions, the FFA, the amygdala, and the inferior frontal gyrus (IFG) were identified for the contrast Face>Scrambled Face. A cluster of suprathreshold voxels lying at the junction of the PG and PHG (FG-PHG junction) for the contrast Context>Scrambled Context was detected as well (see *Table 3* for full results). Specifically, as one of the most active clusters in response to contexts resided in the fusiform gyrus and extended to the adjacent regions (i.e., parahippocampal gyrus), the peak voxel in the FG-

PHG junction was defined as the voxel with strongest activity within the PHG that was closest to the boundaries of two regions based on AAL atlas. For later analyses on these regions of interest, spherical functional ROI masks for FFA, amygdala, and FG-PHG junction were created on the basis of these results, in addition to the anatomical template of the hippocampus (see "Memory contextualization" in Methods and Materials).

Memory contextualization

Brain regions associated with SMEs independent of context (i.e., all remembered > all forgotten) were identified in the left IFG (p<.05, whole-brain FWE) and left amygdala (p<0.001, SVC), but not in FFA and the FG-PHG junction (not even at a more liberal threshold of p<0.005, uncorrected). A cluster of suprathreshold voxels in the left hippocampus showed marginally significant activation (p=0.058, SVC; see *Figure 2A* and *Table 3*).

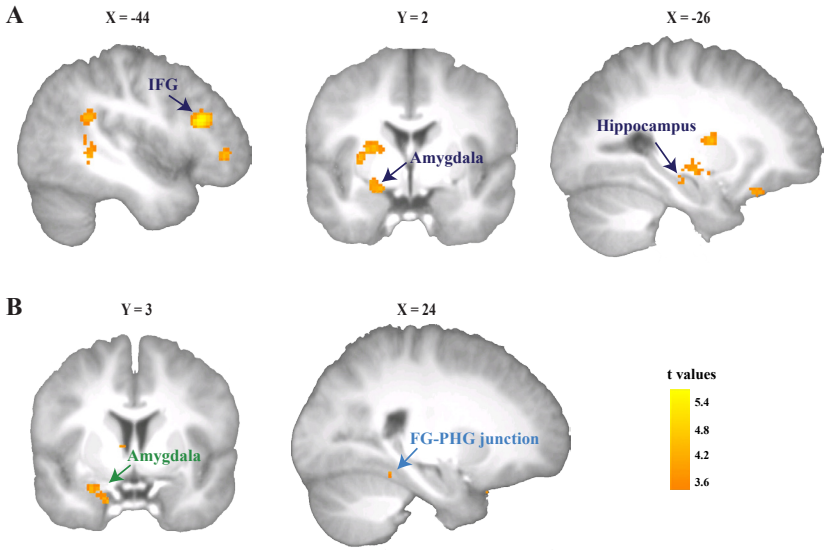

Figure 2. *Brain activity associated with SMEs and contextualization. (A) SMEs were found in the left IFG (left) and left amygdala (middle); a small cluster of suprathreshold voxels in the left hippocampus (right) also showed marginally significant activity. (B) Stronger neural coupling between the left IFG (seed region) and the left amygdala (left) was associated with memory contextualization (greater SME in intact vs. rearranged conditions); neural coupling between the left IFG (seed region) and the right FG–PHG junction was marginally significant for the same contrast (right). The images are thresholded at p < .001 uncorrected, for visualization purposes. Peak voxels of clusters assigned to the left IFG, the amygdala, and the hippocampus (see Table 3) fell within these regions as defined by the Automatic Anatomical Labeling template. The left IFG cluster is located in the triangular part.*

Table 3. Peak Voxel Coordinates in MNI Space and *t* Statistics

Contrast	*Left Hemisphere*				*Right Hemisphere*			
Region	*x*	*y*	*z*	*Peak (t)*	*x*	*y*	*z*	*Peak (t)*
Localizer								
Face > scrambled face								
Amygdala	−26	−2	−16	4.02*	22	−2	−18	5.29*
Fusiform gyrus	−36	−48	−20	11.23	44	−44	−22	11.73
Inferior occipital cortex	−44	−80	−8	10.24	46	−80	−10	15.87
IFG (opercular)					40	12	26	5.54
IFG (orbital)					36	28	−18	6.27
IFG (triangularis)	−40	20	24	5.52	44	24	28	6.31
Mid occipital cortex	−34	−86	−8	6.26	32	−86	6	5.55
Mid temporal lobe	−50	−64	2	5.75	46	−52	0	6.19
Superior temporal lobe					54	−42	16	5.93
Supramarginal gyrus	−64	−50	28	5.48				
Context > scrambled context								
Calcarine sulcus	−18	−62	12	8.49	24	−58	20	7.98
Cerebellum	−30	−40	−24	6.23				
Fusiform gyrus	−26	−44	−10	11.68	30	−42	−8	13.8
Inferior occipital cortex	−42	−76	−10	6.56	44	−82	−8	7.18
Lingual gyrus	−16	−50	4	5.47	16	−52	4	6.77
Mid occipital cortex	−34	−88	12	12.04	36	−82	18	11.27
FG–PHG junction	−30	−42	−8	11.01[a]	26	−38	−10	7.3[a]
Encoding								
SMEs (remembered > forgotten)								
Left IFG	−44	24	20	5.73				
Left amygdala	−20	−4	−14	4.2**				
Left hippocampus	−26	−12	−10	3.75*				
Subjective contextualization ability (main effect)								
Left IFG (triangularis)	−46	24	18	3.75				
Memory contextualization (PPI, SME in intact > SME in rearranged)								
(left IFG-) Left amygdala	−26	4	−22	4.85**				
(left IFG-) FG / PHG junction	24	−42	−16	3.99*				

All statistical values reported here were significant at $p < .05$, whole-brain FWE-corrected, unless indicated otherwise.

[a] Identified based on voxel intensity and distance to the cluster peak (see Results: Definition of ROIs).

*$p < .05$, small volume corrected.

**$p < .01$, small volume corrected.

We then checked which neural mechanisms at encoding might have mediated the subsequent contextualization memory benefit. We defined memory contextualization at the neural level as SMEs as a function of retrieval context (i.e., interaction between subsequent memory and retrieval context). No significant voxels emerged for this contrast. However, higher trial-by-trial subjective contextualization ability score, which was tested orthogonally to the memory effect (i.e., remembered vs. forgotten), was associated with enhanced activity in a cluster of suprathreshold voxels in the same left IFG region as revealed in the main SME ($p<0.05$, FWE; see *Table 3*). These findings reveal involvement of left IFG both in general memory performance as well as in subjective contextualization ability. These results raised the question whether IFG activity would still predict subsequent memory when controlling for subjective contextualization ability. We tested this effect in a separate model and observed the same IFG cluster (peak voxel: -46,26,20) showed stronger activity in remembered vs. forgotten trials.

Given the association between the left IFG and both objective subsequent memory and subjective contextualization ability, as well as our expectation that the PFC plays a role in information integration, we performed a left IFG-based PPI analysis to investigate if the left-IFG based functional connectivity could potentially explain context dependency of memories. Enhanced connectivity between the left IFG and left amygdala indeed predicted stronger subsequent memory for trials in the intact versus the rearranged condition ($p<0.05$, SVC; see *Figure 2B*). Connectivity with the right FG-PHG junction showed a trend in the same direction ($p=0.054$, SVC; see *Figure 2B*). We then investigated whether the effective connectivity between these regions would also predict inter-individual differences in context-dependent face memory performance. The two PPI-derived neural coupling estimates were added as covariates in separate ANCOVAs with retrieval context as within-subjects factor and memory performance as dependent variable. We found significant interactions between retrieval context and the left IFG-amygdala connectivity, $F(1, 19) = 7.85$, $\eta 2p = 0.29$, $p < 0.05$ (see *Figure 3A*), and between retrieval context and the left IFG-FG/PHG junction connectivity, $F(1, 19) = 7.57$, $\eta 2p = 0.29$, $p < 0.05$ (see *Figure 3B*). Non-parametric correlation tests with 100,000 random permutations further confirmed these findings (IFG-amygdala: $r_{(19)}=0.54$, $p=0.012$; IFG-FG/PHG junction: $r_{(19)}=0.53$, $p=0.013$). Together, these additional tests confirm that stronger left IFG-based coupling with the amygdala and with the FG-PHG junction, all associated with memory contextualization processes, predict stronger context-dependent memory, both within and between participants.

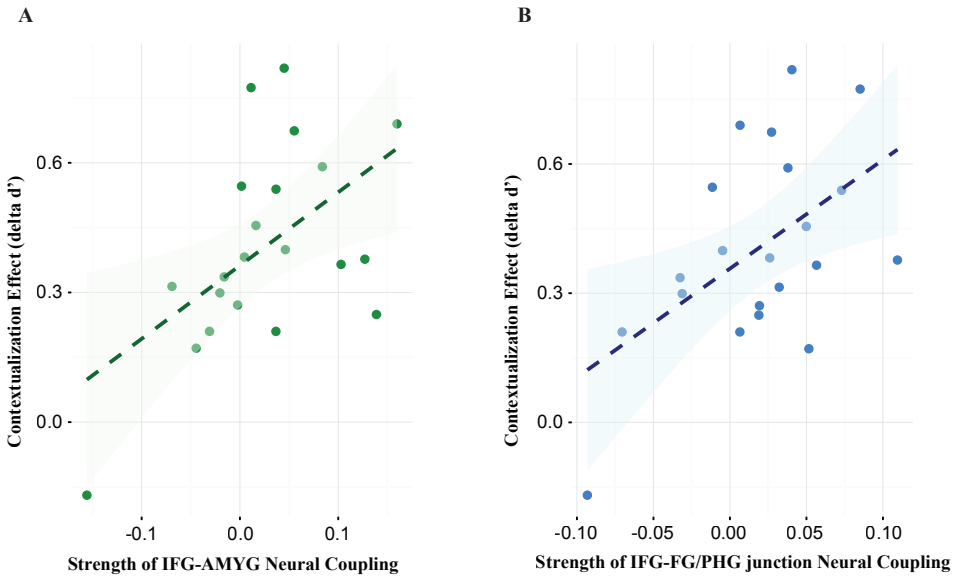

***Figure 3**. Neural coupling predictive of context-dependent memories. (A) The strength of neural coupling between the left IFG and amygdala predicted interindividual differences in context dependency of memory at the behavioral level, as indicated by differences in d' between intact and rearranged retrieval conditions (delta d'). (B) The strength of neural coupling between the left IFG and FG–PHG junction also predicted interindividual differences in context dependency of memory.*

Discussion

The ability to store memories in conjunction with a representation of their encoding context may protect against subsequent dysfunctional memory generalization. Therefore, the current study aimed to reveal the functional neurobiology by which the brain contextualizes biologically meaningful items during encoding, resulting in subsequent context-dependent memories. Indeed, recognition performance was enhanced when the retrieval context was identical to the original encoding context, suggesting effective memory contextualization processes during encoding. Context-dependent memories were associated with stronger neural coupling during encoding between the left IFG and the amygdala, as well as between the left IFG and a region at the junction of FG and PHG. Importantly, the strength of these neural connections also predicted the extent of the context-dependency of memories when tested across participants, providing additional evidence that contextualization processes during encoding are mediated by these regions.

In the current study, we used an incidental memory test to investigate how item recognition memory, in this case for faces, is facilitated by contextual information. This contrasts our study with previous work on relational and associative memory,

which has provided important insight into neural mechanisms underlying item binding, but has commonly used explicit memory tests involving recognition of pairs of items (Davachi, 2006). The advantage of testing implicit context effects on item memory during recognition, combined with incidental encoding of items-in-contexts, is that it most closely mimics real-life memory function: Context-dependent memory is considered a hallmark of human memory function (Tulving & Thomson, 1973). Notably, contemporary animal research shows that, when confronted with a familiar context, hippocampal context codes are automatically re-expressed, thereby priming the relevant memories and reducing the interference from memories associated with other contexts (for a review, see Smith & Bulkin, 2014): There seems to be no need to explicitly encode or assess the association of the item with its context. Thus, our paradigm builds on a long-standing tradition of both animal and human behavioral work showing the power of context to (implicitly) aid memory function.

The two studies by Hayes et al. (2007, 2010) did use a similar experimental setup as ours. However, their findings of the hippocampal and parahippocampal involvement could be explained by processing of more complex visual features due to unbalanced visual input in the contrast. To account for this, we adopted a task that was used in previous behavioral studies into the context-dependency of memories. In this task, all items are encoded against context backgrounds, but 50% of contexts are rearranged during retrieval (van Ast et al., 2013, 2014). Unlike these studies, which used words as items, here we used faces because we specifically intended to investigate brain mechanisms by which emotional or biologically salient items are bound to contexts during encoding. An additional motivation was that faces are known to consistently activate a face-responsive region within the fusiform gyrus (Kanwisher et al., 1997) and the amygdala (Costafreda, Brammer, David, & Fu, 2008; Sergerie, Chochol, & Armony, 2008), a brain structure that is well known for its involvement in processing emotion and salience (Liberzon, Phan, Decker, & Taylor, 2003; Sergerie et al., 2008). Because another area, located within the PHG (i.e., PPA), responds to the presentation of spatial scenes (Epstein et al., 1999), our design allowed us to distinguish item (i.e., face) and context (i.e., scene) representations at the neural level.

Behaviorally, our results revealed that memory recognition was strongly facilitated when the encoding and retrieval contexts were identical. This observation of context-dependency of memories aligns well with previous studies using highly similar experimental paradigms (Cox et al., 2014; Meyer et al., 2017; Staudigl & Hanslmayr, 2013; Talamini et al., 2010; van Ast et al., 2013, 2014). New was that we assessed the subjective ability to contextualize items on a trial-by-trial basis during encoding. We observed that better trial-by-trial contextualization ability yielded better subsequent item recognition performance. More importantly, the degree to which the original encoding context could help later retrieval was predicted by this

contextualization ability. This is in line with the notion that information presented in a more vivid and detailed manner helps to enhance future recall of that information (Buchsbaum, Lemire-Rodger, Fang, & Abdi, 2012). Individual imagery ability, indicated by measures of the vividness of visual imagery, has likewise been suggested to positively affect memory (Baddeley & Andrade, 2000; McKelvie, 1984; McKelvie & Demers, 1979). The current findings are in line with these studies, but also extend these by showing a predictive effect of contextualization ability on context-dependency of memories. This finding suggests that stronger associative imagery during encoding particularly benefits later recognition memory performance in the presence of contextual cues.

With respect to the neural correlates of memory contextualization, we could not identify regions in which the amplitude of regional BOLD responses was predictive of context-dependent memory. It thus appears that contextualization is not strongly predicted by the magnitude of neural responses in any specific brain region. Rather, *functional coupling* between the left IFG and the amygdala, as well as between left IFG and the FG-PHG junction, was positively related to face recognition as a function of retrieval context. Additionally, the neural coupling strength of these regions predicted individual differences in the extent of context-dependent memory. The encoding-related activity of the IFG, part of the PFC, has been consistently reported as being associated with SMEs (Kim, 2011). More specifically, it seems to process both relational and item-specific information as part of the ventrolateral PFC (Blumenfeld, Parks, Yonelinas, & Ranganath, 2011; Murray & Ranganath, 2007; Ranganath, 2010b), to generate associations between items (Addis & McAndrews, 2006; Uncapher & Rugg, 2005), and to support the durability of episodic memories (Uncapher & Rugg, 2005). Our findings broaden understanding of the mnemonic functions of this region by providing compelling evidence that the left IFG is a key region enabling effective memory contextualization.

The observation that IFG-connectivity rather than regional activity was associated with contextualization points toward a role for the IFG in actively integrating information across distributed regions. These distant regions included the amygdala, a core face-responsive region (Costafreda et al., 2008; Mende-siedlecki et al., 2013) that processes information forwarded by more face-selective regions such as the FFA (Todorov, 2012). Here, we found left IFG-amygdala rather than IFG-FFA connectivity, suggesting that memory contextualization of biologically meaningful stimuli such as faces might require more salient feature processing that involves the amygdala. Left IFG-connectivity with a region at the junction of PHG and FG was also predictive of memory contextualization. We first identified this region as responsive to the spatial contexts employed in our localizer task. Previous studies have found that an adjacent region within the PHG, the parahippocampal place area (PPA), responds selectively to images of houses or buildings (Aminoff, Kveraga, & Bar, 2013; Epstein & Kanwisher, 1998). The difference between these findings and

ours may be explained by the fact that we chose scene images with more complex features, to increase distinctiveness. Together, these findings indicate that strongly contextualized memories result from an IFG-based coordination of mnemonic processes across distant regions representing distinct aspects of a memory, likely including perceptual features, spatiotemporal context, and motivational salience.

The hippocampus is also known to play a critical role in memory formation (Eichenbaum, 2000; Gabrieli, 1998; Scoville & Milner, 2000; Squire & Zola-Morgan, 1991), and has been highlighted as the "binding" center where features or elements of episodes and environments that are essential for recollection are bound together (Yonelinas, 2013). Here, we observed a marginally significant main effect of subsequent memory (SME) in the hippocampus, which is consistent with previous studies on its critical role in memory formation (Wagner, 1998). However, we did not find hippocampal involvement associated with memory contextualization. Perhaps the current experimental design was more likely to invoke an active and complex process of information integration that strongly depends on higher-order cognitive processes supported by prefrontal regions such as the IFG. The hippocampus, on the other hand, may become more important during memory consolidation, a process that persists well beyond the time of initial encoding (Knowlton & Fanselow, 1998; McClelland, McNaughton, & O'Reilly, 1995; Squire, 1992) that was not targeted by the current design. Alternatively, the absence of evidence for hippocampal involvement might result from decreased power due to inter-individual variability in functional specialization along the longitudinal axis of the hippocampus (Poppenk, Evensmoen, Moscovitch, & Nadel, 2013; Strange, Witter, Lein, & Moser, 2014). Future studies should use tailored tasks focusing also on the post-encoding period to elucidate hippocampal involvement in memory contextualization with higher anatomical precision.

Inappropriate memory contextualization is considered a hallmark of traumatic memories (Brewin et al., 2010). For instance, low-level memory representations that are improperly contextualized are thought to contribute to memory flashbacks in PTSD (Acheson et al., 2012; Ehlers & Clark, 2000; Liberzon & Sripada, 2007). The brain structures we identified as being involved in memory contextualization are especially sensitive to stress-related neuromodulatory changes (Arnsten, 2009, 2015; Hermans, Henckens, Joëls, & Fernández, 2014). Stress levels of noradrenergic activation lead to occupation of lower-affinity alpha-1 adrenoceptors in the PFC, thus impairing functioning of this region (Birnbaum, Gobeske, Auerbach, Taylor, & Arnsten, 1999). Acute stress has an opposite effect on functioning of the amygdala, where beta-1 adrenoceptors become engaged at elevated levels of noradrenergic activity (Arnsten, 2000). Such dual effects are thought to be amplified by glucocorticoid activation (Roozendaal, McEwen, & Chattarji, 2009). In agreement, a previous study by (van Ast et al., 2013) using a similar task indeed found impaired memory contextualization after a pharmacological elevation of glucocorticoid levels.

Notably, reduced memory contextualization as assessed by the same task as used in the present study, has been shown to predict more traumatic memory intrusions and related distress upon seeing a 'trauma movie' (trauma analogue in the lab) (Meyer et al., 2017). These studies, together with the present findings, suggest that extreme stress associated with traumatic events could lead to unusually strong amygdala-based representations, while a transient suppression of PFC functioning may give rise to a lack of mnemonic integration, resulting in de-contextualization, fragmentation, and generalization of memories. This interpretation is in line with the revised dual representation theory of PTSD, which states that traumatic experiences can be stored as sensory-bound memories isolated from original encoding contexts, which would allow for the retrieval of traumatic memories triggered by perceptual cues reminiscent of the original trauma without retrieval of the appropriate context (Bisby, Horner, Hørlyck, & Burgess, 2016; Brewin et al., 2010). Our data, however, indicate that this model may place too much emphasis on hippocampal instead of PFC dysfunction as central factor (Diamond, Campbell, Park, Halonen, & Zoladz, 2007). It should be noted that in the current study, we only used neutral faces as item stimuli to investigate memory contextualization. Given the aversive and negatively arousing properties of traumatic events, studies directly manipulating the emotional valence and arousal of items are required to further explore the clinical implications of our findings regarding the neural substrates of memory contextualization. Additionally, some studies have shown that emotional valence of the encoding context can influence memory retrieval that seems to recruit similar neural circuits activated during encoding (Erk et al., 2003; Erk, Martin, & Walter, 2005; Hofstetter, Achaibou, & Vuilleumier, 2012; Sterpenich et al., 2006). It is therefore important to investigate how emotional valence of contexts could contribute to inappropriate memory contextualization as well.

To conclude, our results indicate that memory contextualization depends on the integration of information across neural circuits that are involved in item and context representations. Our findings in particular highlight a key role for the left IFG in coordinating this mnemonic process. Given the vulnerability of the prefrontal regions to the effects of acute stress, our findings thereby provide a novel framework for understanding the pathogenesis of traumatic memories that are often seen in stress-related disorders such as PTSD.

References

Acheson, D. T., Gresack, J. E., & Risbrough, V. B. (2012). Hippocampal dysfunction effects on context memory: Possible etiology for posttraumatic stress disorder. *Neuropharmacology*, *62*(2), 674–685.

Addis, D. R., & McAndrews, M. P. (2006). Prefrontal and hippocampal contributions to the generation and binding of semantic associations during successful encoding. *NeuroImage*, *33*(4), 1194–1206.

Aminoff, E. M., Kveraga, K., & Bar, M. (2013). The role of the parahippocampal cortex in cognition. *Trends in Cognitive Sciences*, *17*(8), 379–390.

Arnsten, A. F. T. (2000). Through the Looking Glass: Differential Noradenergic Modulation of Prefrontal Cortical Function. *Neural Plasticity*, *7*(1–2), 133–146.

Arnsten, A. F. T. (2009). Stress signalling pathways that impair prefrontal cortex structure and function. *Nature Reviews. Neuroscience*, *10*(6), 410–422.

Arnsten, A. F. T. (2015). Stress weakens prefrontal networks: molecular insults to higher cognition. *Nature Neuroscience*, *18*(10), 1376–1385.

Baddeley, A. D., & Andrade, J. (2000). Working memory and the vividness of imagery. *Journal of Experimental Psychology: General*, *129*(1), 126–145.

Birnbaum, S., Gobeske, K. T., Auerbach, J., Taylor, J. R., & Arnsten, A. F. T. (1999). A role for norepinephrine in stress-induced cognitive deficits: a-1-Adrenoceptor mediation in the prefrontal cortex. *Biological Psychiatry*, *46*(9), 1266–1274.

Bisby, J. A., Horner, A. J., Hørlyck, L. D., & Burgess, N. (2016). Opposing effects of negative emotion on amygdalar and hippocampal memory for items and associations. *Social Cognitive and Affective Neuroscience*, *11*(6), 981–990.

Blumenfeld, R. S., Parks, C. M., Yonelinas, A. P., & Ranganath, C. (2011). Putting the pieces together: the role of dorsolateral prefrontal cortex in relational memory encoding. *Journal of Cognitive Neuroscience*, *23*(1), 257–265.

Brewer, J. B., Zhao, Z., Desmond, J. E., Glover, G. H., & Gabrieli, J. D. (1998). Making memories: brain activity that predicts how well visual experience will be remembered. *Science*, *281*(5380), 1185–1187.

Brewin, C. R., Gregory, J. D., Lipton, M., & Burgess, N. (2010). Intrusive images in psychological disorders: characteristics, neural mechanisms, and treatment implications. *Psychological Review*, *117*(1), 210–232.

Buchsbaum, B. R., Lemire-Rodger, S., Fang, C., & Abdi, H. (2012). The neural basis of vivid memory is patterned on perception. *Journal of Cognitive Neuroscience*, *24*(9), 1867–1883.

Chun, M. M., & Phelps, E. a. (1999). Memory deficits for implicit contextual information in amnesic subjects with hippocampal damage. *Nature Neuroscience*, *2*(9), 844–847.

Costafreda, S. G., Brammer, M. J., David, A. S., & Fu, C. H. Y. (2008). Predictors of amygdala activation during the processing of emotional stimuli: A meta-analysis of 385 PET and fMRI studies. *Brain Research Reviews*, *58*(1), 57–70.

Cox, R., Tijdens, R. R., Meeter, M. M., Sweegers, C. C. G., & Talamini, L. M. (2014). Time, not sleep, unbinds contexts from item memory. *PLoS ONE*, *9*(2), 1–6.

Davachi, L. (2006). Item, context and relational episodic encoding in humans. *Current Opinion in Neurobiology*, *16*(6), 693–700.

Davachi, L., & DuBrow, S. (2015). How the hippocampus preserves order: The role of prediction and context. *Trends in Cognitive Sciences*, *19*(2), 92–99.

De Beni, R., & Pazzaglia, F. (1995). Memory for different kinds of mental images: role of contextual and autobiographic variables. *Neuropsychologia*, *33*(11), 1359–1371.

Diamond, D. M., Campbell, A. M., Park, C. R., Halonen, J., & Zoladz, P. R. (2007). The temporal dynamics model of emotional memory processing: A synthesis on the neurobiological basis of stress-induced amnesia, flashbulb and traumatic memories, and the Yerkes-Dodson law. *Neural Plasticity*, *2007*.

Diana, R. A., Yonelinas, A. P., & Ranganath, C. (2007). Imaging recollection and familiarity in the medial temporal lobe: a three-component model. *Trends in Cognitive Sciences*, *11*(9), 379–386.

Ehlers, A., & Clark, D. M. (2000). A cognitive model of posttraumatic stress disorder. *Behaviour Research and Therapy*, *38*(4), 319–345. https://doi.org/S0005-7967(99)00123-0

Eichenbaum, H. (2000). A cortical-hippocampal system for declarative memory. *Nature Reviews. Neuroscience*, *1*(1), 41–50.

Eichenbaum, H. (2004). Hippocampus: Cognitive processes and neural representations that underlie declarative memory. *Neuron*, *44*(1), 109–120.

Eichenbaum, H., Sauvage, M., Fortin, N., Komorowski, R., & Lipton, P. (2012). Towards a functional organization of episodic memory in the medial temporal lobe. *Neuroscience and Biobehavioral Reviews*, *36*(7), 1597–1608.

Emmerich, D. S. (1967). Signal Detection Theory and Psychophysics . David M. Green , John A. Swets. *The Quarterly Review of Biology*, *42*(4), 578–578.

Epstein, R., Harris, A., Stanley, D., & Kanwisher, N. (1999). The parahippocampal place area: Recognition, navigation, or encoding? *Neuron*, *23*(1), 115–125.

Epstein, R., & Kanwisher, N. (1998). A cortical representation of the local visual environment. *Nature*, *392*(6676), 598–601.

Erk, S., Kiefer, M., Grothe, J., Wunderlich, A. P., Spitzer, M., & Walter, H. (2003). Emotional context modulates subsequent memory effect. *NeuroImage*, *18*(2), 439–447.

Erk, S., Martin, S., & Walter, H. (2005). Emotional context during encoding of neutral items modulates brain activation not only during encoding but also during recognition. *NeuroImage*, *26*(3), 829–838.

Gabrieli, J. D. E. (1998). Cognitive neuroscience of human memory. *Annual Review of Psychology*, *49*(1), 87–115.

Gabrieli, J. D. E., Brewer, J. B., Desmond, J. E., & Glover, G. H. (1997). Separate neural bases of two fundamental memory processes in the human medial temporal lobe. *Science*, *276*(5310), 264–266.

Gitelman, D. R., Penny, W. D., Ashburner, J., & Friston, K. J. (2003). Modeling regional and psychophysiologic interactions in fMRI: The importance of hemodynamic deconvolution. *NeuroImage*, *19*(1), 200–207.

Godden, D. R., & Baddeley, A. D. (1975). Context-dependent memory in two natural environments: On land and underwater. *British Journal of Psychology*, *66*(3), 325–331.

Graf, P., & Schacter, D. L. (1985). Implicit and explicit memory for new associations in normal and amnesic subjects. *Journal of Experimental Psychology: Learning, Memory, and Cognition*, *11*(3), 501–518.

Hayes, S. M., Baena, E., Truong, T.-K., & Cabeza, R. (2010). Neural mechanisms of context effects on face recognition: automatic binding and context shift decrements. *J Cogn Neurosci*, *22*(11), 2541–2554.

Hayes, S. M., Nadel, L., & Ryan, L. (2007). The effect of scene context on episodic object recognition: Parahippocampal cortex mediates memory encoding and retrieval

success. *Hippocampus*, *17*(9), 873–889.

Hermans, E. J., Henckens, M. J. A. G., Joëls, M., & Fernández, G. (2014). Dynamic adaptation of large-scale brain networks in response to acute stressors. *Trends in Neurosciences*, *37*(6), 304–314.

Hofstetter, C., Achaibou, A., & Vuilleumier, P. (2012). Reactivation of visual cortex during memory retrieval: Content specificity and emotional modulation. *NeuroImage*, *60*(3), 1734–1745.

Hutton, C., Bork, A., Josephs, O., Deichmann, R., Ashburner, J., & Turner, R. (2002). Image distortion correction in fMRI: A quantitative evaluation. *Neuroimage*, *16*(1), 217–240.

Jenkins, L. J., & Ranganath, C. (2010). Prefrontal and Medial Temporal Lobe Activity at Encoding Predicts Temporal Context Memory. *Journal of Neuroscience*, *30*(46), 15558–15565.

Kanwisher, N., McDermott, J., & Chun, M. M. (1997). The fusiform face area: a module in human extrastriate cortex specialized for face perception. *The Journal of Neuroscience : The Official Journal of the Society for Neuroscience*, *17*(11), 4302–4311.

Kanwisher, N., & Yovel, G. (2006). The fusiform face area: a cortical region specialized for the perception of faces. *Philosophical Transactions of the Royal Society of London. Series B, Biological Sciences*, *361*(1476), 2109–2128.

Kapur, S., Craik, F. I., Tulving, E., Wilson, A. A., Houle, S., & Brown, G. M. (1994). Neuroanatomical correlates of encoding in episodic memory: levels of processing effect. *Proceedings of the National Academy of Sciences of the United States of America*, *91*(6), 2008–2011.

Kim, H. (2011). Neural activity that predicts subsequent memory and forgetting: A meta-analysis of 74 fMRI studies. *NeuroImage*, *54*(3), 2446–2461.

Kirchhoff, B. A., Wagner, A. D., Maril, A., & Stern, C. E. (2000). Prefrontal-Temporal Circuitry for Episodic Encoding and Subsequent Memory. *J. Neurosci.*, *20*(16), 6173–6180.

Kirwan, C. B., Wixted, J. T., & Squire, L. R. (2008). Activity in the Medial Temporal Lobe Predicts Memory Strength, Whereas Activity in the Prefrontal Cortex Predicts Recollection. *Journal of Neuroscience*, *28*(42), 10541–10548.

Knowlton, B. J., & Fanselow, M. S. (1998, April). The hippocampus, consolidation and on-line memory. *Current Opinion in Neurobiology*.

Langner, O., Dotsch, R., Bijlstra, G., Wigboldus, D. H. J., Hawk, S. T., & van Knippenberg, A. (2010). Presentation and validation of the Radboud Faces Database. *Cognition & Emotion*, *24*(8), 1377–1388.

Liberzon, I., Phan, K. L., Decker, L. R., & Taylor, S. F. (2003). Extended amygdala and emotional salience: a PET activation study of positive and negative affect. *Neuropsychopharmacology : Official Publication of the American College of Neuropsychopharmacology*, *28*(4), 726–733.

Liberzon, I., & Sripada, C. S. (2007). The functional neuroanatomy of PTSD: a critical review. In *Progress in Brain Research* (Vol. 167, pp. 151–169).

Long, N. M., & Kahana, M. J. (2015). Successful memory formation is driven by contextual encoding in the core memory network. *NeuroImage*, *119*, 332–337.

Lundqvist, D., Flykt, A., & Ohman, A. (1998). The Karolinska directed emotional faces (KDEF). *CD ROM from Department of Clinical Neuroscience, Psychology Section, Karolinska Institutet*, 91–630.

McClelland, J. L., McNaughton, B. L., & O'Reilly, R. C. (1995). Why there are complementary learning systems in the hippocampus and neocortex: Insights from the successes and failures of connectionist models of learning and memory. *Psychological Review*,

102(3), 419–457.

McKelvie, S. J. (1984). Reported visual imagery for faces and facial recognition memory. *Perceptual and Motor Skills*, *59*(3), 825–826.

McKelvie, S. J., & Demers, E. G. (1979). Individual differences in reported visual imagery and memory performance. *British Journal of Psychology (London, England : 1953)*, *70*(1), 51–57.

Mende-siedlecki, P., Said, C. P., & Todorov, A. (2013). The social evaluation of faces: A meta-analysis of functional neuroimaging studies. *Social Cognitive and Affective Neuroscience*, *8*(3), 285–299.

Meyer, T., Krans, J., van Ast, V., & Smeets, T. (2017). Visuospatial context learning and configuration learning is associated with analogue traumatic intrusions. *Journal of Behavior Therapy and Experimental Psychiatry*, *54*, 120–127.

Meyer, T., Smeets, T., Giesbrecht, T., Quaedflieg, C. W. E. M., Girardelli, M. M., Mackay, G. R. N., & Merckelbach, H. (2013). Individual differences in spatial configuration learning predict the occurrence of intrusive memories. *Cognitive, Affective, & Behavioral Neuroscience*, *13*(1), 186–196.

Mumby, D. G., Gaskin, S., Glenn, M. J., Schramek, T. E., & Lehmann, H. (2002). Hippocampal damage and exploratory preferences in rats: memory for objects, places, and contexts. *Learning & Memory (Cold Spring Harbor, N.Y.)*, *9*(2), 49–57.

Murray, L. J., & Ranganath, C. (2007). The dorsolateral prefrontal cortex contributes to successful relational memory encoding. *J Neurosci*, *27*(20), 5515–5522.

Nichols, T. E., & Holmes, A. P. (2001). Nonparametric Permutation Tests for {PET} functional Neuroimaging Experiments: A Primer with examples. *Human Brain Mapping*, *15*(1), 1–25.

Nyberg, L., Cabeza, R., & Tulving, E. (1996). PET studies of encoding and retrieval: The HERA model. *Psychonomic Bulletin & Review*, *3*(2), 135–148.

Paller, K. A., & Wagner, A. D. (2002). Observing the transformation of experience into memory. *Trends in Cognitive Sciences*, *6*(2), 93–102.

Phillips, R. G., & LeDoux, J. E. (1992). Differential contribution of amygdala and hippocampus to cued and contextual fear conditioning. *Behavioral Neuroscience*, *106*(2), 274–285.

Poppenk, J., Evensmoen, H. R., Moscovitch, M., & Nadel, L. (2013). Long-axis specialization of the human hippocampus. *Trends in Cognitive Sciences*, *17*(5), 230–240.

Poser, B. A., Versluis, M. J., Hoogduin, J. M., & Norris, D. G. (2006). BOLD contrast sensitivity enhancement and artifact reduction with multiecho EPI: Parallel-acquired inhomogeneity-desensitized fMRI. *Magnetic Resonance in Medicine*, *55*(6), 1227–1235.

Prince, S. E. (2005). Neural Correlates of Relational Memory: Successful Encoding and Retrieval of Semantic and Perceptual Associations. *Journal of Neuroscience*, *25*(5), 1203–1210.

Quaedflieg, C. W. E. M., van de Ven, V., Meyer, T., Siep, N., Merckelbach, H., & Smeets, T. (2015). Temporal Dynamics of Stress-Induced Alternations of Intrinsic Amygdala Connectivity and Neuroendocrine Levels. *PLOS ONE*, *10*(5), e0124141.

Ranganath, C. (2010a). A unified framework for the functional organization of the medial temporal lobes and the phenomenology of episodic memory. *Hippocampus*, *20*(11), 1263–1290.

Ranganath, C. (2010b). Binding Items and Contexts: The Cognitive Neuroscience of Episodic Memory. *Current Directions in Psychological Science*, *19*, 131–137.

Richardson, J. T. E. (1980). *Mental imagery and human memory.* London: Macmillan.
Rimmele, U., Davachi, L., & Phelps, E. A. (2012). Memory for Time and Place Contributes to Enhanced Confidence in Memories for Emotional Events. *Emotion*, *12*(4), 834–846.
Roozendaal, B., McEwen, B. S., & Chattarji, S. (2009). Stress, memory and the amygdala. *Nature Reviews Neuroscience*, *10*(6), 423–433.
Scoville, W. B., & Milner, B. (2000). Loss of recent memory after bilateral hippocampal lesions. 1957. *The Journal of Neuropsychiatry and Clinical Neurosciences*, *12*(1), 103–113.
Sergerie, K., Chochol, C., & Armony, J. L. (2008). The role of the amygdala in emotional processing: A quantitative meta-analysis of functional neuroimaging studies. *Neuroscience and Biobehavioral Reviews*, *32*(4), 811–830.
Slotnick, S. D., & Dodson, C. S. (2005). Support for a continuous (single-process) model of recognition memory and source memory. *Memory & Cognition*, *33*(1), 151–170.
Smith, D. M., & Bulkin, D. A. (2014). The form and function of hippocampal context representations. *Neuroscience and Biobehavioral Reviews*.
Smith, S. M., & Vela, E. (2001). Environmental context-dependent memory: A review and meta-analysis. *Psychonomic Bulletin & Review*, *8*(2), 203–220.
Squire, L. (1992). Memory and the hippocampus: a synthesis from findings with rats, monkeys, and humans. *Psychological Review*, *99*(2), 195–231.
Squire, L., & Zola-Morgan, S. (1991). The medial temporal lobe memory system. *Science*, *253*(5026), 1380–1386.
Staudigl, T., & Hanslmayr, S. (2013). Theta oscillations at encoding mediate the context-dependent nature of human episodic memory. *Current Biology : CB*, *23*(12), 1101–1106.
Sterpenich, V., D'Argembeau, A., Desseilles, M., Balteau, E., Albouy, G., Vandewalle, G., … Maquet, P. (2006). The Locus Ceruleus Is Involved in the Successful Retrieval of Emotional Memories in Humans. *Journal of Neuroscience*, *26*(28), 7416–7423.
Strange, B. a, Witter, M. P., Lein, E. S., & Moser, E. I. (2014). Functional organization of the hippocampal longitudinal axis. *Nature Reviews Neuroscience*, *15*(10), 655–669.
Summerfield, C., Greene, M., Wager, T., Egner, T., Hirsch, J., & Mangels, J. (2006). Neocortical connectivity during episodic memory formation. *PLoS Biology*, *4*(5), 855–864.
Talamini, L. M., de Haan, L., Nieman, D. H., Linszen, D. H., & Meeter, M. (2010). Reduced context effects on retrieval in first-episode schizophrenia. *PloS One*, *5*(4), e10356.
Talamini, L. M., & Gorree, E. (2012). Aging memories: Differential decay of episodic memory components. *Learning & Memory*, *19*(6), 239–246.
The MathWorks Inc. (2012). Matlab2012b. Massachusetts: Natick.
Todorov, A. (2012). The role of the amygdala in face perception and evaluation. *Motivation and Emotion*, *36*(1), 16–26.
Tottenham, N., Tanaka, J. W., Leon, A. C., McCarry, T., Nurse, M., Hare, T. a., … Nelson, C. (2009). The NimStim set of facial expressions: judgments from untrained research participants. *Psychiatry Research*, *168*(3), 242–249.
Tsivilis, D., Otten, L. J., & Rugg, M. D. (2001). Context Effects on the Neural Correlates of Recognition Memory. *Neuron*, *31*(3), 497–505.
Tulving, E. (1986). Episodic and semantic memory: Where should we go from here? *Behavioral and Brain Sciences*, *9*(3), 573.
Tulving, E., & Thomson, D. M. (1973). Encoding specificity and retrieval processes in episodic memory. *Psychological Review*, *80*(5), 352–373.
Tzourio-Mazoyer, N., Landeau, B., Papathanassiou, D., Crivello, F., Etard, O., Delcroix, N.,

… Joliot, M. (2002). Automated anatomical labeling of activations in SPM using a macroscopic anatomical parcellation of the MNI MRI single-subject brain. *NeuroImage*, *15*(1), 273–289.

Uncapher, M. R., & Rugg, M. D. (2005). Encoding and the durability of episodic memory: A functional magnetic resonance imaging study. *Journal of Neuroscience*, *25*(31), 7260–7267.

van Ast, V. a, Cornelisse, S., Meeter, M., Joëls, M., & Kindt, M. (2013). Time-dependent effects of cortisol on the contextualization of emotional memories. *Biological Psychiatry*, *74*(11), 809–816.

van Ast, V. a, Cornelisse, S., Meeter, M., & Kindt, M. (2014). Cortisol mediates the effects of stress on the contextual dependency of memories. *Psychoneuroendocrinology*, *41*, 97–110.

Wagner, A. (1998). Prefrontal cortex and recognition memory. Functional-MRI evidence for context-dependent retrieval processes. *Brain*, *121*(10), 1985–2002.

Yonelinas, A. P. (2013). The hippocampus supports high-resolution binding in the service of perception, working memory and long-term memory. *Behavioural Brain Research*, *254*, 34–44.

Zeidman, P., Mullally, S. L., & Maguire, E. A. (2015). Constructing, perceiving, and maintaining scenes: Hippocampal activity and connectivity. *Cerebral Cortex*, *25*(10), 3836–3855.

CHAPTER VI

VI

SUMMARY
AND
GENERAL DISCUSSION

What are the neurobiological mechanisms underlying individual differences in stress sensitivity? The aim of this thesis was to elucidate biological processes in acute stress exposure that can provide insight into long-term consequences for mental health. To this end, I first defined biomarkers of potential interest using a variety of statistical techniques, based on acute stress-induced changes in resting-state functional connectivity (rs-FC) measured in a large sample of 340 police recruits. Thereafter, I tested predictive effects of selected potential biomarkers on stress-related symptom development upon trauma exposure in police recruits who had had the most impactful traumatic experience of their life during the period of emergency aid training.

Below, I will first summarize the main findings of my thesis in the order of the research questions listed in **Chapter 1**. Thereafter, I will discuss these findings in light of existing knowledge and the potential questions to address for future investigations.

Summary of findings

1. *How do large-scale intrinsic networks respond to acute stressors with regard to functional connectivity (FC)?*

   In **Chapter 2**, I tested changes in rs-FC of three major intrinsic networks – namely, the DMN, SN and CEN – following a formal acute stress induction. I found increased rs-FC within the SN that was associated with individual cortisol stress responsiveness. Cortisol stress responsiveness was also associated with rs-FC within the DMN as well as rs-FC between the overall DMN and brain regions outside this network. These findings suggest that acute stress alterations in the rs-FC of these large-scale networks may function as a biomarker for individual stress reactivity.

2. *What are the sub-structures of the large-scale brain networks that are most strongly affected by acute stress induction?*

   In **Chapter 3**, I used a supervised machine learning approach to explore the most relevant brain structures within three major brain networks that were affected by acute stress. These brain structures were derived from FC-based parcellation and thus had enhanced specificity with respect to local functionality – in contrast to studies using anatomically defined structures. My analyses used rs-fMRI data to identify several critical brain structures from the DMN and SN of which the connectivity pattern could accurately discriminate the stressed from the non-stressed brain states. Next, I found a correlation between discriminative features and individual cortisol reactivity, further validating the relevance of the identified networks. In addition to confirming the involvement of the dorsal ACC, amygdala, PCC

and PCu in stress-related processing, the findings from this study point toward potential candidate structures for studying stress effects which have been largely overlooked by previous investigations (i.e., the angular gyrus and inferior parietal lobule).

3. *Can acute stress responses at the endocrine and neural-network level predict the development of PTSD symptom levels?*

   In additional to hormonal and behavioral reactivity, acute stress-induced rs-FC changes at the network level, as identified in **Chapter 2,** were used in **Chapter 4** to predict stress-related symptom development after trauma exposure. I further tested potential abnormalities in acute stress reactivity that were acquired after trauma exposure. The results show that relatively weak coupling between the overall SN and several regions, including PCC/PCu from the DMN, following acute stress prospectively predicted increases in perceived stress after trauma. However, reduced coupling between the SN and anterior cerebellum in response to acute stressors from Wave 1 to Wave 2 was observed in participants with higher clinician-rated PTSD symptoms at follow-up. Together, these findings suggest SN synchronization after stress induction as a biomarker for predictive as well as acquired stress symptoms.

4. *What are the neural correlates of memory contextualization?*

   In **Chapter 5**, I discussed the first step in exploring a cognitive process, namely memory contextualization, which is considered potentially relevant to PTSD symptomatology. I designed a task to manipulate the degree of contextualizing faces with places and tested the neural correlates of this process. I found a PFC-based information integration that was associated with stronger memory contextualization effects. It would be of interest for future studies to test whether such effects and associated neural correlates can be linked to post-trauma symptom levels.

Integration of Findings

SN-based synchronization in response to stress

The salience network is involved in detecting and orienting to salient external stimuli and internal events. It has been consistently implicated in stress-related processing with increased activity and connectivity in response to experimentally induced acute stressors (for example, Young et al., 2017; for review see van Oort et al., 2017). Dysfunction of the SN has been suggested to underlie stress-related psychopathology, including stress-related PTSD, anxiety and depression (see reviews for Akiki, Averill, & Abdallah, 2017; Freitas-Ferrari et al., 2010; Mulders, van

Eijndhoven, Schene, Beckmann, & Tendolkar, 2015). In general, a breakdown of the SN gives rise to impaired detection and signaling of salient stimuli or events, resulting in significant consequences for cognition and emotion. The characterization of the SN and its interactions with other large-scale brain networks such as the DMN and CEN has been proposed as an important way to understand dysfunction in a variety of neuropsychiatric disorders.

Chapter 2 elaborates on my observations concerning increased connectivity within the SN following acute stress induction and the correlation between the magnitude of this increase and individual cortisol stress -responsiveness. In parallel, decreased DMN connectivity was found after stress induction, which also exhibited an association with higher cortisol stress-responsiveness. These findings may suggest potential interactions between these large-scale networks and the HPA axis that give rise to individual variability in cortisol responsivity. This result is generally in line with previous studies suggesting the critical roles played by the amygdala, hippocampus and medial PFC – also the key regions from the SN and DMN – in regulating cortisol secretion in response to acute stress. With these findings, I identified neural markers at the network level that exhibit sensitivity to individual differences and that could potentially be relevant to stress-related psychopathology. In **Chapter 4**, I discussed the link between these connectivity changes and subsequent PTSD symptom development after trauma and reported the finding that SN connectivity patterns with posterior DNM prospectively predicted perceived stress levels, while changes in SN connectivity (i.e., SN-cerebellum connectivity) over time also explained symptoms at follow-up. Interestingly, the specific DMN connectivity changes in Chapter 2 showed neither predictive nor acquired effects of PTSD symptoms after trauma in the study reported in Chapter 4. However, DNM was involved in predicting post-trauma stress levels via its interaction with the overall SN. These results align well with the current literature reporting the SN-DMN interactions, predominantly based on connectivity between key regions of these networks, in relation to stress-related processing and psychopathology (Veer et al., 2010; Sripada et al., 2012; Van Der Werff et al., 2013; Lei et al., 2015; Koch et al., 2016; Akiki et al., 2017). This involvement of SN-DMN interaction in stress-related processing was further supported by the findings reported in **Chapter 3**, where I directly investigated inter-regional interactions within and across these large-scale networks (i.e., connectivity patterns) in relation to acute stress induction. Using a novel analytic approach, I identified critical interactions of key regions from the SN (i.e., dACC and amygdala) and DMN (i.e., PCC and PCu) that, together, substantiated the discrimination between the stressed and non-stressed brain states. Again, these results suggest that connectivity patterns of the SN and DMN might be the most relevant neural signature for stress sensitivity and can thus be informative for studying long-term consequences for mental health. In conclusion, these findings demonstrate that neural responses to challenging situations can be useful 1) for understanding inter-individual variability in stress reactivity and possibly in stress adaptation, and 2) for

linking that variance to long-term consequences.

Strengths, Implications and Limitations

Strengths

From an evolutionary point of view, stress responses evolved as adaptive processes. However, severe and prolonged stress responses may lead to undesired consequences (Selye, 1956). How these presumably adaptive responses can become destructive is a key to understanding individual differences in stress resilience versus vulnerability. Furthermore, such insight can potentially facilitate precise assessments and alternative classifications beyond the DSM categories of PTSD by identifying varying dysfunctions in general biological and psychological systems (Cuthbert and Insel, 2013; Howlett and Stein, 2016; McFarlane et al., 2017). In the studies reported in this thesis, based on indications that reactivity to challenges might provide useful biomarkers for stress vulnerability (see reivew for Michopoulos, Norrholm, & Jovanovic, 2015), I used a formal acute stress induction to experimentally probe stress responses – particularly at the neural-network level. Importantly, having used a longitudinal design, the work described in this thesis also fits well with a recently proposed framework for resilience research in which prospective longitudinal studies are urged to investigate resilience factors and thereby complement traditional pathophysiological research on stress (Kalisch et al., 2017). Hence, the findings reported in this thesis can also be considered relevant for studying resilience factors.

Implications

At the clinical level, the majority of investigations into stress-related network-level connectivity have used a cross-sectional design, leaving the predisposed and acquired neural effects unclear. Results reported in this thesis show that acute stress-induced reconfiguration of large-scale networks, particularly the SN reconfiguration, can be highly relevant for further clinical studies. More specifically, insufficient SN-DMN interactions in response to stress may lead to unwanted high stress levels after trauma exposure, whereas SN-cerebellum interactions under stress may become sensitized with increased symptom levels (as shown in **Chapter 4**). Although the studies in the thesis focused on a relatively resilient sample with sub-clinical symptoms, the findings reported here are, to a certain degree, in line with the existing theories and hypotheses about the neurocircuitry of PTSD. For example, based on neuroimaging findings, Admon et al. (2013) proposed a causal model for PTSD with abnormalities within the amygdala and dACC – the core regions of the SN – being predisposing risk factors of PTSD. In this research, instead of within-SN abnormalities, we observed weakened SN synchronization with other brain circuits (i.e., the DMN) being predictive of higher post-trauma stress levels.

The discrepancy here might result from the different experimental designs used in the current research and in the prospective studies reviewed by Admon and colleagues. Nevertheless, these findings all point toward the SN as a potential biomarker for PTSD vulnerability. Interestingly, in contrast to the abnormalities in the DMN (i.e., the hippocampal-vmPFC) that were proposed as the acquired deficits (Admon et al., 2013), this research observed intensified SN-cerebellum synchronization in participants with higher symptom levels after trauma. Again, the inconsistency may arise from different experimental designs. Yet, the alterations in SN connectivity pattern match well the existing observations for discrete structures of the SN connectivity in PTSD (see review for Koch et al., 2016), as well as the findings from large-scale network-based studies on PTSD (see review for Akiki et al., 2017). In short, the current research provides empirical evidence supporting aberrant SN function as a predisposing risk factor for PTSD. In line with the existing models for PTSD biomarkers, this thesis highlights the critical role of SN connectivity in stress-related processing and potentially relevant psychopathology – not only at the local regional level, but also at a cohesive and unified network level.

Limitations

This thesis is not without limitations. For example, the experimental setup for inducing acute stress only allowed for capturing of the neural processing that was plausibly a mixture of stress reactivity and stress recovery. Specifically, although at the group level, cortisol level in the current sample peaked 20 minutes after the onset of stress induction and remained high for another 10 minutes; some participants showed a decline from the peak level, while others exhibited a sustained elevation even 30 minutes after the onset. As the acquisition of rs-fMRI took place in the timeframe between 20 and 30 minutes after the stress onset, the observed neural responses for some participants may be more relevant to stress reactivity than to stress recovery and for others vice versa. Consequently, disentangling these interrelated, yet conceptually distinct processes may help identify neural circuits associated with and the factors that can influence individual variances in these processes. Teasing these processes apart with a higher temporal resolution of neuroimaging measures may also provide better insight into the relationship between the short-term adaptation to a stressor and the long-term consequences for mental health.

Additionally, the sample studied in this research was relatively resilient and demonstrated low overall levels of PTSD symptoms after trauma. Therefore, the observed neural-network responses to acute stress and their association with subsequent symptom development may well involve processes relevant to stress resilience as well. To delineate the underpinning processes for resilience versus vulnerability, future investigations may consider the use of much higher sampling frequency during and after trauma for studying trajectories of stress responses,

assuming that stress resilience is a dynamic process of successful adaptation to adversity that is presumably time-varying and individually variable (Kalisch et al., 2017). It may also help to take into account genetic make-up and early-life experiences that, together, are suggested to program individuals with improved resilience for later-life challenges when adverse experiences in early and later life are similar or with enhanced vulnerability when there is a mismatch (Daskalakis et al., 2013).

Lastly, the network-level focus in this research inevitably missed neural processing at a more refined regional or sub-regional level, which may direct one to more specific neural circuits pertinent to stress-related processing. However, in acknowledgment of this drawback, I applied a more data-driven method to identify sub-regions from these large-scale networks in relation to acute stress responses; whether these functional units can offer more information about long-term stress effects remains untested.

Open Questions and Future Directions

The studies reported in this thesis aimed to identify predictive biomarkers of stress-related symptom development. I focused primarily on large-scale network connectivity but also made an effort to explore inter-regional interaction within and across those networks. As mentioned earlier, it remains unknown whether the observed interactions at more local level (i.e., between sub-regions) that significantly responded to acute stress can provide us more information on long-term stress effects. This question is relevant because, if we can break down acute stress-induced brain reconfiguration from the network level to regional and sub-regional level and demonstrate the association between these more local-level functional characteristics and long-term stress consequences, we may be able to specify neural mechanisms for distinct yet highly overlapped processes, such as stress reactivity and stress recovery. In fact, previous investigations into prolonged stress effects provided a hint of different connection patterns involved in stress recovery as opposed to reactivity, which appeared to be associated with cortisol stress response (Veer et al., 2011; Vaisvaser et al., 2013; Quaedflieg et al., 2015; Dimitrov et al., 2018).

Another relevant question concerns the outcome measures for stress symptoms used in this research. I used three outcome measures and found different results (i.e., results in PSS and CAPS but not in PCL), which may be due to different aspects of the measures (i.e., PCL was less sensitive to the current sub-clinical sample). Alternatively, these differences may have arisen from different administration methods (i.e., the CAPS being administered via telephone interview). One possible way to reconcile all these outcome measures is to combine the information from all the stress measurements. In relation to this aspect, a number of recent studies

set out to sub-type tested samples for a better understanding of complex disorders, such as PTSD. One approach used in these studies is latent variable modeling, which allows for the discovery of a set of invisible (thus, latent) variables based on the observed variables. This data-driven approach appears to better characterize individuals with reported symptom scores as well as with information about trauma experience and socio-demographic characteristics. Further investigations can then follow to identify the associated neurophysiological mechanisms for characterized symptom groups (Bondjers, Willebrand, & Arnberg, 2018; Galatzer-Levy, Nickerson, Litz, & Marmar, 2013; Murphy, Ross, Busuttil, Greenberg, & Armour, 2019; Rahman et al., 2018). As PTSD is highly heterogeneous and comorbid with several other psychiatric disorders (Spinhoven, Penninx, van Hemert, de Rooij, & Elzinga, 2014), it is important to find efficient ways to better describe and characterize the tested samples (i.e., phenotyping), as this may not only advance our understanding of this complex disorder but also ultimately benefit clinical populations through the use of targeted treatment strategies. For example, with the identification of neural and behavioral signatures for a specific PTSD subgroup, non-invasive brain stimulation approaches are now suggested for treating patients with PTSD (Etkin et al., 2019). Interventions using a real-time fMRI-based neurofeedback technique are also emerging and showing promising outcomes for targeting specific brain regions known to be involved in the pathophysiology of PTSD (Nicholson et al., 2017, 2018).

Concluding remarks

"It's not stress that kills us; it is our reaction to it." – Hans Selye

Exposure to stressful situations can lead to undesirable consequences for mental health. Such exposure can also potentially prepare us for challenges later in life, thus facilitating resilience. It is, therefore, important to uncover brain processes that result in divergent pathways of long-term stress effects. This research investigated potential biomarkers for stress vulnerability at the neural, endocrine and subjective levels. The findings suggest that focusing on acute stress responses at a large-scale network level is a promising way to investigate long-term stress effects. In particular, SN-based reconfiguration upon acute stress may serve as a potential marker for stress vulnerability.

References

Admon R, Milad MR, Hendler T (2013) A causal model of post-traumatic stress disorder: Disentangling predisposed from acquired neural abnormalities. Trends Cogn Sci 17:337–347.

Akiki TJ, Averill CL, Abdallah CG (2017) A Network-Based Neurobiological Model of PTSD: Evidence From Structural and Functional Neuroimaging Studies. Curr Psychiatry Rep 19, 81.

Bondjers K, Willebrand M, Arnberg FK (2018) Similarity in symptom patterns of posttraumatic stress among disaster-survivors: a three-step latent profile analysis. Eur J Psychotraumatol 9:1546083.

Cuthbert BN, Insel TR (2013) Toward the future of psychiatric diagnosis: The seven pillars of RDoC. BMC Med 11.

Daskalakis NP, Bagot RC, Parker KJ, Vinkers CH, de Kloet ER (2013) The three-hit concept of vulnerability and resilience: toward understanding adaptation to early-life adversity outcome. Psychoneuroendocrinology 38:1858–1873.

Dimitrov A, Demin K, Fehlner P, Walter H, Erk S, Veer IM (2018) Differences in Neural Recovery From Acute Stress Between Cortisol Responders and Non-responders. Front Psychiatry 9.

Etkin A et al. (2019) Using fMRI connectivity to define a treatment-resistant form of post-traumatic stress disorder. Sci Transl Med 11:eaal3236.

Freitas-Ferrari MC, Hallak JEC, Trzesniak C, Filho AS, Machado-de-Sousa JP, Chagas MHN, Nardi AE, Crippa JAS (2010) Neuroimaging in social anxiety disorder: A systematic review of the literature. Prog Neuro-Psychopharmacology Biol Psychiatry 34:565–580.

Galatzer-Levy IR, Nickerson A, Litz BT, Marmar CR (2013) Patterns of lifetime PTSD comorbidity: A latent class analysis. Depress Anxiety 30:489–496.

Howlett JR, Stein MB (2016) Prevention of Trauma and Stressor-Related Disorders: A Review. Neuropsychopharmacology 41:357–369.

Kalisch R et al. (2017) The resilience framework as a strategy to combat stress-related disorders. Nat Hum Behav 1:784–790.

Koch SBJ, van Zuiden M, Nawijn L, Frijling JL, Veltman DJ, Olff M (2016) Aberrant resting-state brain activity in posttraumatic stress disorder: A meta-analysis and systematic review. Depress Anxiety 33:592–605.

Lei D, Li K, Li L, Chen F, Huang X, Lui S, Li J, Bi F, Gong Q (2015) Disrupted Functional Brain Connectome in Patients with Posttraumatic Stress Disorder. Radiology 276:818–827.

McFarlane AC, Lawrence-Wood E, Van Hooff M, Malhi GS, Yehuda R (2017) The Need to Take a Staging Approach to the Biological Mechanisms of PTSD and its Treatment. Curr Psychiatry Rep 19.

Michopoulos V, Norrholm SD, Jovanovic T (2015) Diagnostic Biomarkers for Posttraumatic Stress Disorder: Promising Horizons from Translational Neuroscience Research. Biol Psychiatry 78:344–353.

Mulders PC, van Eijndhoven PF, Schene AH, Beckmann CF, Tendolkar I (2015) Resting-state functional connectivity in major depressive disorder: A review. Neurosci Biobehav Rev 56:330–344.

Murphy D, Ross J, Busuttil W, Greenberg N, Armour C (2019) A latent profile analysis of PTSD symptoms among UK treatment seeking veterans. Eur J Psychotraumatol 10:1558706.

Nicholson AA, Rabellino D, Densmore M, Frewen PA, Paret C, Kluetsch R, Schmahl C, Théberge

J, Neufeld RWJ, McKinnon MC, Reiss J, Jetly R, Lanius RA (2017) The neurobiology of emotion regulation in posttraumatic stress disorder: Amygdala downregulation via real-time fMRI neurofeedback. Hum Brain Mapp 38:541–560.

Nicholson AA, Rabellino D, Densmore M, Frewen PA, Paret C, Kluetsch R, Schmahl C, Théberge J, Ros T, Neufeld RWJ, McKinnon MC, Reiss JP, Jetly R, Lanius RA (2018) Intrinsic connectivity network dynamics in PTSD during amygdala downregulation using real-time fMRI neurofeedback: A preliminary analysis. Hum Brain Mapp 39:4258–4275.

Quaedflieg CWEM, van de Ven V, Meyer T, Siep N, Merckelbach H, Smeets T (2015) Temporal Dynamics of Stress-Induced Alternations of Intrinsic Amygdala Connectivity and Neuroendocrine Levels Yu R, ed. PLoS One 10:e0124141.

Rahman AF, Manatunga A, Guo Y, Peng L, Warnock M, Ressler KJ, Jovanovic T (2018) A latent class analysis of PTSD symptoms among inner city primary care patients. J Psychiatr Res 98:1–8.

Spinhoven P, Penninx BW, van Hemert AM, de Rooij M, Elzinga BM (2014) Comorbidity of PTSD in anxiety and depressive disorders: Prevalence and shared risk factors. Child Abus Negl 38:1320–1330.

Sripada RK, King AP, Welsh RC, Garfinkel SN, Wang X, Sripada CS, Liberzon I (2012) Neural dysregulation in posttraumatic stress disorder: evidence for disrupted equilibrium between salience and default mode brain networks. Psychosom Med 74:904–911.

Vaisvaser S, Lin T, Admon R, Podlipsky I, Greenman Y, Stern N, Fruchter E, Wald I, Pine DS, Tarrasch R, Bar-Haim Y, Hendler T (2013) Neural traces of stress: cortisol related sustained enhancement of amygdala-hippocampal functional connectivity. Front Hum Neurosci 7:313.

Van Der Werff SJA, Pannekoek JN, Veer IM, Van Tol MJ, Aleman A, Veltman DJ, Zitman FG, Rombouts SARB, Elzinga BM, Van Der Wee NJA (2013) Resting-state functional connectivity in adults with childhood emotional maltreatment. Psychol Med 43:1825–1836.

Veer IM, Oei NYL, Spinhoven P, van Buchem M a, Elzinga BM, Rombouts SARB (2011) Beyond acute social stress: increased functional connectivity between amygdala and cortical midline structures. Neuroimage 57:1534–1541.

Veer IM, Oei NYL, Van Buchem MA, Elzinga BM, Rombouts SA (2010) Acute Social Stress Increases Amygdala Functional Connectivity with Posterior Cingulate Cortex and Medial Orbitofrontal Cortex. Proc Intl Soc MAg Reson Med 18:3509–3509.

Summary

Why some people develop stress symptoms and others do not, even when being exposed to similar stressors or traumatic events? This thesis contributes to the answer to this question and tested whether individual differences in acute stress responses might be predictive of long-term stress vulnerability.

In specific, the studies in the current thesis first identified the neural biomarkers that are of potential interest for acute stress responses, such as the changes in functional connectivity of large-scale networks. Whether these potential biomarkers could predict stress-related symptom development in a longitudinal fashion was investigated subsequently. A total of 340 police recruits before and after a stressful period in their training phase characterized by numerous trauma exposures were tested. Results reported in this thesis show that the connectivity changes of the default mode and salience networks in response to acute stress induction were most relevant for predicting stress-related symptom development. The findings suggest that salience network-based reconfiguration upon acute stress may serve as a potential marker for stress vulnerability.

Acknowledgement

When I look back, I see many people, many kind, smart, and funny people that I had the privilege to work with, to get inspirations from, and to share not-necessarily-always-academic-but-nevertheless-very-precious moments with. On this special occasion, I want to let them know how grateful I have been for having them next to me along this journey.

首先要特别感谢我的父母和姐姐，没有他们的支持和鼓励，我大概率不能坚持做自己想做的事情。博士论文能够顺利完成，也要谢谢家人的包容和关爱。么么哒！

I want to thank my PhD supervisors: Karin and Floris. I know that I am not the easiest type of student to supervise. Being described as stubborn, sometimes I may focus too much on my own thoughts, and possibly argue too much. Nevertheless, you both have always been very patient and tolerant, trying the best to teach me, guide me and convince me. I really appreciate that! I want to thank you for treating my stubbornness positively and for considering it as a potential quality of a good researcher. I also appreciated greatly your encouragement and your help along the way of my PhD training. Thank you!

My collaborators, it has been a great pleasure for me to work with you!
Erno, I am so grateful for your guidance and teaching in my first experimental fMRI study. I can still recall vividly how you explained the complicated design matrix for interaction conditions with a drawing on the white board. I of course cannot forget either how many Matlab codes you have provided me for extracting and analyzing heart-rate data. Thank you!
Vanessa, in my memory about our working experiences, the context appears very bight and fun. When I just started my PhD, I literally knew nothing about memory contextualization. Thank you for being patient and nice to such a terrible student! P.S. Hope one day I will have the chance to watch your live cello performance.
Christian, I am a fan of your cynical humor. I also admire your knowledge and insight. I am greatly thankful that I have had the opportunity to work with you since my master study. Thank you for all the valuable teachings and advice!
Hola, Alberto ;) We didn't get to work together until not so long ago but it feels like I have known you for some years. I want to thank you for taking me one step closer (I hope?) to the front door of your math world. I am particularly grateful for your step-by-step explanations. I also enjoyed very much our chats on random stuff. I am very happy to get to know you, as a colleague, but also as a friend. One day if you managed to get your scuba diving certificate, I will consider to be your diving buddy. Haha..

I want to thank my old roomies: Daniel, Peter and Thomas. We started our PhD almost the same time and have shared the office until .. we had to separate lol. I am so glad that I had you guys beside me when I was in the most difficult phase of my entire PhD training. I enjoyed our scientific and non-scientific discussions. I loved our exchange of thoughts and feelings. I feel so lucky to have you guys in my life. Although most of us has left Nijmegen now, I do hope one day there will be a reunion. In Montreal next year or in Seoul the year after, how about that? ;)

My Polish squad! Anna, and Maria, and Peter, Nessa, Leonore … sorry, I don't know why but somehow it becomes a Polish squad. Guess because spiritually we are the minorities here?! I thank you all for being part of my life in Nijmegen. Maria, I loved your broadcasting about all sorts of gossips, I was so amazed by your unbeatable gossip radar! Anna, I know I impressed you as the only Chinese you know who actually enjoys drinking. I also appreciate it that you meet my expectations about Polish in terms of drinking. Not that you drink a lot, but at least you do drink, more than just one rosie beer. You know what/who I am talking about. Nessa, sorry I 'ignored you' (in your word) the first time when we met during a Christmas dinner. But I am happy I got to know you after. I cannot forget the awful cigarettes we bought in Germany. Did you take the rest? Leonore, I felt I had this click with you when you joined our project as a RA some years ago. It's a strange feeling to be so sure right from the beginning that you can get along with this person outside the work as well. Oh, don't tell me if I am wrong, just 'let me live that fantacy' lol.

And Zahra, hmm.. will you come to my defense party, and drink? That determines what will follow here. just joking. I don't remember how we got to know each other, but you have been a window for me to get to know a different culture that I would not have been able to otherwise. I want to thank you particularly for that, but also for your unforgettable eggplant grilling show and many other similar performances. I thank you for all the laughter we had! I hope a visit to Pakistan together is still on your agenda, somewhere?

I also want to thank my EPAN group members, and particularly PIA members. Having worked on such a demanding research project, I really appreciated it that we were a team. Floris, Saskia, Mao, Reinoud, Naomi, Leonore, Geoffery, Inge, Tiele, Lisanne and many more students and assistants, thank you all for helping me achieve my PhD research project. All the EPAN members, I want to thank you for your valuable feedback and suggestions on my work. Thank you!

And SINers! There is a part of me that I feel belongs to the SIN group, partly because I did my master internship there and partly because I love the vibe of the group. Maarten and Eric, I particularly want to thank you for your suggestions and advice regarding the motion corrections. You have always been very kind and helpful to me, I really appreciate that! Roselyne, I believe my time in 2.268 would have been

much more stressful if I hadn't had your company there. Thank you! And also thank you already for a couch that I can crush on in CA in the near future ;) Jill, just want to say I really enjoyed that bed in Vancouver, thanks to you and Zahra. I also appreciate your witty and funny remarks. Happy to get to know you.

I should not forget to mention Marek, Mike, Hong and Edward from TG, and Nicole, Ayse, Sandra and Tildie from Admin. You guys are amazing!! I appreciated your help and I appreciate it even more after having left the Donders! And Paul, you were my super saver! I don't remember how many times I have asked you to help with our experiments in those years. I really learned a lot from you. It has been a privilege to have the support from all of you during my entire stay at the DCCN. Thank you all! Truly grateful!

I'd also like to give a big thank you to Rasim and Jenni for helping me set up the scanning protocols, to Marcel for offering me mentor advice at the early stage of my PhD.

Also, I want to thank my paranymphs, Peter and Leonore, and the Corona members, Prof. dr. Guillén Fernández, Prof. dr. Bernet Elzinga, Dr. Ilya Veer, Prof. dr. Tom Smeets, Prof. dr. Elbert Geuze, Dr. Mirjam van Zuiden and Dr. Marloes Henckens. Thank you all for making my PhD defense ceremony possible.

And lastly, my faraway friends…
阿宝同学，这些年辛苦你时不时远程消化我的抱怨，终于我也和你一样成灭绝师太了，哈哈。学术路上有人同行，有友人同行，是我的幸运。
수영언니, 고마워. 내가 박사과정에서 가장 힘들었을 때 언니한테 갔던 것 같아. 그 땐큰 든든했던.. 그 외에도 여러가지로 늘 고마워하고 있다는 것!

最后的最后，感谢自己随心，随性，不放弃。

About the Author

Wei was born in November 26, 1979 in Chongqing, China. She left for Beijing for the college and then moved to Seoul, South Korea after. She obtained her first master degree in Psychology (M.A.) at Korean University, South Korea and the second in Cognitive Neuroscience (M.Sc.) at Radboud University, The Netherlands. She then joined the EPAN lab, led by Professor dr. Karin Roelofs and worked together also with dr. Floris Klumpers for her PhD training in affective neuroscience at the Donders Institute. Currently, she is a postdoctoral research associate at Washington University in Saint Louis in the United States. Wei's academic interests lie broadly in affective and cognitive neuroscience with a focus on the brain state as a function of emotions, and its relation to psychopathologies. Outside science, Wei loves going into the wild nature and enjoys adventurous explorations.

Publication List

Zhang, W., Groen, W., Mennes, M., Greven, C., Buitelaar, J., & Rommelse, N. (2017). Revisiting subcortical brain volume correlates of autism in the ABIDE dataset: effects of age and sex. Psychological Medicine, pp. 1– 15.

Zhang, W., van Ast, V. A., Klumpers, F., Roelofs, K., & Hermans, E. J. (2018). Memory contextualization: The role of prefrontal cortex in functional integration across item and context representational regions. Journal of Cognitive Neuroscience, 30(4), 1–15

Zhang, W., Hashemi, M. M., Kaldewaij, R., Koch, S. B. J., Christian, B., Klumpers, F. & Roelofs, K. (2019). Acute stress alters the 'default' brain processing. NeuroImage, 189:870-877.

Rausch, A., **Zhang, W.**, Haak, K., Mennes, M., Hermans, E. J., ... Groen, W. B. (2016). Altered functional connectivity of the amygdaloid input nuclei in adolescents and young adults with autism spectrum disorder: A resting state fMRI study. Molecular Autism, 7(13).

Rausch, A., **Zhang, W.**, Beckmann, C. F., Buitelaar, J., Groen, W., & aak, K. V. (2017). Connectivity-based parcellation of the amygdala predicts social skills in adolescents with Autism Spectrum Disorder. Journal of Autism and Developmental Disorders, 48(2), 572-582.

Koch, S., Klumpers, F., **Zhang, W.,** Hashemi, M., Kaldewaij, R., van Ast, V., Smith, S.A., & Roelofs, K. (2017). The role of automatic defensive responses in the development of posttraumatic stress symptoms in police recruits: protocol of a prospective study. Eur J. Psychotraumatol, 8(1): 1412226.

Hashemi, M., T. Gladwin, de Valk, N., **Zhang, W.,** Kaldewaij, R., van Ast, V., Koch, S., Klumpers, F. & Roelofs, K. (2019). Neural Dynamics of shooting decisions and the switch from freeze to fight. Scientific Report, 9(1):4240.

Kaldewaij, R., Koch, S., **Zhang, W.**, Hashemi, M., Klumpers, F. & Roelofs, K. (2019). High endogenous testosterone levels are associated with diminished neural emotional control in aggressive police recruits. Psychological Science, 30(8):1161-1173.

Kaldewaij, R., Koch, S., **Zhang, W.**, Hashemi, M., Klumpers, F. & Roelofs, K. (2019). Frontal Control Over Automatic Emotional Action Tendencies Predicts Acute Stress Responsivity. Biol Psychaitry Cogn Neurosci Neuroimaging, S2451-9022(19)30176-4.

Donders Graduate School for Cognitive Neuroscience

For a successful research Institute, it is vital to train the next generation of young scientists. To achieve this goal, the Donders Institute for Brain, Cognition and Behaviour established the Donders Graduate School for Cognitive Neuroscience (DGCN), which was officially recognised as a national graduate school in 2009. The Graduate School covers training at both Master's and PhD level and provides an excellent educational context fully aligned with the research programme of the Donders Institute.

The school successfully attracts highly talented national and international students in biology, physics, psycholinguistics, psychology, behavioral science, medicine and related disciplines. Selective admission and assessment centers guarantee the enrolment of the best and most motivated students.

The DGCN tracks the career of PhD graduates carefully. More than 50% of PhD alumni show a continuation in academia with postdoc positions at top institutes worldwide, e.g. Stanford University, University of Oxford, University of Cambridge, UCL London, MPI Leipzig, Hanyang University in South Korea, NTNU Norway, University of Illinois, North Western University, Northeastern University in Boston, ETH Zürich, University of Vienna etc.. Positions outside academia spread among the following sectors: specialists in a medical environment, mainly in genetics, geriatrics, psychiatry and neurology. Specialists in a psychological environment, e.g. as specialist in neuropsychology, psychological diagnostics or therapy. Positions in higher education as coordinators or lecturers. A smaller percentage enters business as research consultants, analysts or head of research and development. Fewer graduates stay in a research environment as lab coordinators, technical support or policy advisors. Upcoming possibilities are positions in the IT sector and management position in pharmaceutical industry. In general, the PhDs graduates almost invariably continue with high-quality positions that play an important role in our knowledge economy.

For more information on the DGCN as well as past and upcoming defenses please visit: http://www.ru.nl/donders/graduate-school/phd/